KAPITAŁ LUDZKI
NARODOWA STRATEGIA SPÓJNOŚCI

Politechnika Wrocławska

UNIA EUROPEJSKA
EUROPEJSKI
FUNDUSZ SPOŁECZNY

ROZWÓJ POTENCJAŁU I OFERTY DYDAKTYCZNEJ POLITECHNIKI WROCŁAWSKIEJ

Wrocław University of Technology

Control in Electrical Power Engineering

Waldemar Rebizant, Andrzej Wiszniewski

DIGITAL SIGNAL PROCESSING FOR PROTECTION AND CONTROL

Wrocław 2011

Projekt współfinansowany ze środków Unii Europejskiej w ramach
Europejskiego Funduszu Społecznego

Wrocław University of Technology

Control in Electrical Power Engineering

Waldemar Rebizant, Andrzej Wiszniewski

DIGITAL SIGNAL PROCESSING FOR PROTECTION AND CONTROL

Wrocław 2011

Reviewer: Bogdan Miedziński

ISBN 978-83-62098-59-0

Published by PRINTPAP Łódź, www.printpap.pl

CONTENTS

1. INTRODUCTION

The age of protection began some 105 years ago, when control apparatus were for the first time connected to current and voltage transformers, which reduced the primary currents and voltages to secondary levels. The secondary currents and voltages could be processed to generate TRIP or NO TRIP decisions.

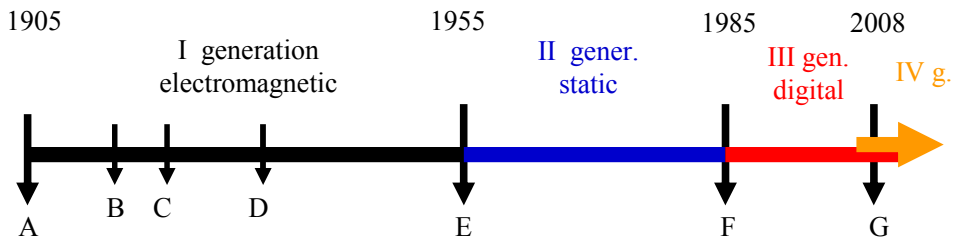

A – overcurrent & undervoltage relays with CTs & VTs
B – inverse time overcurrent relays
C – differential relays and directional relays
D – distance relays with time graded characteristics
E – static relays with filters and comparators
F – digital relays measuring phasors
G – first Wide Area Measuring protective systems

Fig. 1.1 History of protection technology

The first relays were simple overcurrent and undervoltage apparatus (1905). Both were electromagnetic or magnetoelectric in nature and resembled the measuring apparatus. Both were actuated either by r.m.s. values or mean values of rectified signals. They had moving parts and their delay was due to the time needed to close the output contacts.

Next step (around 1915) was introduction of inverse time overcurrent relays, either thermal, or with rotating discs. Some 5 years later the differential principle was adopted, and it was a great step forward in protection of the power system apparatus. The differential relays compared two currents.

From differential relays there was only one step to distance relays (1930), which compared currents and voltages, their r.m.s. or mean values. They had the delay which

was a function of the measured impedance U/I. All those relays were magnetoelectric or electromagnetic, all had moving parts and we consider them as the first generation of protective devices.

The big change was caused by the invention of transistors (1947). They were introduced to protective relays around 1955. It enabled to build the static devices (without moving parts, except the output element) that began the era of second generation of protective relays. The static relays had the operational criteria the same as electromagnetic ones; however, their decisions (to trip or not to trip) were based on the modified ways of signal processing. Because of that they offered a number of advantages:

- improvement of cooperation with CTs and VTs,
- reduced dimensions and modularity,
- facilitation of testing, maintenance and repairs,
- complex operational characteristics,
- increased speed of operation.

The third generation of protective devices started with the widespread application of inexpensive digital processors and memories (around 1985). The block diagram of the digital relay is presented in Fig. 1.2.

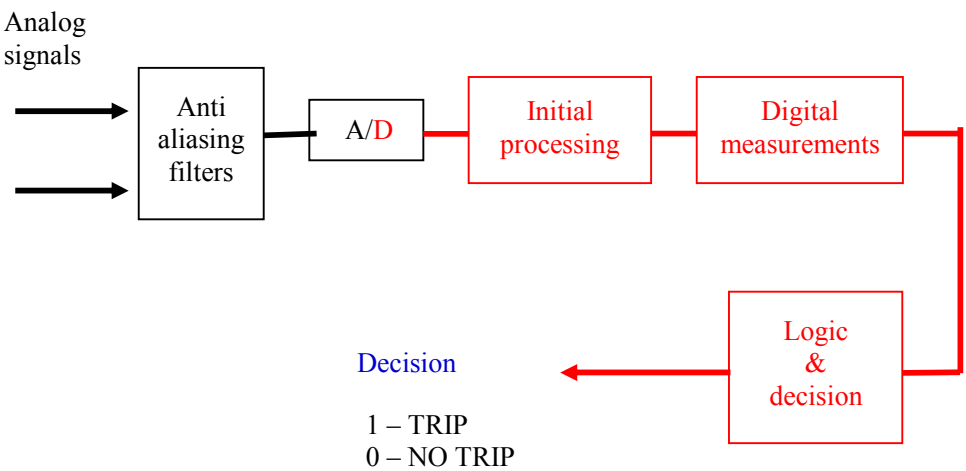

Fig. 1.2 Block diagram of digital relays

Processing of relay input signals is realized in 5 basic stages:

- input of analog signals, which usually are currents and voltages derived from CTs and VTs, enter the antialiasing low pass filters that remove components of high frequency which could irreversibly corrupt the digital signals;

- from the antialiasing filter the signals – still in the analog form – enter the A/D converter and at the output of that block they have forms of trains of samples;
- the digital signals enter the block of initial processing, where they are filtered, orthogonalized, etc.;
- the results of initial processing enter the block of digital measurements, in which the signals, their parameters and mutual relations are calculated;
- the final block generates the final decisions, which are based on adopted criteria checked on the ground of digital signal processing.

One has to remark that the relays of previous generations did not actually measure particular signals. Their operations were based on comparators, which only decided, if the given quantity was smaller or greater than the operational threshold. In cases of digital relays the signals are actually measured and the comparison with the thresholds comes afterwards.

Starting from around 1985 the digital relays became dominant in the offer of manufacturers. It is so, because they offer a number of advantages:

- integration of functions,
- further reduction of power derived from secondary terminals of CTs and VTs,
- reduction of secondary cabling,
- complex algorithms, which process digital signals using values of the samples,
- increased speed of operation,
- facility of communication,
- self testing capabilities.

The digital processing of signals, and progress in telecommunication enables to enter the era of 4-th generation of protective devices. It is the era of Wide Area Measurement and Protection Systems (WAMPS), which combine sophisticated digital processing with the fast and reliable exchange of information via telecommunication links.

The 4-th generation came in timely, because the philosophy of relaying has recently slightly changed. Previously the principal requirement was to assure reliable and fast protection of given power system apparatus. Therefore they were object oriented. The relays ought to be:

- reliable,
- sensitive,
- selective,
- high speed.

However, nowadays the priorities of relaying slightly changed. The first one is protection of the power system against developing disturbances, which could lead to blackouts. Although the needs to protect given power system component is still fundamental, but the relays ought to be system-oriented. Therefore, undesirable tripping may be considered as dangerous as the delayed tripping of the fault.

The 4-th generation has the following properties:

- wide area measuring of signals and transfer of the results to the decision making points,
- integration of protection, control, monitoring and measurements,
- adaptability to the existing conditions,
- intelligent decisions, estimation of actual conditions and possible consequences.

All the advantages of 3-rd and 4-th generation of protective devices require efficient digital processing of signals. Both theoretical basics and specific algorithms for signal conditioning, calculation of criteria values and decision making are provided in the following sections of this book.

2. ANALOG PROCESSING AND SAMPLING

An exemplary sampled signal is presented in Fig. 2.1. One may see that the sampling time T_S is the time span between two consecutive samples. One may also define the sampling frequency $f_S = 1/T_S$ and the sampling angular frequency $\omega_S = 2\pi/T_S$.

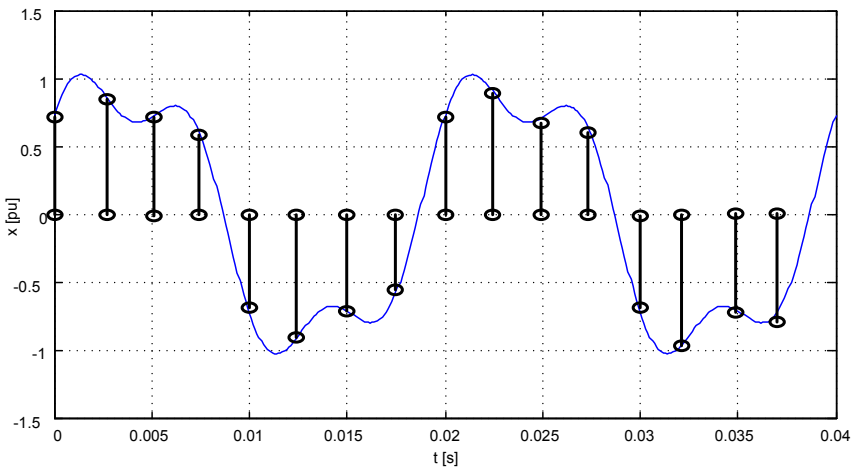

Fig. 2.1. Sampled signal

While designing the analog processing of the signal one has to decide two things:

- selection of sampling frequency – in cases of sinusoidal signals it is the number of samples within one period of the basic frequency of the signal,
- cut off frequency of the antialiasing low pass filter.

If the input signal is a current in transient state caused by the short circuit, it may be presented in the form:

$$i(\tau) = I_1 \cos(\omega_1 \tau - \alpha_1) + I_0 \exp\left(-\frac{\tau}{T_a}\right) + \sum_{k=2}^{p} I_k (k\omega_1 \tau - \alpha_k) + \\ + \sum_{h=1}^{r} I_h \left[\exp\left(-\frac{\tau}{T_h}\right)\right] \cos(\omega_h \tau - \beta_h) \tag{2.1}$$

One may observe that the signal consists of the following components:

I_1 – fundamental frequency component (phasor magnitude),

I_0 – decaying DC component,

I_k – higher frequency component,

I_h – transient oscillatory decaying component.

The useful information is contained in the fundamental frequency component, and sometimes in the selected higher frequency components (2-nd, 3-rd or 5-th). Therefore, all the other components are to be rejected. Particularly dangerous are very high frequency components (I_k and I_h), which have frequencies close to the sampling frequency, because they may cause irreversible corruption of the digital signal.

Therefore, selection of the sampling frequency f_S is a compromise. It must not be too low, to enable reproduction of the component which is vital for the relaying decisions. On the other hand it must not be too high, to make unnecessary burden for the digital processing.

Basically, the minimum sampling frequency results from the Shannon-Kotielnikov theorem that defines conditions for possibility of signal reconstruction after sampling. According to that, there should be at least two samples of the signal taken within the period of the signal component that should be represented in digital form without loss of information about frequency.

If the component to be reproduced correctly has the frequency f_{k1} then the sampling frequency ought to be:

$$f_S \geq 2 f_{k1} \tag{2.2}$$

In real installations the sampling frequency is seldom lower than 800 Hz (16 samples per one period of the fundamental frequency component, 4 samples per one period of the 4th harmonic, etc). Contemporary digital protection relays offer sampling rates up to several kHz. Special solutions, where higher frequency components are used for generating the trip decision, may have sampling rates in the range of many hundreds of kHz.

Before sampling the signal goes through the antialiasing low pass filters that are used to pass all the components with frequencies lower than f_{k1}, and to eliminate frequencies higher than that. The cut off frequency of the filter f_C ought to meet the following requirements:

$$f_{k1} < f_C \leq \frac{f_S - f_k}{3} \tag{2.3}$$

This would make all the components with frequencies lower than f_{k1} pass with the minimal distortion, while the components with frequencies greater than that would be suppressed.

The analog input filters are in most cases implemented in form of cascade RC circuits. Required slope of the transition part of filter spectrum is obtained by choosing appropriate filter order, which means that respective number of the first order RC four-poles is connected in series.

3. FUNDAMENTALS OF SIGNAL PROCESSING

3.1. APPROXIMATION OF A SIGNAL IN THE DATA WINDOW

Let us consider a periodic signal containing the fundamental and higher harmonics as shown in Fig. 3.1.

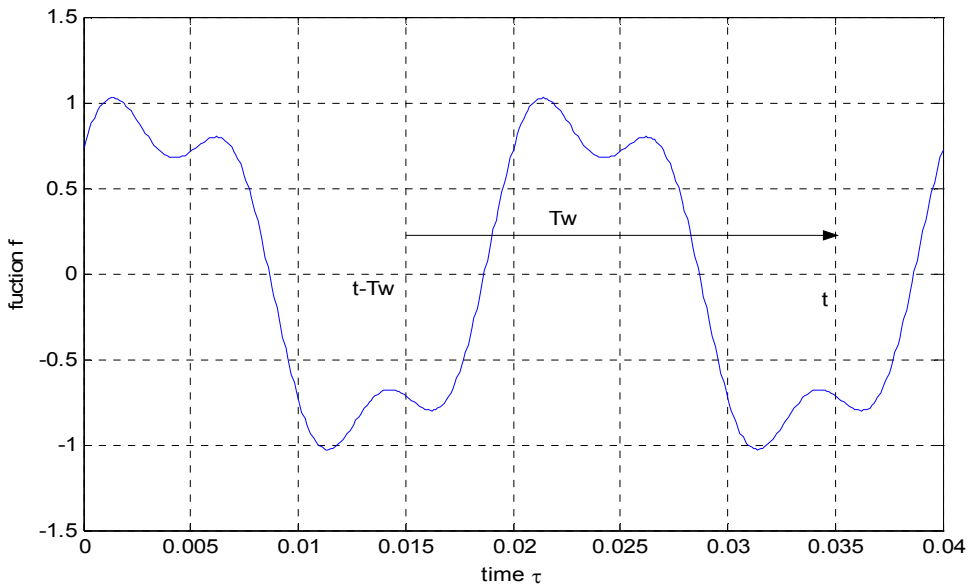

Fig. 3.1. Example of a periodic signal

On the axis of time τ there is a given moment t. In the time $\tau \leq t$ the signal is known (was already recorded), while for $\tau > t$ the signal is unknown yet.

Let in the period between t and $t - T_w$ (where T_w is the so called Data Window, DW) the signal is to be approximated by two orthogonal correlating functions $f_{r1}(\tau)$ and $f_{r2}(\tau)$:

$$f(\tau) \approx C_1 f_{r1}(\tau) + C_2 f_{r2}(\tau), \tag{3.1}$$

where: C_1 and C_2 are coefficients of the approximation.

Two functions may be called *orthogonal* if their product integrated in the data window is zero:

$$\int_{t-T_w}^{t} f_{r1}(\tau) f_{r2}(\tau) d\tau = 0 . \tag{3.2}$$

The best approximation is achieved, if the selection of the coefficients is done in such a way that the mean square error ε

$$\varepsilon = \int_{t-T_w}^{t} [f(\tau) - C_1 f_{r1}(\tau) - C_2 f_{r2}(\tau)]^2 d\tau \tag{3.3}$$

is minimum.

To achieve that there are specified the following conditions, which enable calculating the coefficients C_1 and C_2:

$$\frac{d\varepsilon}{dC_1} = 0 \quad \text{and} \quad \frac{d\varepsilon}{dC_2} = 0 .$$

It gives two independent equations, which in case of orthogonal functions f_1 and f_2, lead to simple calculation of the coefficients of approximation:

$$C_1 = \frac{\int_{t-T_w}^{t} f(\tau) f_{r1}(\tau) d\tau}{\int_{t-T_w}^{t} f_{r1}^2(\tau) d\tau} , \tag{3.4}$$

$$C_2 = \frac{\int_{t-T_w}^{t} f(\tau) f_{r2}(\tau) d\tau}{\int_{t-T_w}^{t} f_{r2}^2(\tau) d\tau} . \tag{3.5}$$

Similar formulas may be developed for any number of approximating functions which are mutually orthogonal in the data window.

3.2. FOURIER SERIES

Approximation of the function $f(\tau)$ by the infinite series of sinusoidal / cosinusoidal functions being mutually orthogonal is called a Fourier series:

$$f(\tau) \approx \frac{a_0}{2} + \sum_{m=1}^{\infty} \left[a_m \cos(m\omega_w \tau) + b_m \sin(m\omega_w \tau) \right], \tag{3.6}$$

where: $\omega_w = \dfrac{2\pi}{T_w}$.

Minimizing the mean square error of approximation in the same way as above, one gets the general formulas describing the values of a_m and b_m using the correlating functions $f_{r1} = \cos(m\omega_w \tau)$ and $f_{r2} = \sin(m\omega_w \tau)$:

$$a_m = \frac{\int_{t-T_w}^{t} f(\tau) f_{r1}(\tau) d\tau}{\int_{t-T_w}^{t} f_{r1}^2 d\tau} = \frac{\int_{t-T_w}^{t} f(\tau) \cos(m\omega_w \tau) d\tau}{\int_{t-T_w}^{t} \cos^2(m\omega_w \tau) d\tau} = \left(\frac{2}{T_w} \right) \int_{t-T_w}^{t} f(\tau) \cos(m\omega_w \tau) d\tau \tag{3.7}$$

$$b_m = \frac{\int_{t-T_w}^{t} f(\tau) f_{r2}(\tau) d\tau}{\int_{t-T_w}^{t} f_{r2}^2 d\tau} = \frac{\int_{t-T_w}^{t} f(\tau) \sin(m\omega_w \tau) d\tau}{\int_{t-T_w}^{t} \sin^2(m\omega_w \tau) d\tau} = \left(\frac{2}{T_w} \right) \int_{t-T_w}^{t} f(\tau) \sin(m\omega_w \tau) d\tau \tag{3.8}$$

3.3. CALCULATION OF PHASORS

The antialiasing filtering of the input signal removes the oscillatory transient components (and the very high frequency harmonics as well) and the signal, which enters an A/D converter, consists of the fundamental frequency component, some harmonics and the decaying DC component. It may be presented in the following form:

$$f(\tau) = \underbrace{F_1 \cos(\omega_1 \tau - \beta_1)}_{\text{Fundamental (Phasor)}} + \underbrace{F_0 \exp\left(\frac{-\tau}{T_a} \right)}_{\text{DC}} + \underbrace{\sum_{k=2}^{p} F_k \cos(k\omega_1 \tau - \beta_k)}_{\text{Harmonics}}, \tag{3.9}$$

where: T_1 – duration of one period of the fundamental frequency component,
$\omega_1 = 2\pi/T_1$ – fundamental angular frequency.

Amplitude of the fundamental frequency component f_1 may be determined by the Fourier coefficients (3.7) and (3.8). It is given by two orthogonal components: sinusoidal (lagging) and cosinusoidal (leading). Those components determine the ampli-

tude and phase of the fundamental component, thus they determine the *phasor*. Neglecting all other components the fundamental frequency signal can be approximated by:

$$f_1(\tau) = (F_1 \cos\beta_1)\cos(\omega_1\tau) + (F_1 \sin\beta_1)\sin(\omega_1\tau). \tag{3.10}$$

Therefore amplitudes of the leading (+) and lagging (-) orthogonal components of the fundamental harmonic are:

$$a_1 = f_+ = F_1 \cos\beta_1 \tag{3.11}$$

$$b_1 = f_- = F_1 \sin\beta_1 \tag{3.12}$$

and the amplitude and phase of the phasor may be calculated as follows:

$$F_1 = \sqrt{f_+^2 + f_-^2}\ , \tag{3.13}$$

$$\beta_1 = arctg\left(\frac{f_-}{f_+}\right) = arctg\left(\frac{b_1}{a_1}\right). \tag{3.14}$$

In calculation the orthogonal phasor components f_+ and f_- there are two basic ways for selecting the correlating functions. The first one calculates non rotating phasor components, while the second calculates the rotating components.

3.3.1. NON-ROTATING ORTHOGONAL COMPONENTS

Let the correlating functions are the following:

$$f_{r1} = \cos(\omega_1\tau),\ f_{r2} = \sin(\omega_1\tau).$$

Then the orthogonal components are calculated as it was demonstrated by equations (3.7) and (3.8).

If in the data window neither the frequency of the phasor nor its amplitude changed, and if the period of the phasor is equal to the data window duration, then the values of calculated orthogonal components f_+ and f_- are constant (see Fig. 3.2). Therefore, the angle β_1 may be defined as the angle of the phasor with respect to the function $\cos(\omega_1\tau)$.

However, one must bear in mind that the simple formulas (3.7), (3.8) may be used only if the correlating functions f_{r1} and f_{r2} are mutually orthogonal. It is so if the duration of the data window is equal to the period of the calculated phasor: $T_w = T_1 = 2\pi/\omega_1$, or if it is equal to the half of the period: $T_w = 0.5(2\pi/\omega_1)$. In the former case the calculation of the phasor efficiently rejects higher frequency components and the DC component. In the latter case rejection is far from being perfect, and the components corrupt the result of phasor calculation.

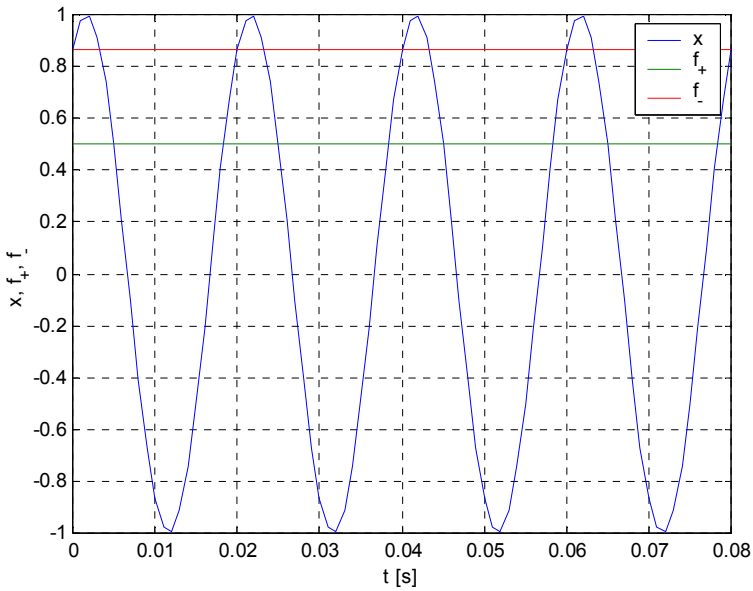

Fig. 3.2. Example of a pure sine signal and its non-rotating orthogonal components

3.3.2. ROTATING ORTHOGONAL COMPONENTS

To avoid limitations related to the non-rotating orthogonal components that could be calculated only if the correlating functions were orthogonal in the data window (this window ought to be equal to one period or half the period of the fundamental frequency) one may use the so called rotating orthogonal components. If the correlating functions are the same in the data windows and are orthogonal in that window for at value of t, they ought to be selected as follows:

$$f_{r1} = \cos\left[\omega_1(\tau - t) + \frac{T_w}{2}\right], \tag{3.15}$$

$$f_{r2} = \sin\left[\omega_1(\tau - t) + \frac{T_w}{2}\right]. \tag{3.16}$$

Therefore one gets:

$$a_1 = \frac{\int_{t-T_w}^{t} f(\tau) f_{r1}(\tau) d\tau}{\int_{t-T_w}^{t} f_{r1}^2 d(\tau)} = F_1 \cos\left[\omega_1\left(t - \frac{T_w}{2}\right) - \beta\right] = f_+, \tag{3.17}$$

$$b_1 = \frac{\int_{t-T_w}^{t} f(\tau) f_{r2}(\tau) d\tau}{\int_{t-T_w}^{t} f_{r2}^2 d(\tau)} = F_1 \sin\left[\omega_1\left(t - \frac{T_w}{2}\right) - \beta\right] = f_- . \tag{3.18}$$

Both orthogonal components rotate with the change of time. However, the amplitude of the phasor may be calculated in the same way as before:

$$F_1 = \sqrt{f_+^2 + f_-^2} . \tag{3.19}$$

The advantage of the rotating orthogonal components is that the correlating functions are mutually orthogonal for any duration of the data window T_w, therefore the formulas (3.7) and (3.8) may be applied for any T_w.

An illustration of the concept for a pure 50Hz sine signal and full-cycle data window is shown in Fig. 3.3. One can see that the components f_+, f_- have the same amplitude as the input signal (hidden under the f_- curve) and are shifted one by 90 deg.

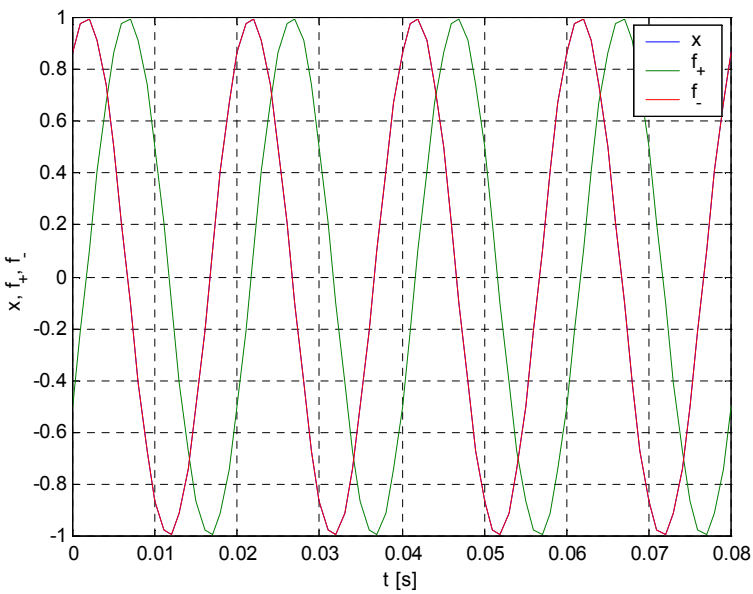

Fig. 3.3. Example of a pure sine signal and its rotating orthogonal components

3.4. DIGITAL CALCULATION OF PHASORS

3.4.1. APPLICATION OF FOURIER SERIES

The input signal presented as a train of samples is shown in Fig. 3.4.

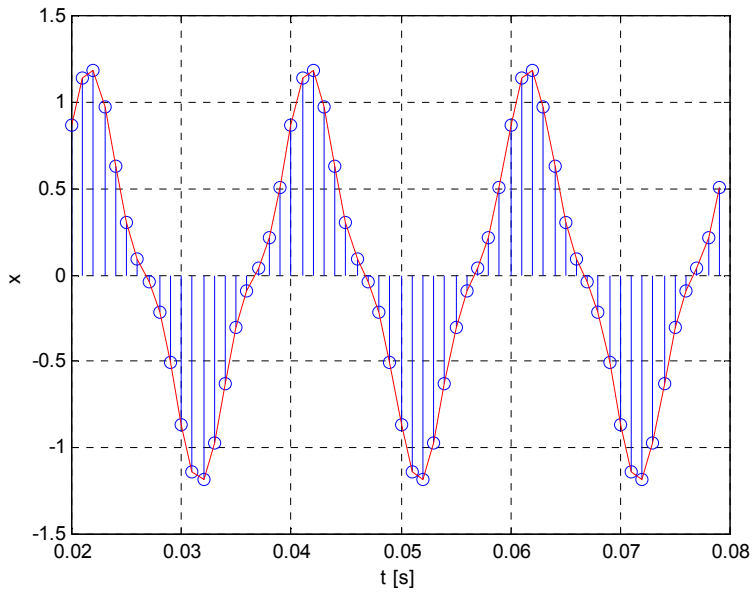

Fig. 3.4. An input signal (50Hz + 20% of the 3rd harmonic) in digital form as a train of samples

The actual moment t may be expressed in the alternative form $t = nT_S$, where: n – current number of the sample, T_S – sampling period.

Therefore, the digital form of calculation the Fourier coefficients, which in the continuous form are given by (3.7) and (3.8), is the following:

$$a_m(n) = \left(\frac{2T_S}{T_w}\right) \sum_{m=n-p}^{n} f(m) \cos(m\omega_w T_S), \tag{3.20}$$

$$b_m(n) = \left(\frac{2T_S}{T_w}\right) \sum_{m=n-p}^{n} f(m) \sin(m\omega_w T_S), \tag{3.21}$$

where: $T_w = (p+1)T_S$ – duration of the data window,

$(p+1)$ – number of samples in the data window.

Therefore, while calculating the non-rotating phasor for duration of the data window T_w being equal to the period of the phasor T_1, the formulas are:

$$a_1(n) = \left(\frac{2T_S}{T_w}\right) \sum_{m=n-p}^{n} f(m) \cos(m\omega_1 T_S) = f_{1+}, \tag{3.22}$$

$$b_1(n) = \left(\frac{2T_S}{T_w}\right) \sum_{m=n-p}^{n} f(m) \sin(m\omega_1 T_S) = f_{1-}. \tag{3.23}$$

The formulas (3.22) and (3.23) may also be presented in the recursive form to reduce the number of multiplications:

$$a_1 = a_1(n-1) + \left(\frac{2T_S}{T_w}\right)\left[f(n)\cos(n\omega_1 T_S) - f(n-p-1)\cos\left((n-p-1)\omega_1 T_S\right)\right], \tag{3.24}$$

$$b_1 = b_1(n-1) + \left(\frac{2T_S}{T_w}\right)\left[f(n)\sin(n\omega_1 T_S) - f(n-p-1)\sin\left((n-p-1)\omega_1 T_S\right)\right]. \tag{3.25}$$

As a result the computational burden is greatly reduced. The formulae may even be more efficient, if one observes that:

$$\cos(n\omega_1 T_S) = \cos\left[(n-p-1)\omega_1 T_S\right],$$
$$\sin(n\omega_1 T_S) = \sin\left[(n-p-1)\omega_1 T_S\right].$$

Non-rotating phasor components may be calculated in the very efficient form; however, as stated before the method may be used only if the duration of the data window is equal to the period or a half of the period of the phasor.

If orthogonal components of a rotating phasor are calculated, then correlating functions are digital forms of formulas (3.17) and (3.18), and for $T_w = T_1$:

$$a_1(n) = \left(\frac{2T_S}{T_w}\right) \sum_{m=n-p}^{n} f(m) \cos\left[\omega_1 (m-n) T_S + \frac{T_w}{2}\right] = f_+, \tag{3.26}$$

$$b_1(n) = \left(\frac{2T_S}{T_w}\right) \sum_{m=n-p}^{n} f(m) \sin\left[\omega_1 (m-n) T_S + \frac{T_w}{2}\right] = f_-. \tag{3.27}$$

The rotating phasor components can not be calculated in the recursive form, but they may be applied for any duration of the data window. If the duration of the data window T_w is not equal to the period of the phasor T_1, then the formulas are slightly changed:

$$a_1(n) = \frac{2T_S}{T_w + T_1 \sin(\omega T_w)/2\pi} \sum_{m=n-p}^{n} f(m) \cos\left[\omega_1 (m-n) T_S + \frac{T_w}{2}\right] = f_+ \qquad (3.28)$$

$$b_1(n) = \frac{2T_S}{T_w - T_1 \sin(\omega T_w)/2\pi} \sum_{m=n-p}^{n} f(m) \sin\left[\omega_1 (m-n) T_S + \frac{T_w}{2}\right] = f_- . \qquad (3.29)$$

The amplitude of the phasor is to be determined by (3.19). An illustration of the calculation for the signal from Fig. 3.4 is given in Fig. 3.5.

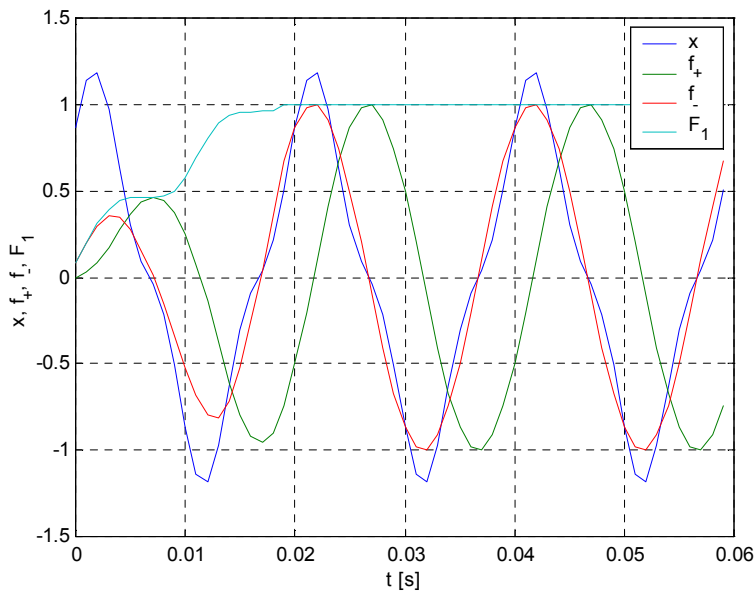

Fig. 3.5. Signal (as in Fig. 3.4), orthogonal components (3.28), (3.29) and amplitude of fundamental harmonic

3.4.1 OTHER METHODS OF CALCULATIONS OF PHASORS

Calculation of phasors by means of correlation with sine/cosine in the data window being equal to the period of the phasor is advantageous, because it rejects the higher frequencies and DC components which are present in the input signal and can corrupt the results of the phasor calculation. However, it introduces a delay which is equal to T_w. If the input signal has none of the corrupting components, simpler and faster methods of calculation may be used. The most common is utilization of the first derivative:

$$f(\tau) = F \sin(\omega_1 \tau + \beta) = f_- , \qquad (3.30)$$

$$\left(\frac{1}{\omega_1}\right)f'(\tau)=F\cos(\omega_1\tau+\beta)=f_+. \tag{3.31}$$

Calculation of the first derivative in a digital form is simple, if the signal between the samples (n) and (n–1) is approximated by the straight line segment. Thus one can get:

$$f(n-0.5)\approx\frac{f(n)+f(n-1)}{2}\approx F\sin[\omega_1(n-0.5)T_S+\beta]=f_- \tag{3.32}$$

$$\left(\frac{1}{\omega_1}\right)f'(n-0.5)\approx\frac{f(n)-f(n-1)}{\omega_1 T_S}\approx F\cos[\omega_1(n-0.5)T_S+\beta]=f_+ \tag{3.33}$$

To increase accuracy of the calculation one may introduce a corrective factor:

$$f_+=\frac{f(n)-f(n-1)}{2\sin\left(\frac{\omega_1 T_S}{2}\right)}, \tag{3.34}$$

$$f_-=\frac{f(n)+f(n-1)}{2\cos\left(\frac{\omega_1 T_S}{2}\right)}. \tag{3.35}$$

Alternatively, the fast calculation of the phasor may be based on the time delay:

$$f(n)=F\sin(\omega_1 nT_S+\beta), \tag{3.36}$$

$$f(n-k)=F\sin[\omega_1(n-k)T_S+\beta]. \tag{3.37}$$

Therefore:

$$f(n-k)=F[\sin(\omega_1 nT_S+\beta)\cos(\omega_1 kT_S)-\cos(\omega_1 nT_S+\beta)\sin(\omega_1 kT_S)]. \tag{3.38}$$

It may be rewritten in the form:

$$F\cos(\omega_1 nT_S+\beta)=[f(n)ctg(\omega_1 kT_S)-f(n-k)]\frac{1}{\sin(\omega_1 kT_S)}. \tag{3.39}$$

Therefore:

$$f_+=F\cos(\omega_1 nT_S+\beta)=\left[f(n)ctg(\omega_1 kT_S)-f(n-k)\frac{1}{\sin(\omega_1 kT_S)}\right], \tag{3.40}$$

$$f_-=F\sin(\omega_1 nT_S+\beta)=f(n), \tag{3.41}$$

where k is selected arbitrary. The fastest calculation is when k=1, while the simplest calculation is for $k=\pi / (2\omega_1 T_S)$.

In the latter case:

$$f_+ = -f(n-k),$$

$$f_- = f(n).$$

An illustration of the calculation using eqs. (3.40) and (3.41) for k=1 is provided in Fig. 3.6. One can see that the measurement dynamics is very high, however, the accuracy is poor, what results as an effect of presence of the 3rd harmonic.

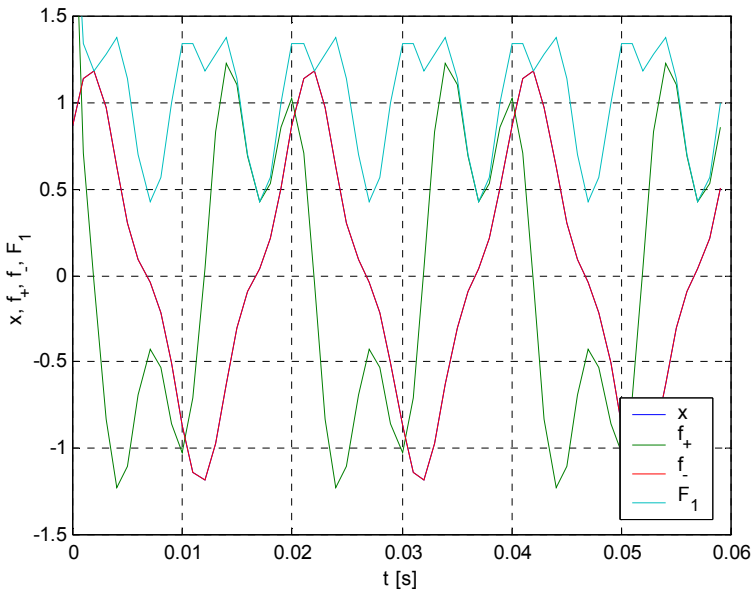

Fig. 3.6. Signal (as in Fig. 3.4), orthogonal components (3.40), (3.41) and amplitude of fundamental harmonic

3.5. NON-PERIODIC INPUT SIGNALS

3.5.1 CONVOLUTION

Among non-periodic functions a special place occupies the Dirac's pulse $\delta(x)$:

$$\delta(x) = 0 \quad \text{for} \quad x \neq 0$$
$$\delta(x) = \textit{infinity} \text{ for } x = 0$$

$$\int_{-\infty}^{\infty} \delta(x)dx = 1(x)$$

The pulse $\delta(t-\tau)$ is presented in Fig. 3.7.

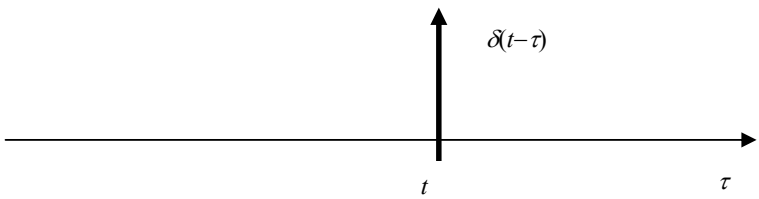

Fig. 3.7. Illustration of the Dirac's pulse

The Dirac's pulse has a very interesting property:

$$\int_{-\infty}^{\infty} f(\tau)\delta(t-\tau)d\tau = f(t). \tag{3.42}$$

If the Dirac's pulse enters a linear circuit then so called *weighting function* $h(t-\tau)$ appears at the circuit output. Therefore, since the circuit is linear, what implies homogenity and additivity, the following steps presented in the Fig. 3.8 are true:

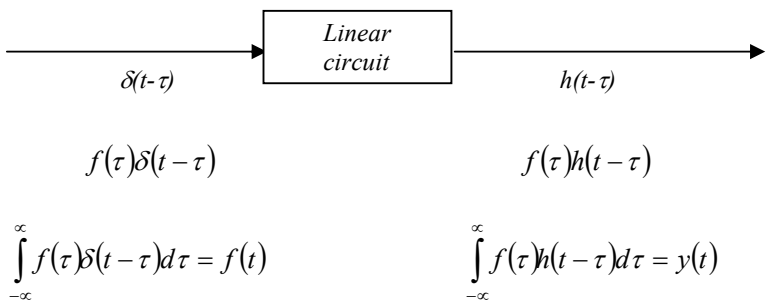

Fig. 3.8. Processing of the continuous signals

Therefore, if $f(t)$ is the circuit input signal then the output signal $y(t)$ is a convolution of the function $f(\tau)$ and the weighting function $h(t-\tau)$.

One may observe that if:

for $\tau < 0$, $f(\tau) = 0$

and if for $t-\tau < 0$, $h(t-\tau) = 0$, then:

$$y(t) = \int_0^t f(\tau)h(t-\tau)d\tau = \int_0^t f(t-\tau)h(\tau)d\tau\,. \tag{3.43}$$

3.5.2. FOURIER INTEGRAL AND FOURIER TRANSFORM

Fourier series, being so useful in processing of the periodic signal, must be modified, if it comes to non-periodic signals. This modification is based on exponential representation of sine/cosine functions, and the assumption, that it is a semi periodic signal of the period T_W being equal to infinity. It leads to the following relation, which is a Fourier transform. It is a spectral representation, or a frequency domain representation of the time domain signal $f(\tau)$:

$$F(j\omega) = \int_{-\infty}^{\infty} f(\tau)e^{-j\omega\tau}d\tau\,. \tag{3.44}$$

The reversed process called the Inverse Fourier Transform shows how to determine the time domain signal $f(\tau)$ for the given spectral signal $F(j\omega)$:

$$f(\tau) = \left(\frac{1}{2\pi}\right)\int_{-\infty}^{\infty} F(j\omega)e^{j\omega\tau}d\omega. \tag{3.45}$$

Relations between the time and frequency domain signals are given in any mathematical manual. However, some more frequently used relations are given below.

$$f(\tau) \Rightarrow F(j\omega)$$

$$1(\tau)e^{-a\tau} \Rightarrow \frac{1}{a+j\omega}$$

$$f(a\tau) \Rightarrow \left(\frac{1}{a}\right)F\left(\frac{j\omega}{a}\right)$$

$$f(\tau - t_0) \Rightarrow e^{-j\omega t_0}F(j\omega)$$

$$f\left(\tau e^{-j\omega_0\tau}\right) \Rightarrow F[j(\omega-\omega_0)]$$

$$\frac{df(\tau)}{d\tau} \Rightarrow j\omega F(j\omega)$$

$$\int_0^t f(\tau)h(t-\tau)d\tau \Rightarrow F(j\omega)H(j\omega)$$

$$h(\tau) \Rightarrow H(j\omega)$$

The spectral representation $H(j\omega)$ of a weighting function $h(\tau)$ is called a Fourier domain transfer function.

3.5.3. LAPLACE TRANSFORM

The Fourier transform has a limitation, because the time domain function must meet the following condition:

$$\int_{-\infty}^{\infty} |f(\tau)| d\tau < \infty .$$

To avoid it the imaginary operator $j\omega$ may be replaced by the complex operator s. However, it imposes another limitation, because the time domain function $f(\tau)$ must be zero for $\tau < 0$. As a result one gets the Laplace representation of the time domain function.

For the majority of the time domain functions, there is a very simple relation between the Fourier representation and the Laplace representation. It is just by replacing the Fourier operator $j\omega$ by the Laplace operator s. Therefore:

$$F(s) = \int_{0}^{\infty} f(\tau) e^{-s\tau} d\tau . \tag{3.46}$$

It leads to the following basic relations:

$$f(\tau) \Rightarrow F(s)$$

$$f(\tau - t_0) \Rightarrow e^{-st_0} F(s)$$

$$\left(\frac{df(\tau)}{d\tau} \right) \Rightarrow sF(s)$$

$$\int_{0}^{t} f(\tau) d\tau \Rightarrow \left(\frac{1}{s} \right) F(s)$$

$$\int_{0}^{t} f(\tau) h(t - \tau) d\tau \Rightarrow F(s) H(s)$$

$$h(\tau) \Rightarrow H(s)$$

The Laplace function $H(s)$, which is a Laplace transform of the weighting function $h(\tau)$, is called a Laplace transfer function of the linear continuous system.

3.5.4. DISCRETE SIGNALS AND LAURENT'S TRANSFORM

In cases of continuous non-periodic signals the Dirac's pulse plays a special role. For discrete signals such a role plays the unit pulse, presented in Fig. 3.9.

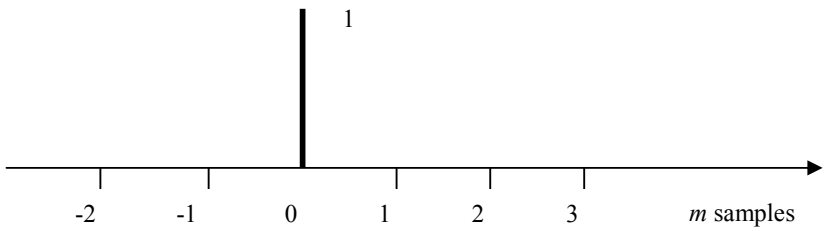

Fig. 3.9. Illustration of the unit pulse $\delta^*(m)$

The unit pulse is $\delta^*(m)=0$ for $m\neq 0$, and $\delta^*(m)=1$ for $m=0$.

A discrete signal is a train of time-shifted pulses:

$$f(n)=\sum_{m=-\infty}^{\infty} f(m)\delta^*(n-m). \tag{3.47}$$

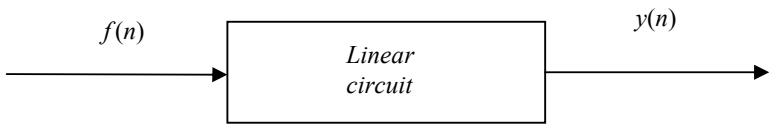

Fig. 3.10. Processing of a discrete signal

If a train of pulses enters a linear processing block, like in the Fig. 3.6, then the output is described by a formula:

$$y(n)=\sum_{m=-\infty}^{\infty} f(m)h(n-m), \tag{3.48}$$

where: $h(m)$ is a discrete weighting function, being an output of the block if the input is a unit pulse $\delta^*(m)$.

Equation (3.48) is a discrete convolution of the signals f and h.

If for $m<0$ the function $f(m)=0$ and for $n-m<0$ the weighting function $h(n-m)=0$, then:

$$y(n)=\sum_{m=0}^{n} f(m)h(n-m). \tag{3.49}$$

However, it is possible to convert the discrete function *y(n)* into an equivalent continuous function *y*(*t*), according to:

$$y(n)T_S = T_S \sum_{m=0}^{n} f(m)h(n-m) \approx \int_0^{nT_S} f(\tau)h(t-\tau)d\tau = y(nT_S) = y(t). \tag{3.50}$$

what gives a link between the sampled signal and the continuous signal.

The spectrum of the sampled signal *f*(*n*) may be described in the following form:

$$F(j\omega) = \sum_{m=-\infty}^{\infty} f(m)e^{-mT_S(j\omega)}. \tag{3.51}$$

The spectrum of the output function *y*(*n*) becomes:

$$Y(j\omega) = \sum_{m=-\infty}^{\infty} f(m)h(n-m)e^{-mT_S(j\omega)} = F(j\omega)H(j\omega). \tag{3.52}$$

However, on the ground of continuous representation of a sampled signal (3.50) one may present the spectrum of a sampled signal by almost equivalent spectrum of a continuous signal:

$$Y(j\omega) \approx \left(\frac{1}{T_S}\right) F(j\omega)H(j\omega). \tag{3.53}$$

where: $F(j\omega)$ and $H(j\omega)$ are spectra of the continuous input signal and the block continuous weighting function, respectively.

Discrete signals may be well represented by the Laurent's "z" transform:

$$f(n) = \sum_{m=-\infty}^{\infty} f(m)\delta^*(n-m).$$

Thus the Laplace transform of the sampled signal becomes:

$$F(s) = \sum_{m=0}^{n} f(m)e^{-msT_S}. \tag{3.54}$$

Now substituting

$$e^{sT_S} = z$$

one obtains:

$$F(z) = \sum_{m=0}^{n} f(m)z^{-m} \tag{3.55}$$

and consequently:

$$Y(z) = \sum_{m=0}^{n} f(m)h(n-m)z^{-m} = F(z)H(z) \tag{3.56}$$

Some more often used z-transform relations are as follows:

$$f(n) \Rightarrow F(z)$$
$$f(n-1) \Rightarrow z^{-1}F(z)$$
$$f(n-k) \Rightarrow z^{-k}F(z)$$
$$\sum_{m=0}^{n} f(m)h(n-m) \Rightarrow F(z)H(z)$$
$$h(n) \Rightarrow H(z)$$

3.6. DISCRETE INTEGRATION AND SIMULATION OF TRANSFER FUNCTIONS

Integration in the time domain is given by the formula:

$$y(t) = \int_0^t f(\tau)d\tau \,.$$

In the Laplace domain the integration representation becomes:

$$Y(s) = \left(\frac{1}{s}\right)F(s).$$

The discrete integration of the sampled signal may be done in several ways.

3.6.1. EULER'S METHOD OF INTEGRATION

The simplest formula of digital integration is described by:

$$y(n) = y(n-1) + T_S f(n-1) \tag{3.57}$$

Thus the *z-transform* of (3.57) is:

$$Y(z) = z^{-1}Y(z) + T_S z^{-1}F(z). \tag{3.58}$$

Therefore:

$$Y(z)=\left(\frac{T_S z^{-1}}{1-z^{-1}}\right)F(z). \tag{3.59}$$

This enables to present the process of integration in time domain, Laplace domain and *"z"* domain:

$$\int_0^t f(\tau)d\tau \Rightarrow \left(\frac{1}{s}\right)F(s)\Rightarrow\left(\frac{T_S z^{-1}}{1-z^{-1}}\right)F(z) \tag{3.60}$$

Therefore, the transfer function *G(s)* may be replaced by the digital form:

$$G(s)\Rightarrow G(x), \tag{3.61}$$

where: $x=\dfrac{1-z^{-1}}{T_S z^{-1}}$.

Graphical illustration of the integration process according to (3.57) is given in Fig. 3.11.

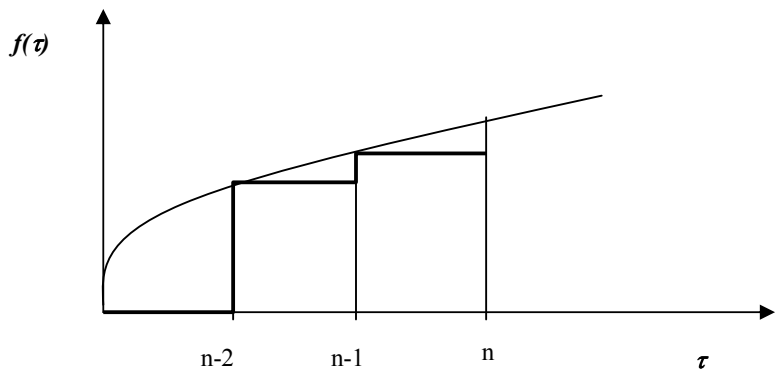

Fig. 3.11. Graphical representation of the formula (3.57)

The basic Euler's method may be modified, if in (3.55) *f*(*n*) is replaced by *f*(*n*-1). Then the formula (3.59) becomes:

$$Y(z)=\left(\frac{T_S}{1-z^{-1}}\right)F(z). \tag{3.62}$$

This method may be graphically presented in Fig. 3.12.

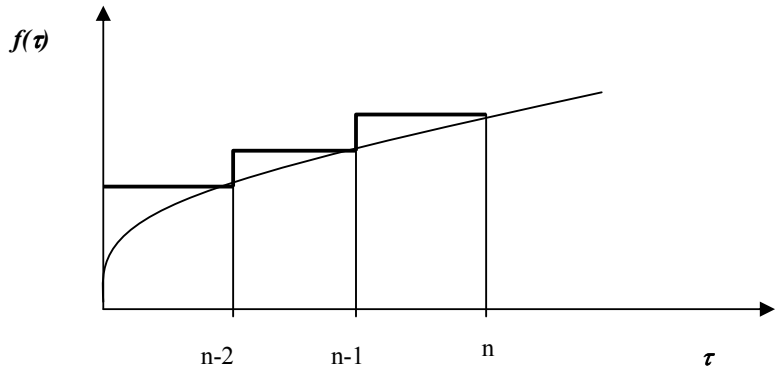

Fig. 3.12. Graphical representation of the formula (3.62)

3.6.2. TRAPEZOIDAL (TUSTIN'S) METHOD OF INTEGRATION

Euler's method of integration may be interpreted as summation of rectangles, which represent the function $f(\tau)$ in each sampling period. To improve the accuracy of integration one may represent it as a trapezoid, what leads to the formula:

$$y(n) = y(n-1) + 0.5T_S\left[f(n) + f(n-1)\right], \tag{3.63}$$

and, in the Z domain:

$$Y(z) = 0.5T_S\left(\frac{1+z^{-1}}{1-z^{-1}}\right)F(z)\,. \tag{3.64}$$

3.6.3. ADAMS – MOULTON FORMULA OF INTEGRATION

Several alternative, more accurate (but less frequently used) formulas have been developed. Among them there is an Adams–Moulton formula of integration, which is based on the basic relation:

$$y(n) = y(n-1) + \left(\frac{T_S}{12}\right)\left[5f(n) + 8f(n-1) - f(n-2)\right], \tag{3.65}$$

what gives the following *z-transform* relationship:

$$Y(z) = \left(\frac{T_S}{12}\right)\left(\frac{5+8z^{-1}-z^{-2}}{1-z^{-1}}\right)F(z)\,. \tag{3.66}$$

The discrete formulas of integration enable to transform a continuous transfer function $Y(s)$ in Laplace domain into a digital expression, by simple replacement of the Laplace integration operator s^{-1} by one of the discrete equivalents:

$$s^{-1} \Rightarrow \frac{T_S z^{-1}}{1 - z^{-1}}$$

$$s^{-1} \Rightarrow \frac{T_S}{1 - z^{-1}}$$

$$s^{-1} \Rightarrow 0.5 T_S \left(\frac{1 + z^{-1}}{1 - z^{-1}} \right)$$

$$s^{-1} \Rightarrow \left(\frac{T_S}{12} \right) \left(\frac{5 + 8z^{-1} - z^{-2}}{1 - z^{-1}} \right)$$

This process may be illustrated by a very simple example.

The Laplace domain transfer function of a continuous processing block is given by an expression:

$$H(s) = \frac{Y(s)}{F(S)} = \frac{a_0}{b_1 s + 1} = \frac{a_0 s^{-1}}{b_1 + s^{-1}}$$

Now, substituting the Euler's operator of integration:

$$s^{-1} \Rightarrow \frac{T_S z^{-1}}{1 - z^{-1}}$$

one gets:

$$H(z) = \frac{Y(z)}{F(z)} = \frac{a_0 T_S z^{-1}}{b_1 + (T_S - b_1) z^{-1}}.$$

Therefore:

$$Y(z) = \left(\frac{1}{b_1} \right) \left[(b_1 - T_S) z^{-1} Y(z) + a_0 T_S z^{-1} F(z) \right].$$

Since multiplication by z^{-1} in the z domain corresponds to the delay by one sample in the time domain, thus the calculation of $y(n)$ may be done according to the formula:

$$y(n) = \frac{b_1 - T_S}{b_1} y(n-1) + \frac{a_0 T_S}{b_1} f(n-1).$$

Processing of the transfer function by means of integration operators can also be seen as a very efficient tool of infinite impulse response digital filters design.

4. DIGITAL FILTERS

4.1. GENERAL CONSIDERATIONS

Apart from analog antialiasing filtering described in Section 2, the sampled signals are also quite frequently subjected to further digital filtering, with the aim to extract signal components carrying the information important from the protection task viewpoint. The digital filters, which are symbolically presented in Fig. 4.1, are of two kinds: Infinite Impulse Response (IIR) filters and Finite Impulse Response (FIR) filters. The former are units, in which a single pulse at the input $f(n) = \delta^*(n)$ generates the output $y(n)$, which lasts for ever. The FIR filters are the ones, in which the single pulse at the input generates the output which lasts only as long as the data window duration.

Fig. 4.1. Digital filter

The IIR filters are in fact digital versions of the analog linear filters, which are always infinite input response in nature. The digital ones process the input signal in the following way:

$$y(n) = a_p f(n-p) + \ldots + a_1 f(n-1) + a_0 f(n) - b_r y(n-r) - \ldots - b_1 y(n-1). \tag{4.1}$$

Taking the z transform of the (4.1) one yields:

$$Y(z) = F(z)\sum_{h=0}^{p} a_h z^{-h} - Y(z)\sum_{h=1}^{r} b_h z^{-h}. \tag{4.2}$$

Therefore, the transfer function of the filter becomes:

$$H(z) = \frac{Y(z)}{F(z)} = \frac{\sum_{h=0}^{p} a_h z^{-h}}{1 + \sum_{h=1}^{r} b_h z^{-h}}. \tag{4.3}$$

Remembering that if one takes the Fourier transform to calculate the spectrum of the filter the operator z^{-1} corresponds to $\exp(-j\omega T_S)$ and the Fourier transform of the filter becomes:

$$H(j\omega) = \frac{\sum_{h=0}^{p} a_h \exp(-jh\omega T_S)}{1 + \sum_{h=1}^{r} b_h \exp(-jh\omega T_S)}. \tag{4.4}$$

The FIR filters process the input signal according to:

$$y(p) = a_p f(n-p) + ... + a_1 f(n-1) + a_0 f(n), \tag{4.5}$$

where, if T_w is a data window duration, and T_S is sampling period, $(p+1)T_S = T_w$.

Therefore the transfer function $H(z)$ of such a filter becomes:

$$H(z) = \sum_{k=0}^{p} a_k z^{-k} \tag{4.6}$$

and the Fourier transform, representing its spectrum, may be expressed in the following way:

$$H(j\omega) = \sum_{k=0}^{p} a_k \exp(-jk\omega T_S). \tag{4.7}$$

4.2. INFINITE IMPULSE RESPONSE FILTERS

All the analog linear filters have infinite impulse response $h(\tau)$. Typical spectral characteristics of the filters are: low pass, band pass, low stop and band stop.

Design of the digital IIR filters usually begins with the typical approximation of the low pass (the most common) filter. Among typical known approximations the best are: Butterworth's, Chebyschev's and Bessel's , each of them may be of various orders. The transfer functions of the second and third order approximations are given in the Table 4.1.

The spectra of all typical approximations have the cut off angular frequency $\omega_c = 1$. One may observe that the better spectral characteristic (possibly narrow transition band) the longer settling time of the step pulse response.

The first step in designing of any IIR filter is to choose a typical approximation and its transfer function $H(s)$. Then the procedure depends on the type of the filter, which is to be designed. It is described in the following paragraphs.

Table 4.1. Typical approximations of LP filters

Order	Butterworth's	Chebyshev's	Bessel's
II	$\frac{1}{s^2 + s\sqrt{2} + 1}$	$\frac{1{,}431}{s^2 + 1{,}421s + 1{,}516}$	$\frac{3}{s^2 + 3s + 3}$
III	$\frac{1}{s^3 + 2s^2 + 2s + 1}$	$\frac{0{,}716}{s^3 + 1{,}253s^2 + 1{,}535s + 0{,}716}$	$\frac{15}{s^3 + 6s^2 + 15s + 15}$

4.2.1. DESIGN OF THE LOW PASS FILTER WITH THE CUT OFF FREQUENCY Ω_{CA}

The typical transfer function with the cut off frequency ω_c is selected. Then the Laplace operator in the transfer function s is replaced by the modified operator s_1:

$$s \Rightarrow \left(\frac{\omega_c}{\omega_{ca}}\right) s_1 ,$$

where: ω_{ca} is the required cut off frequency of the designed filter.

If we choose the one of the standard transfer functions like the ones presented in Table 4.1, then the value of $\omega_c = 1$.

For example, if we select a Bessel's approximation of the second order then the transfer function of the designed filter, which is to have the cut off frequency ω_{ca}, becomes:

$$H_1(s_1) = \frac{3}{\left(\frac{1}{\omega_{ca}}\right)^2 s_1^2 + 3\left(\frac{1}{\omega_{ca}}\right) s_1 + 3} .$$

The digital transfer function of the filter is then obtained by substituting the Laplace operator by one of known discrete equivalents of differentiation (inverse of the integration operand).

4.2.2. HIGH PASS FILTER WITH THE CUT OFF FREQUENCY Ω_{CB}

In order to obtain a high pass filter the Laplace operator in the basic transfer function s is to be replaced by the modified operator s_1:

$$s \Rightarrow \left(\frac{\omega_{cb}}{\omega_c}\right)\left(\frac{1}{s_1}\right).$$

Therefore, the transfer function of the Bessel's second order approximation would be:

$$H_1(s_1) = \frac{3s_1^2}{\omega_{cb}^2 + 3\omega_{cb}s_1 + 3s_1^2}.$$

Again, the digital transfer function of the filter is then obtained by substituting the Laplace operator by one of known discrete equivalents of differentiation/integration.

4.2.3. BAND PASS FILTER WITH CUT OFF FREQUENCIES Ω_{C1} AND Ω_{C2}

The low pass region of the low pass filter is to be shifted to the band pass region. It can be done if the Laplace operator s in the low pass transfer function is replaced by the modified operator s_1:

$$s \Rightarrow \frac{1}{B}\left(s_1 + \frac{\omega_0^2}{s_1}\right),$$

where: B and ω_0 are coefficients which are to be calculated to match the desired band pass spectrum. The conditions are the following:
If $s=j\omega_c$, then $s_1=\omega_{c1}$;
If $s=-j\omega_c$, then $s_1=\omega_{c2}$.
Substituting it to the formula of the modified Laplace operator one gets:

$$B\omega_c = \frac{\omega_{c1}^2 - \omega_0^2}{\omega_{c1}} \qquad \text{and} \qquad -B\omega_c = \frac{\omega_{c2}^2 - \omega_0^2}{\omega_{c2}}.$$

It enables to calculate the coefficient B, which is:

$$B = \frac{\omega_{c1} - \omega_{c2}}{\omega_c},$$

and the coefficient ω_0, which is:

$$\omega_0 = \sqrt{\omega_{c1}\omega_{c2}}.$$

Knowing the coefficients B and ω_0 one may now substitute it to the transfer function. If the starting point was the Bessel's second order low pass approximation, then the band pass transfer function becomes:

$$H_1(s_1) = \frac{3}{\left(\frac{1}{B}\right)^2\left(s_1 + \frac{\omega_0^2}{s_1}\right) + 3\left(\frac{1}{B}\right)\left(s_1 + \frac{\omega_0^2}{s_1}\right) + 3}.$$

It leads to the final formula:

$$H_1(s_1) = \frac{a_2 s_1^2}{b_4 s_1^4 + b_3 s_1^3 + b_2 s_1^2 + b_1 s_1 + b_0},$$

where: a_2, b_0, b_1, b_2, b_3, b_4 are coefficients, which result from the transformation of the previous formula.

4.2.4. BAND STOP FILTER WITH CUT OFF FREQUENCIES Ω_{C1} AND Ω_{C2}

The procedure is performed in two steps. The first one transfers the low pass basic transfer function into the high pass transfer function. It is done by substituting:

$$s \Rightarrow \frac{1}{s_1}.$$

Then in place of s_1 one substitutes the operator s_2:

$$s_1 = \frac{B s_2}{s_2^2 + \omega_0^2}.$$

Calculation of the coefficients B and ω_0 are identical as in case of the band pass filter presented in Section 4.3.3.

If the final Laplace transform of the filter is determined, one has to transfer it into the z domain. This may be done by means of introduction of the integration operator. If for example it is the low pass transfer function based on the Bessel's approximation of the second order, the Laplace transfer function is:

$$H_1(s_1) = \frac{3\omega_{ca}^2 s_1^{-2}}{1 + 3\omega_{ca} s_1^{-1} + 3\omega_{ca}^2 s_1^{-2}}.$$

Now in place of s_1^{-1} one has to introduce the integration operator. If it is the Euler's operator:

$$s_1^{-1} \Rightarrow \frac{T_S}{1 - z^{-1}},$$

after the substitution the *z–domain* transfer function becomes:

$$H_1(z)=\frac{3\omega_{ca}^2\left(\frac{T_S}{1-z^{-1}}\right)^2}{1+3\omega_{ca}\left(\frac{T_S}{1-z^{-1}}\right)+3\omega_{ca}^2\left(\frac{T_S}{1-z^{-1}}\right)^{-2}}.$$

Eventually the transfer function has the shape:

$$H_1(z)=\frac{a_2z^{-2}+a_1z^{-1}+a_0}{b_2z^{-2}+b_1z^{-1}+1}=\frac{Y(z)}{F(z)}.$$

Remembering that multiplication by z^{-1} in the *z-domain* is a delay of one sampling period T_S in the time domain, the filter is given by the following algorithm:

$$y(n)=a_0f(n)+a_1f(n-1)+a_2f(n-2)-b_1y(n-1)-b_2y(n-2).$$

4.3. FINITE IMPULSE RESPONSE FILTERS

4.3.1. GENERAL CONSIDERATIONS

An illustration of the signals in case of the FIR filter is given in Fig. 4.2.

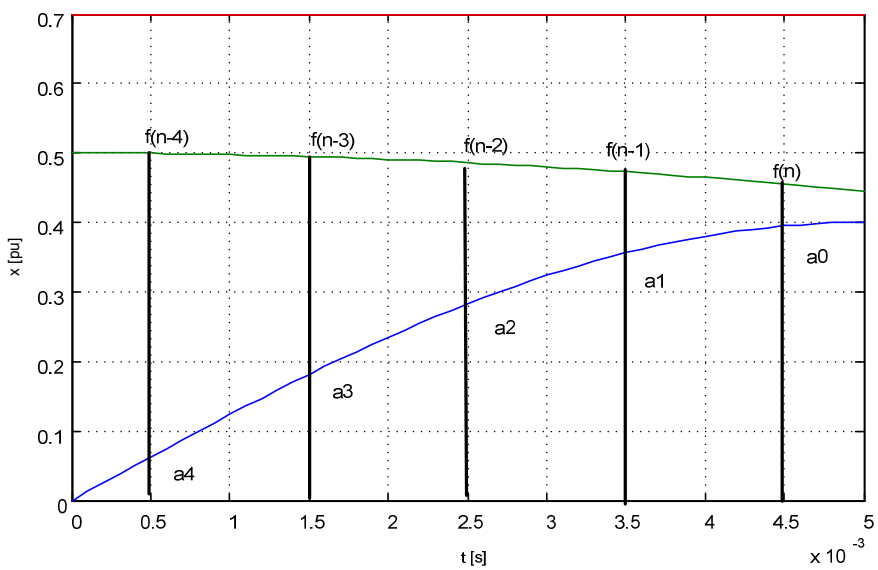

Fig. 4.2. Illustration of the signals of the FIR filter

Generally, the duration of the data window is $T_w = (p+1)T_S$. In the Fig. 4.2 the duration of the data window is $5T_S$. Therefore the output of the data window becomes:

$$y(n) = \sum_{k=0}^{p} a_k f(n-k). \tag{4.8}$$

Deriving the *z* transform of the (4.8) one gets:

$$Y(z) = F^*(z) \sum_{k=0}^{p} a_k z^{-k} \tag{4.9}$$

and the *z – domain* transfer function is:

$$H(z) = \frac{Y(z)}{F(z)} = \sum_{k=0}^{p} a_k z^{-k}. \tag{4.10}$$

Taking the Fourier transform to convert it to the frequency domain one gets:

$$H(j\omega) = \sum_{k=0}^{p} a_k \exp(-j\omega k T_S). \tag{4.11}$$

An example of the digital filter spectrum is presented in Fig. 4.3.

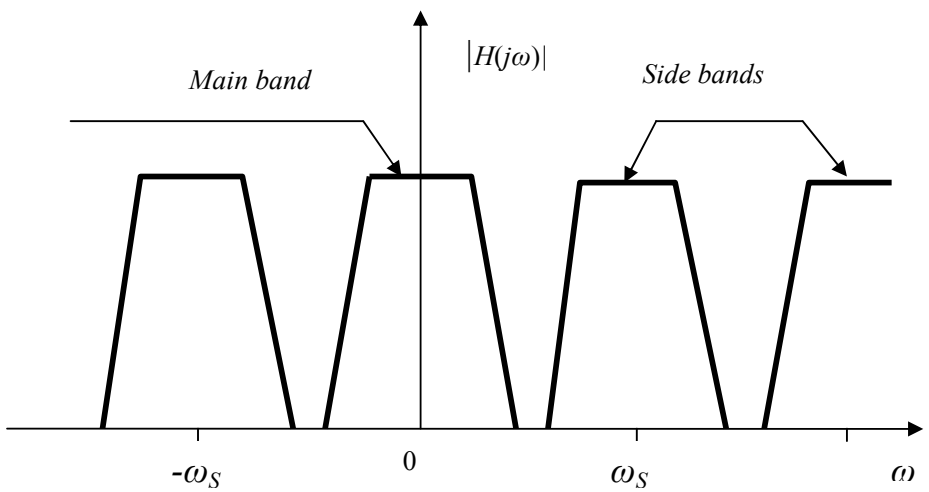

Fig. 4.3. Example of the spectrum of the FR filter transfer function

Simplified calculation of the main band of the spectrum may be done through calculating the convolution of the continues functions $f(\tau)$ and $h(\tau)$:

$$T_S y(n) = T_S \sum_{k=0}^{p} a_k f(n-k) \approx \int_{t-T_W}^{t} f(\tau) h(t-\tau) d\tau \,. \tag{4.12}$$

Therefore:

$$y(n) \approx \frac{1}{T_S} \int_{t-T_W}^{t} f(\tau) h(t-\tau) d\tau \,,$$

or taking the Fourier transform of (4.12):

$$Y(j\omega) \approx \frac{1}{T_S} F(j\omega) H(j\omega) \tag{4.13}$$

and:

$$H(j\omega) \approx \frac{1}{T_S} \int_{t-T_w}^{t} h(\tau) e^{-j\omega\tau} d\tau = \frac{1}{T_S} \int_{0}^{T_w} h(\tau) e^{-j\omega\tau} d\tau \,. \tag{4.14}$$

Therefore, the spectrum of the discrete filter – or, to be more precise, the main band of the spectrum – may be represented by the spectrum of the continuous weighting function $h(\tau)$. It often simplifies calculation of the spectrum, however it neglects the side bands. It is not a great disadvantage, because the frequency regions of sidebands are eliminated by the low pass antialiasing input filters.

Next step in simplifications of the spectrum calculation is to shift the data window, which is the impulse response $h(\tau)$ in such a way that the value of τ=0 is located in the middle of the window:

$$H(j\omega) = \frac{1}{T_S} \int_{0}^{T_w} h(\tau) \exp(-j\omega\tau) d\tau = \exp(-0.5 j\omega T_w) \left(\frac{1}{T_S} \right) \int_{-0.5T_w}^{0.5T_w} h_r(\tau) \exp(-j\omega\tau) d\tau \,, \tag{4.15}$$

where: $h_r(\tau) = h(\tau + 0.5T_w)$.

An example is shown in Fig. 4.4.

One may observe that such a shifting affects only the phase angle of the spectrum:

$$H(j\omega) = \exp(-0.5 j\omega T_w) H_r(j\omega), \tag{4.16}$$

where: $H_r(j\omega)$ – spectrum of the shifted window.

One of the advantages of shifting is that the shifted window is usually either symmetrical $h(\tau) = h(-\tau)$, or antisymmetrical $h(\tau) = -h(-\tau)$.

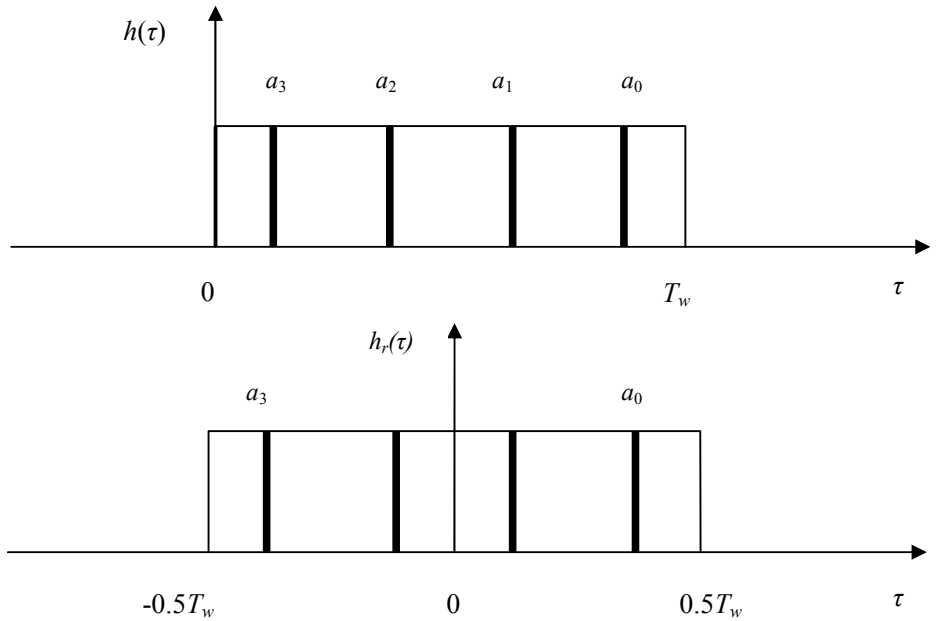

Fig. 4.4. Shifted rectangular window

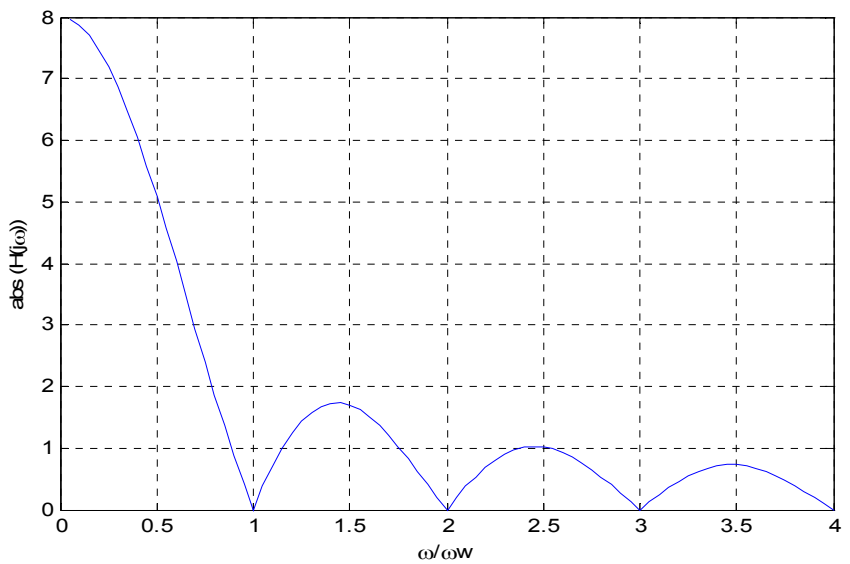

Fig. 4.5. Absolute value of the spectrum of the rectangular window; $\omega_w = 2\pi/T_w$

For symmetrical windows, the spectrum is real, but in cases of antisymmetrical ones the spectrum is imaginary, i.e.

$$H_r(j\omega) \approx \frac{1}{T_S}\int_{-0.5T_w}^{0.5T_w} h_r(\tau)\exp(-j\omega\tau)d\tau = \frac{1}{T_S}\int_{-0.5T_w}^{0.5T_w}\cos(\omega\tau)d\tau = \left(\frac{T_w}{T_S}\right)\frac{\sin(0.5\omega T_w)}{(0.5\omega T_w)} \quad (4.17)$$

or:

$$H_r(j\omega) = (p+1)Sa(0.5\omega T_w). \quad (4.18)$$

The spectrum of rectangle data window is presented in Fig. 4.5.
The numerical calculation of the filter output is as follows:

$$y(n) = \sum_{k=0}^{p} f(n-k). \quad (4.18)$$

It may be expressed in the recursive form, which is more economical numerically:

$$y(n) = y(n-1) + f(n) - f(n-p-1). \quad (4.19)$$

The characteristic shows that it is a low pass filter. However, one must bear in mind that the spectral characteristics of filters with rectangular windows show comparatively high side lobes. It is caused by the abrupt change of the windows at the instants +/- $0.5T_w$. The side lobes are greatly reduced if there is a soft change of the windows, for example if it is a triangular window, shown in Fig. 4.6.

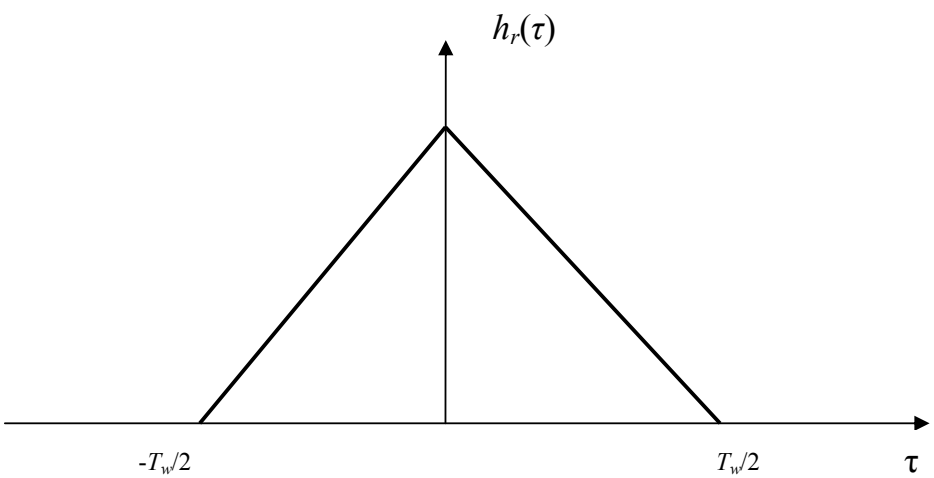

Fig. 4.6. Triangular data window

The spectrum of the triangular window presented in Fig. 4.6 is expressed by the formula:

$$H_r^*(j\omega)=\left(\frac{p+1}{2}\right)Sa^2(0.25\omega T_w) \tag{4.20}$$

and shown in Fig. 4.7.

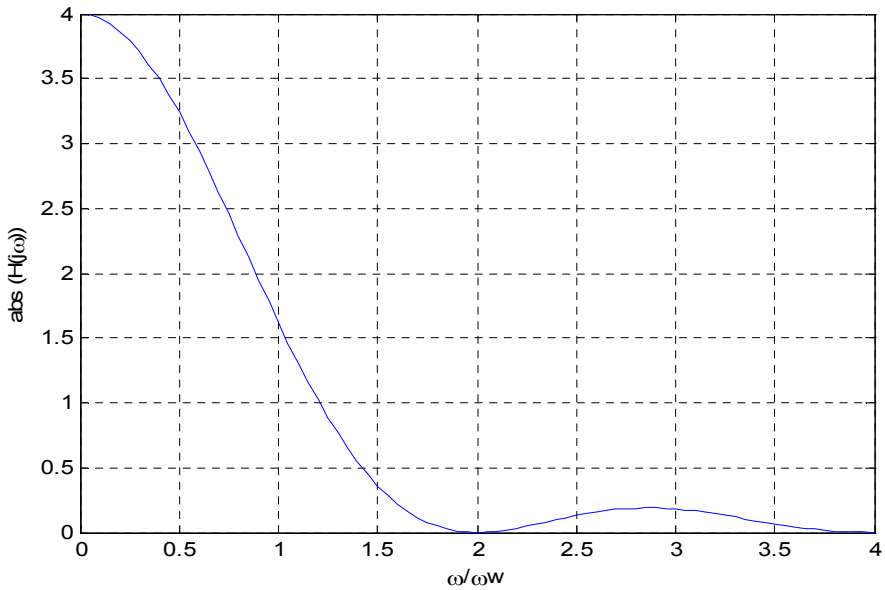

Fig. 4.7. Absolute value of the spectrum of the triangular window

4.3.2. WALSH FUNCTIONS AS DATA WINDOWS

The family of Walsh functions of the order W0, W1, W2 is presented in Fig. 4.8.
The Fourier transfer function of a filter with the *W*1 data window is:

$$H_r(j\omega)=-j(p+1)\left[\frac{1-\cos(0.5\omega T_w)}{0.5\omega T_w}\right]. \tag{4.21}$$

The Fourier transfer function of a filter with the *W2* data window is the following:

$$H_r(j\omega)=(p+1)\left[\frac{\sin(0.25\omega T_w)}{0.25\omega T_w}\right][1-\cos(0.25\omega T_w)]. \tag{4.22}$$

The spectra of the filters are presented in graphical form in Fig. 4.9 and 4.10.

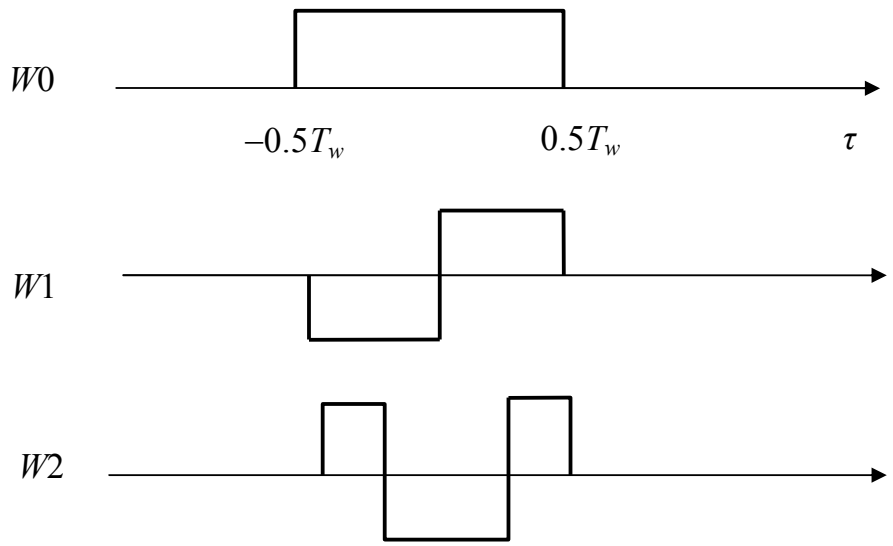

Fig. 4.8. Illustration of the Walsh functions of the 0, 1, and 2 orders

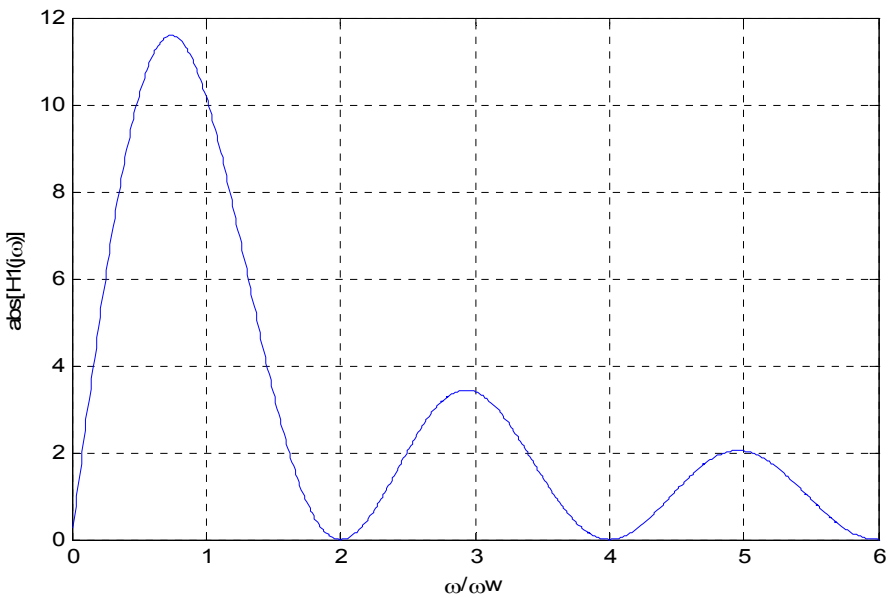

Fig. 4.9. Absolute value of the spectrum of the *W*1 data window

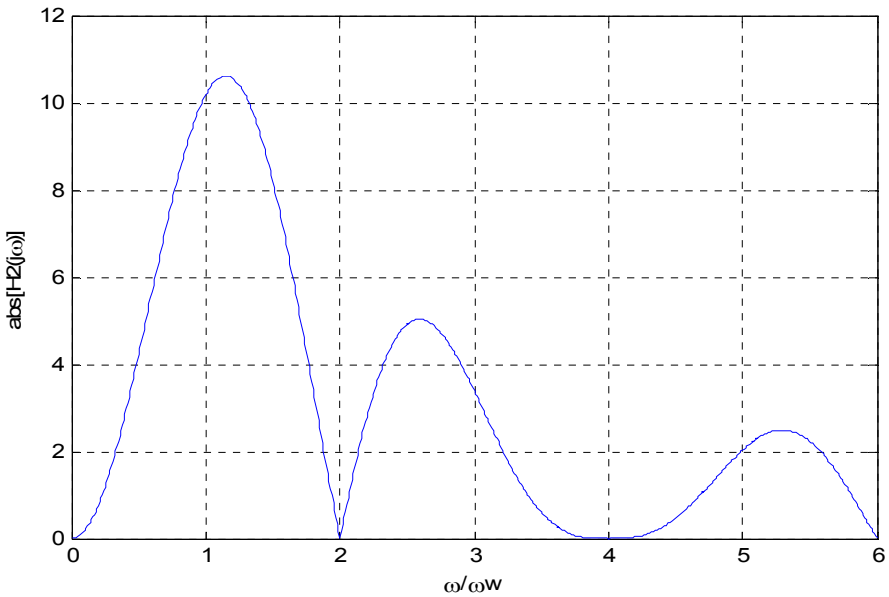

Fig. 4.10. Absolute value of the spectrum of the $W2$ data window

One may note that while the rectangular window spectrum (or in the other words the $W0$ window) represents the low pass filter), the spectra of filters with the $W1$ and $W2$ data windows represent the band pass filters. It is worthwhile to note that the spectra are mutually shifted by 90 degrees, and their absolute values for $\omega_W = \frac{2\pi}{T_w}$ are the same and equal to $0.637(p+1)$.

Digital representation of the filter with $W1$ data window is simple. If the number of samples in the window is even, it becomes:

$$y(n) = \sum_{k=0}^{0.5(p-1)} f(n-k) - \sum_{k=0.5(p+1)}^{p} f(n-k). \tag{4.23}$$

Calculation of the output of the filter with $W2$ data window – again if the number of samples is even, has the shape:

$$y(n) = -\sum_{k=0}^{0.25(p+1)-1} f(n-k) + \sum_{k=0.25(p+1)}^{0.75(p+1)-1} f(n-k) - \sum_{k=0.75(p+1)}^{p} f(n-k). \tag{4.24}$$

Both formulas (4.23) and (4.24) may be expressed also in recursive form, which are computationally more efficient.

4.3.3. SINE/COSINE FUNCTIONS AS DATA WINDOWS

In modern digital relays the FIR filters usually use the sine/cosine data windows, as shown in Fig. 4.11.

The filter coefficients are:

$$a_k = \sin\left[\omega_w (k+0.5) T_S\right] \tag{4.25}$$

$$b_k = \cos\left[\omega_w (k+0.5) T_S\right], \tag{4.26}$$

where: $\omega_w = \dfrac{2\pi}{T_w}$.

Therefore the filter algorithms become:

$$y_S(n) = \sum_{k=0}^{p} a_k f(n-k), \tag{4.27}$$

$$y_C(n) = \sum_{k=0}^{p} b_k f(n-k). \tag{4.28}$$

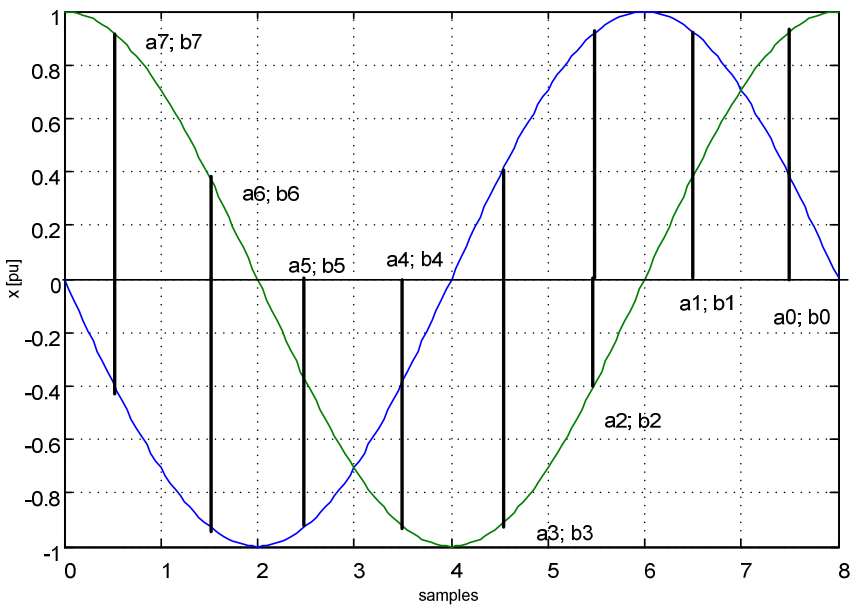

Fig. 4.11. Examples of sine/cosine data windows with 8 samples in the window

The spectra of the sine/cosine data windows are:

$$H_S(j\omega) = -j0.5(p+1)\left[Sa\frac{(\omega-\omega_w)T_w}{2} - Sa\frac{(\omega+\omega_w)T_w}{2} \right], \tag{4.29}$$

$$H_C(j\omega) = 0.5(p+1)\left[Sa\frac{(\omega-\omega_w)T_w}{2} + Sa\frac{(\omega+\omega_w)T_w}{2} \right]. \tag{4.30}$$

The spectra (4.29) and (4.30) are presented in graphical form in Fig. 4.12 and Fig. 4.13, respectively.

One may find that if the input signal is sinusoidal with the angular frequency $\omega = \omega_w$ then the absolute values of the spectra with sinusoidal and cosinusoidal data windows are the same:

$$|H_S(j\omega_w)| = |H_C(j\omega_w)| = 0.5(p+1). \tag{4.31}$$

It may noted that for $\omega = \omega_W$ filtration is exactly the same as extraction of the rotating components of the phasor. Therefore, if the input signal is purely sinusoidal, i.e. has the form

$$f(n) = F\cos(n\omega T_S - \beta)$$

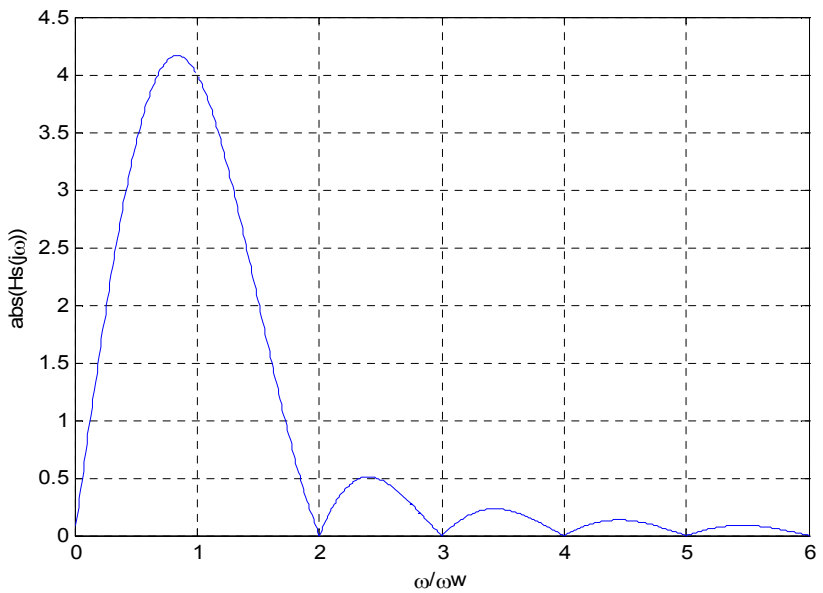

Fig. 4.12. Absolute value of spectrum of the sinusoidal data window

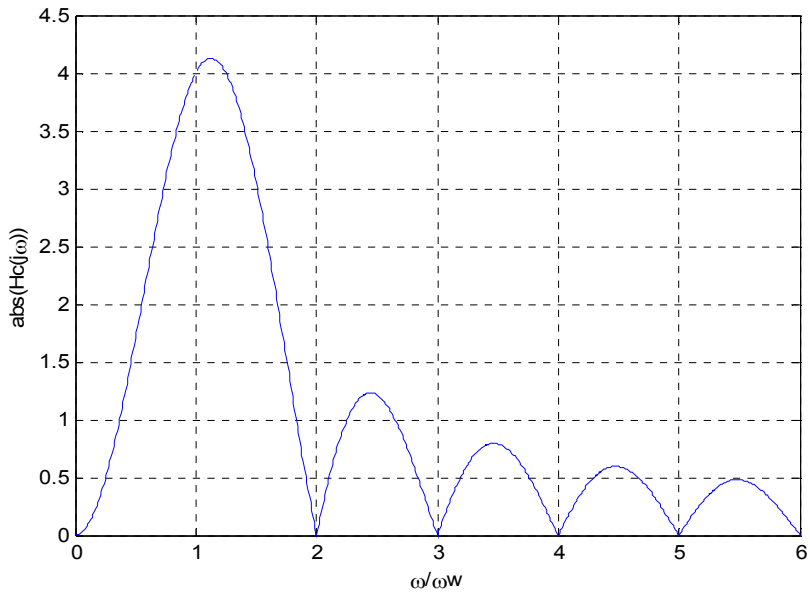

Fig. 4.13. Absolute value of spectrum of the cosinusoidal data window.

The output of the filter with sinusoidal data window becomes:

$$y_s(n) = F\left(\frac{p+1}{2}\right)\cos\left(n\omega T_S - \beta\right)$$

while for cosinusoidal data window it is:

$$y_c(n) = F\left(\frac{p+1}{2}\right)\sin\left(n\omega T_S - \beta\right).$$

It means that the outputs $y_s(n)$ and $y_c(n)$ are orthogonal.

The quality of the filters in terms of their filtering efficiency can be analysed from Fig. 4.14, where the sin/cos filters are compared with the Walsh ones. The signal *i* after the level change from 2 to 5 pu at t=0.06s is corrupted by the 3rd harmonic. The fundamental frequency component amplitude calculated from orthogonal components taken from filter outputs is accurate in case of sine and cosine windows, since both data windows reject all harmonics of the fundamental frequency. The amplitude measured with use of Walsh filters is not perfect (one can observe significant oscillations), which is due to the frequency characteristics of Walsh filters that do not fully suppress odd harmonics.

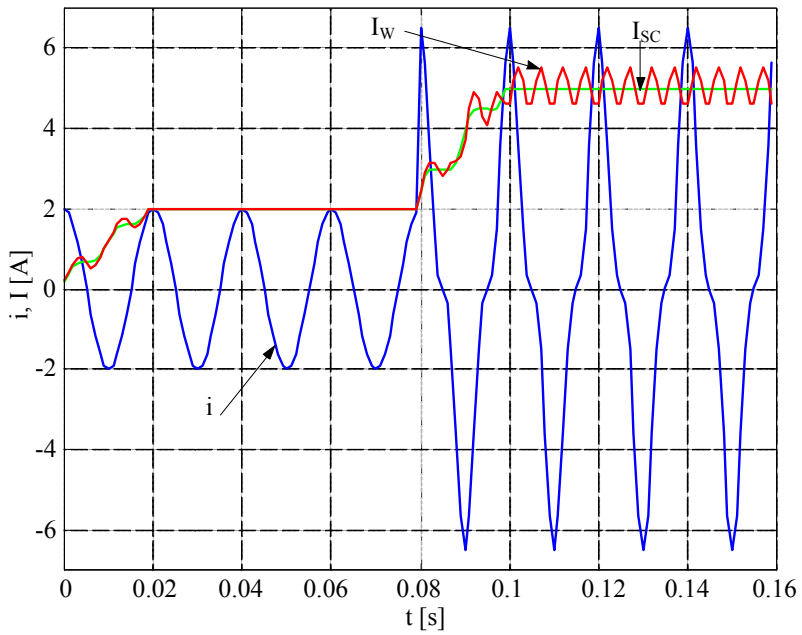

Fig. 4.14. Filtering efficiency with Walsh and sin/cos filters.

4.3.4. DATA WINDOWS FOR REQUIRED SPECTRA

If the desired spectrum of the FIR filter may be approximated by the straight line segments, the data window may be determined in an interesting way, as discussed below.

The spectrum of the continuous window $h(\tau)$ is defined by the well known formula:

$$H(j\omega) = \int_{-\infty}^{\infty} h(\tau)\exp(-j\omega\tau)d\tau\,. \tag{4.32}$$

Differentiating it twice one gets:

$$H'(j\omega) = (-j\tau)\int_{-\infty}^{\infty} h(\tau)\exp(-j\omega\tau)d\tau = (-j\tau)H(j\omega), \tag{4.33}$$

$$H''(j\omega) = -\tau^2 \int_{-\infty}^{\infty} h(\tau)\exp(-j\omega\tau)d\tau = -\tau^2 H(j\omega)\,. \tag{4.34}$$

Let's assume that the desired spectrum is triangular (Fig. 4.15a). The first and second derivative of it are presented in Fig. 4.15b and 4.15c.

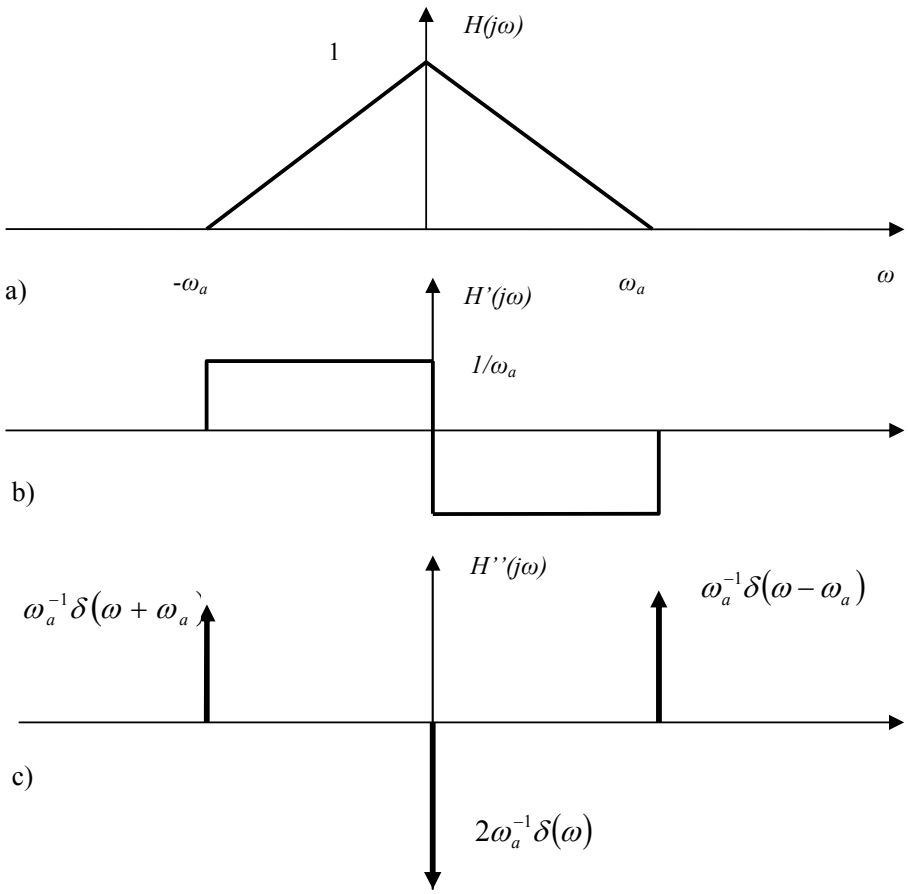

Fig. 4.15. Desired spectrum with its derivatives

The weighting function $h(\tau)$ may be determined on the ground of the value of the transfer function $H(j\omega)$ since it is the inverse Fourier transform. Therefore:

$$h(\tau)=\frac{1}{2\pi}\int_{-\infty}^{\infty}H(j\omega)\exp(j\omega\tau)d\omega. \tag{4.35}$$

Now, using (4.33) and (4.34), one may write:

$$h(\tau)=\frac{-1}{j2\pi\tau}\int H'(j\omega)\exp(j\omega\tau)d\omega \tag{4.36}$$

and:

$$h(\tau)=\frac{-1}{2\omega\tau^2}\int H''(j\omega)\exp(j\omega\tau)d\omega\,. \tag{4.37}$$

However, one may note that $H''(j\omega)$ is a sum of weighted Dirac's pulses, and there is a well known general formula:

$$\int_{-\infty}^{\infty} g(x)\delta(x-x_0)dx = g(x_0)\,. \tag{4.38}$$

Therefore, from (4.37) one may obtain the value of the window function $h(\tau)$:

$$h(\tau)=\frac{-\omega_a^{-1}}{2\pi\tau^2}\left[\exp(j\omega_a\tau)+2+\exp(-j\omega_a\tau)\right] \tag{4.39}$$

or in the trigonometric form:

$$h(\tau)=\frac{1}{\pi\tau^2\omega_a}\left[1-\cos(\omega_a\tau)\right]=\frac{\omega_a}{2\pi}Sa^2\left(\frac{\omega_a\tau}{2}\right). \tag{4.40}$$

The calculated data window is infinite, therefore $h(\tau)$ must be truncated at a certain value of τ, which will determine the duration of the data window.

4.3.5. SPECTRUM OF THE GIVEN DATA WINDOW

If the data window may be approximated by the straight lines one may use a technique which is similar to the ones described in section 4.3.4. Starting from the formula (4.35) and differentiating it twice one gets:

$$h_r'(\tau)=\frac{j\omega}{2\pi}\int_{-\infty}^{\infty}H_r(j\omega)\exp(j\omega\tau)d\tau=(j\omega)h_r(\tau), \tag{4.41}$$

$$h_r''(\tau)=\frac{-\omega^2}{2\pi}\int_{-\infty}^{\infty}H_r(j\omega)\exp(j\omega\tau)d\tau=-\omega^2h_r(\tau). \tag{4.42}$$

On the other hand, one may write:

$$\begin{aligned}H_r(j\omega)&=\int_{-\infty}^{\infty}h_r(\tau)\exp(-j\omega\tau)d\tau=\left(\frac{1}{j\omega}\right)\int_{-\infty}^{\infty}h'(\tau)\exp(-j\omega\tau)d\tau=\\&=\left(\frac{-1}{\omega^2}\right)\int_{-\infty}^{\infty}h''(\tau)\exp(-j\omega\tau)d\tau\end{aligned}\,. \tag{4.43}$$

As an example, the spectrum of the rectangular data window calculation is illustrated in Fig. 4.16.

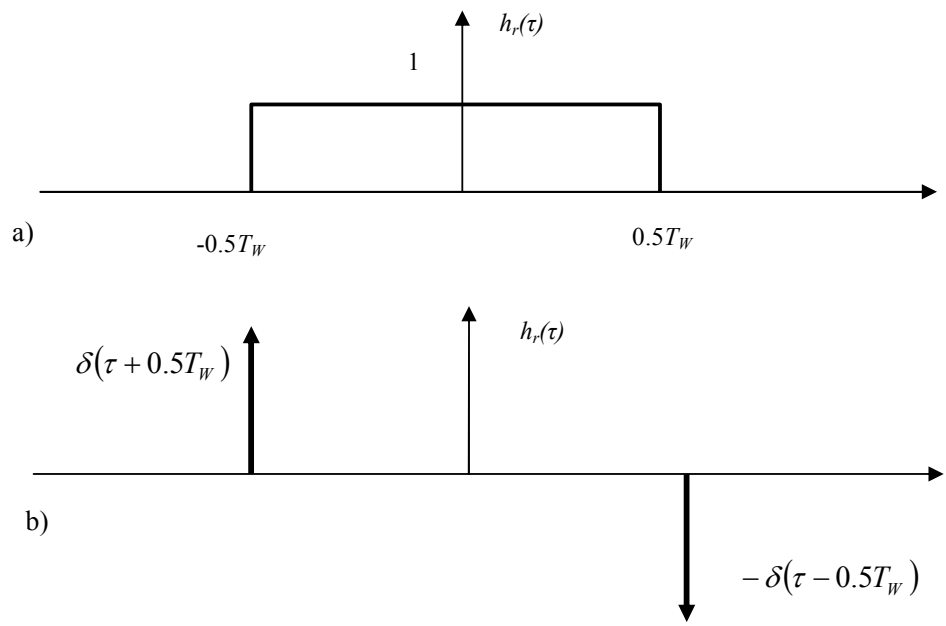

Fig. 4.16. Rectangular data window (a) and its first derivative (b)

On the ground of (4.43) one may write:

$$H_r(j\omega) = \int_{-\infty}^{\infty} h_r(\tau)\exp(-j\omega\tau)d\tau = \left(\frac{1}{j\omega}\right)\int_{-\infty}^{\infty} h_r'(\tau)\exp(-j\omega\tau).$$

Since the first derivative h_r' consists only of the Dirac's pulses then, using the formula (4.38), the spectrum may be easily calculated as:

$$H_r(j\omega) = \left(\frac{1}{j\omega}\right)(\exp(j\omega T_w) - \exp(-j\omega T_w)) = \left(\frac{2}{\omega}\right)\sin(0.5\omega T_w) = T_w Sa(0.5\omega T_w).$$

This is the spectrum of the continuous rectangular data window. The spectrum of the discrete data window becomes:

$$H_r(j\omega) = \frac{T_w}{T_S} Sa(0.5\omega T_w) = (p+1)Sa(0.5\omega T_w).$$

It is the same result as it was calculated previously with (4.17).

4.3.6. SEQUENTIAL FILTERS

Two filters connected in series are depicted in Fig. 4.17.

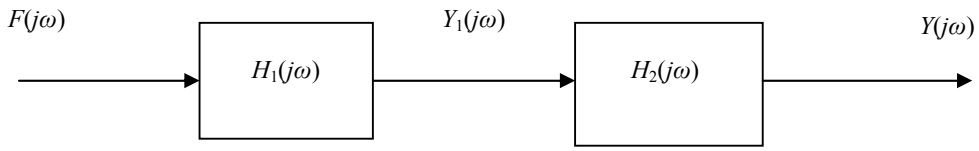

Fig. 4.17. Sequential filters

In such a case one may write:

$$Y_1(j\omega) = F(j\omega)H_1(j\omega), \tag{4.44}$$

$$Y(j\omega) = Y_1(j\omega)H_2(j\omega). \tag{4.45}$$

Therefore:

$$Y(j\omega) = F(j\omega)H_1(j\omega)H_2(j\omega). \tag{4.46}$$

and finally the resulting Fourier transfer function (spectrum) is:

$$H(j\omega) = \frac{Y(j\omega)}{F(j\omega)} = H_1(j\omega)H_2(j\omega). \tag{4.47}$$

In some cases this approach may simplify the digital algorithm of the filter with the desired spectrum. For example, two sequential filters with rectangular data windows represent a filter with the triangular data window.

5. CALCULATION OF SYMMETRICAL COMPONENTS

5.1 GENERAL CONSIDERATIONS

If the three phase sinusoidal signals are given in form of phasors, then, taking the phase L1 as a reference phase, the symmetrical components are given by the well known formulae:

$$\underline{I_0} = \frac{1}{3}\left(\underline{I_{L1}} + \underline{I_{L2}} + \underline{I_{L3}}\right),$$

$$\underline{I_1} = \frac{1}{3}\left(\underline{I_{L1}} + a\underline{I_{L2}} + a^2\underline{I_{L3}}\right), \tag{5.1}$$

$$\underline{I_2} = \frac{1}{3}\left(\underline{I_{L1}} + a^2\underline{I_{L2}} + a\underline{I_{L3}}\right),$$

where: $\underline{I_0}$, $\underline{I_1}$, $\underline{I_2}$ – phasors of symmetrical components,
$\underline{I_{L1}}$, $\underline{I_{L2}}$, $\underline{I_{L3}}$ – phasors of the three phase currents,
$a = \exp(j\pi/3)$ – coefficient shifting the signal by 120 deg.

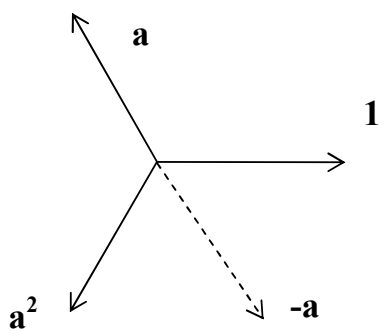

Fig. 5.1. Illustration of the complex coefficients a and a^2

If the three phase current phasors are presented by time dependent forms, one may write:

$$i_{L1}(t) = I_{L1}\sin(\omega_1 t - \beta_1)$$
$$i_{L2}(t) = I_{L2}\sin(\omega_1 t - \beta_2).$$
$$i_{L3}(t) = I_{L3}\sin(\omega_1 t - \beta_3)$$

However, one must remember that multiplication by a shifts the signal by $\lambda_1 = +\frac{2\pi}{3} = +120\,\text{deg}$ what is tantamount to the delay by $\frac{4\pi}{3} = 240\,\text{deg}$. Therefore multiplication by a^2 shifts the signal by $\lambda_2 = +\frac{4\pi}{3} = +240\,\text{deg}$, what in turn is equivalent to the delay by $\frac{2\pi}{3} = 120\,\text{deg}$. Thus:

$$a = \exp(j\frac{2\pi}{3}) = \exp\left(-j\frac{4\pi}{3}\right) = -\exp\left(-j\frac{\pi}{3}\right),$$

$$a^2 = \exp\left(j\frac{4\pi}{3}\right) = \exp\left(-j\frac{2\pi}{3}\right).$$

The phase shift in the time domain may be presented as the time delay:

$$\underline{I}\exp\left(-j\frac{2\pi}{3}\right) \Rightarrow i\left(t - \frac{T_1}{3}\right) = i\left(n - \frac{p+1}{3}\right),$$

$$\underline{I}\exp\left(-j\frac{\pi}{3}\right) \Rightarrow i\left(t - \frac{T_1}{6}\right) = i\left(n - \frac{p+1}{6}\right).$$

5.2. CALCULATION OF SYMMETRICAL COMPONENTS WITH USE OF ORTHOGONAL COMPONENTS

5.2.1. NON ROTATING ORTHOGONAL COMPONENTS

Two first coefficients of the Fourier series are non rotating phasor components. Therefore, if the fundamental component of the input signal is:

$$i(m) = I_1\cos(m\omega_1 T_S - \beta).$$

the orthogonal components are:

$$I_{1+} = I_1\cos\beta$$
$$I_{1-} = I_1\sin\beta$$

Therefore the current amplitude in the complex form is:

$$\underline{I}_1 = I_{1-} + jI_{1+}\,. \tag{5.2}$$

If the phase currents in the complex notation are expressed in the form:

$$\begin{aligned} \underline{I}_{L1} &= I_{-L1} + jI_{+L1} \\ \underline{I}_{L2} &= I_{-L2} + jI_{+L2}\,, \\ \underline{I}_{L3} &= I_{-L3} + jI_{+L3} \end{aligned} \tag{5.3}$$

then one may write:

$$\begin{aligned} \underline{I}_{L2}a &= \left(I_{-L2} + jI_{+L2}\right)\left(-0.5 + j\frac{\sqrt{3}}{2}\right) \\ \underline{I}_{L2}a^2 &= \left(I_{-L2} + jI_{+L2}\right)\left(-0.5 - j\frac{\sqrt{3}}{2}\right) \end{aligned}, \tag{5.4}$$

$$\begin{aligned} \underline{I}_{L3}a &= \left(I_{-L3} + jI_{+L3}\right)\left(-0.5 + j\frac{\sqrt{3}}{2}\right) \\ \underline{I}_{L3}a^2 &= \left(I_{-L3} + jI_{+L3}\right)\left(-0.5 - j\frac{\sqrt{3}}{2}\right) \end{aligned}. \tag{5.5}$$

Substituting (5.4) and (5.5) into (5.1) one gets the symmetrical components. However, one has to remember that the complex quantities represent amplitudes of the components and that the phase L1 is selected as a reference one.

5.2.2. ROTATING ORTHOGONAL COMPONENTS

Remembering, that in the time domain the phase shift corresponds to the time delay (as it was explained in the par. 5.1), and if the phase L_1 is selected as the basic one, one may write:

$$3i_0(t) = I_{L1}\sin(\omega_1 t - \beta_1) + I_{L2}\sin(\omega_1 t - \beta_2) + I_{L3}\sin(\omega_1 t - \beta_3), \tag{5.6}$$

$$3i_1(t) = I_{L1}\sin(\omega_1 t - \beta_1) - I_{L2}\sin(\omega_1 t - \beta_2 - \lambda_2) + I_{L3}\sin(\omega_1 t - \beta_3 - \lambda_1), \tag{5.7}$$

$$3i_2(t) = I_{L1}\sin(\omega_1 t - \beta_1) + I_{L2}\sin(\omega_1 t - \beta_2 - \lambda_1) - I_{L3}\sin(\omega_1 t - \beta_3 - \lambda_2), \tag{5.8}$$

where:

$$\lambda_1 = \omega_1 \frac{T_1}{6} = \frac{\pi}{3}$$
$$\lambda_2 = \omega_1 \frac{T_1}{3} = \frac{2\pi}{3}.$$

Now, if the orthogonal rotating components are known, one may use them to calculate symmetrical components. The lagging and leading orthogonal components of the currents in each phase are therefore given as follows:

$$\begin{aligned} i_{-L1} &= I_{L1} \sin(\omega_1 t - \beta_1) \\ i_{+L1} &= I_{L1} \cos(\omega_1 t - \beta_1) \\ i_{-L2} &= I_{L2} \sin(\omega_1 t - \beta_2) \\ i_{+L2} &= I_{L2} \cos(\omega_1 t - \beta_2) \\ i_{-L3} &= I_{L3} \sin(\omega_1 t - \beta_3) \\ i_{+L3} &= I_{L3} \cos(\omega_1 t - \beta_3) \end{aligned}. \tag{5.9}$$

Now, substituting it to the equations (5.6) – (5.8), the symmetrical components become:

$$\begin{aligned} 3i_0(t) &= i_{-L1}(t) + i_{-L2}(t) + i_{-L3}(t) \\ 3i_1(t) &= i_{-L1}(t) - 0.5\left[i_{-L2}(t) + \sqrt{3} i_{+L2}(t) + i_{-L3}(t) - \sqrt{3} i_{+L3}(t)\right] \\ 3i_2(t) &= i_{-L1}(t) - 0.5\left[i_{-L2}(t) - \sqrt{3} i_{+L2}(t) + i_{-L3}(t) + \sqrt{3} i_{+L3}(t)\right] \end{aligned}. \tag{5.10}$$

Therefore in the digital form it is:

$$\begin{aligned} 3i_0(n) &= i_{-L1}(n) + i_{-L2}(n) + i_{-L3}(n) \\ 3i_1(n) &= i_{-L1}(n) - 0.5\left[i_{-L2}(n) + \sqrt{3} i_{+L2}(n) + i_{-L3}(n) - \sqrt{3} i_{+L3}(n)\right] \\ 3i_2(n) &= i_{-L1}(n) - 0.5\left[i_{-L2}(n) - \sqrt{3} i_{+L2}(n) + i_{-L3}(n) + \sqrt{3} i_{+L3}(n)\right] \end{aligned}. \tag{5.11}$$

Thus, instantaneous values of the symmetrical components are determined on the ground of calculated orthogonal components of the three phase currents. In case of voltages the formulae are identical.

In Figs. 5.2 and 5.3 an illustration of symmetrical components calculation is presented for a case of simulated three-phase fault on a HV transmission line. One can see that both before and after fault inception the positive sequence component is present only (Fig. 5.2), which is correct since the situation is symmetrical. In real case, when CT secondary currents are processed (Fig. 5.3), the signals become transiently saturated. Thus, the other sequence components also appear, and the calculated positive sequence current is at the beginning lower than on the CT primary side.

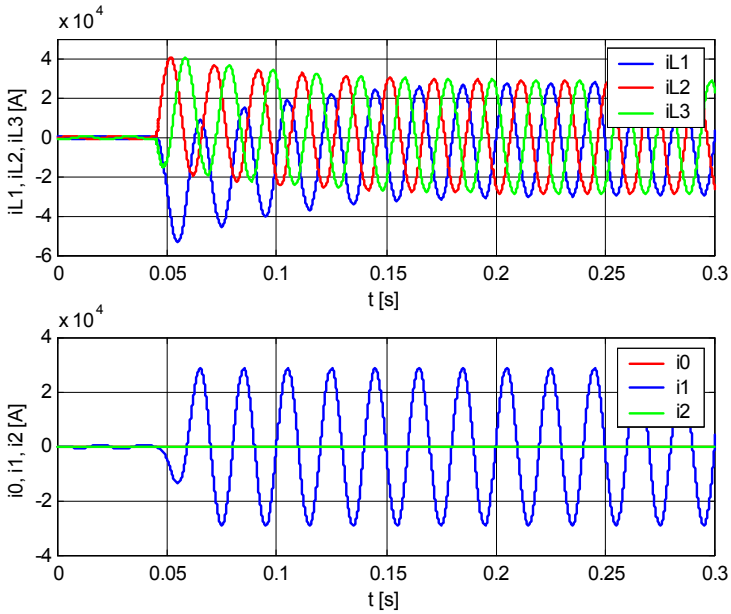

Fig. 5.2. Extraction of symmetrical components with eq. (5.11),
orthogonal components obtained with full cycle Fourier filters; CT primary signals

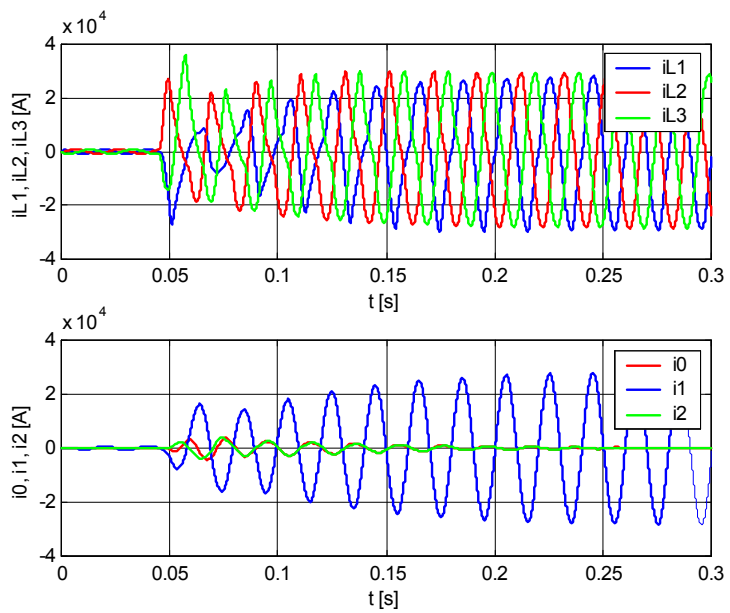

Fig. 5.3. Extraction of symmetrical components with eq. (5.11),
orthogonal components obtained with full cycle Fourier filters; CT secondary signals

5.3. CALCULATION OF SYMMETRICAL COMPONENTS BY MEANS OF SIGNAL DELAYING

Another way to calculate symmetrical components is to use time delay for the three phase signals. The delays τ_1 and τ_2 correspond to angles $2\pi/3$ and to $4\pi/3$:

$$\begin{aligned}\tau_1 &= \frac{T_1}{3}\\ \tau_2 &= \frac{2T_1}{3}\end{aligned}.$$

Besides, one may note that:

$$\sin\left[\omega_1(\tau-\tau_2)-\beta\right] = -\sin\left[\omega_1(\tau-0.5\tau_1)-\beta\right].$$

what leads to the digital formulae:

$$\begin{aligned}3i_0(n) &= i_{L1}(n)+i_{L2}(n)+i_{L3}(n)\\ 3i_1(n) &= i_{L1}(n)-i_{L2}\left(n-\frac{p+1}{6}\right)+i_{L3}\left(n-\frac{p+1}{3}\right)\\ 3i_2(n) &= i_{L1}(n)+i_{L2}\left(n-\frac{p+1}{3}\right)-i_{L3}\left(n-\frac{p+1}{6}\right)\end{aligned}, \tag{5.12}$$

where: $(p+1)\ T_S = T_1$.

However, $(p+1)/3$ and $(p+1)/6$ may not be integer numbers. In such a case one may write:

$$\begin{aligned}\frac{p+1}{6} &= k_1 + r_1\\ \frac{p+1}{3} &= k_2 + r_2\end{aligned}, \tag{5.13}$$

where: k_1 and k_2 are integers, while r_1 and r_2 are fractional numbers less than 1. In such a case :

$$\begin{aligned}i\left(n-\frac{p+1}{6}\right) &\approx i(n-k_1)[1-r_1]+i(n-k_1-1)r_1\\ i\left(n-\frac{p+1}{3}\right) &\approx i(n-k_2)[1-r_2]+i(n-k_2-1)r_2\end{aligned}. \tag{5.14}$$

Applying (5.14) the symmetrical components may be easily calculated with the sufficient accuracy, otherwise the calculation would be corrupted by significant errors.

6. CALCULATION OF PROTECTION CRITERIA VALUES

6.1. CALCULATION OF AMPLITUDES OF SINUSOIDAL SIGNALS

6.1.1. CALCULATION BY MEANS OF ORTHOGONAL COMPONENTS

The orthogonal components of a phasor may be calculated by use of formulas (3.22) – (3.41) or (4.25) – (4.28). If they are available, the simplest way to determine an amplitude of the phasor becomes:

$$\begin{aligned} f_{-}(n) &= F_1(n)\sin(n\omega_1 T_S - \beta) \\ f_{+}(n) &= F_1(n)\cos(n\omega_1 T_S - \beta) \end{aligned} \tag{6.1}$$

and consequently:

$$F_1(n) = \sqrt{f_{-}^2(n) + f_{+}^2(n)}\,. \tag{6.2}$$

The argument of the phasor may also be easily calculated:

$$(n\omega_1 T_S - \beta) = arctg\frac{f_{-}(n)}{f_{+}(n)} = \arcsin\frac{f_{-}(n)}{F_1(n)} = \arccos\frac{f_{+}(n)}{F_1(n)}\,. \tag{6.3}$$

One may observe that perhaps the easiest way to determine orthogonal components of the sinusoidal signal is to use the value of the signal and its derivative (3.30) – (3.35):

$$\begin{aligned} f_{-}(n) &= f(n-0.5) \\ f_{+}(n) &= \left(\frac{1}{\omega_1}\right) f'(n-0.5) \end{aligned}.$$

One can also employ a pair of orthogonal FIR filters having symmetrical and anti-symmetrical data windows. The orthogonalization with time delay (single or double) with or without additional filtering of noise is possible as well.

In Fig. 6.1 the comparison of measurement results obtained with full-cycle Fourier filters and orthogonalization with single delay can be made. For pure sine wave the steady-state accuracy of both approaches is the same, however, the estimation dynamics is different, with advantage for the delay method.

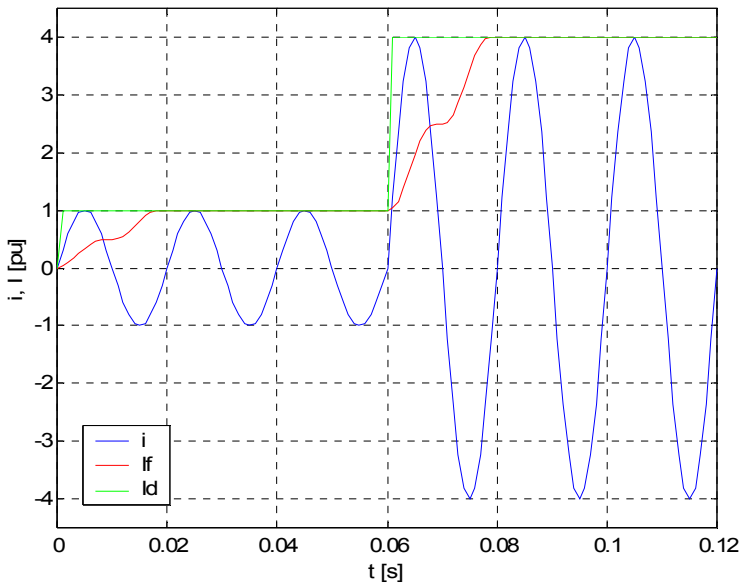

Fig. 6.1. Signal amplitude measurement with two orthogonalization methods for pure sine input

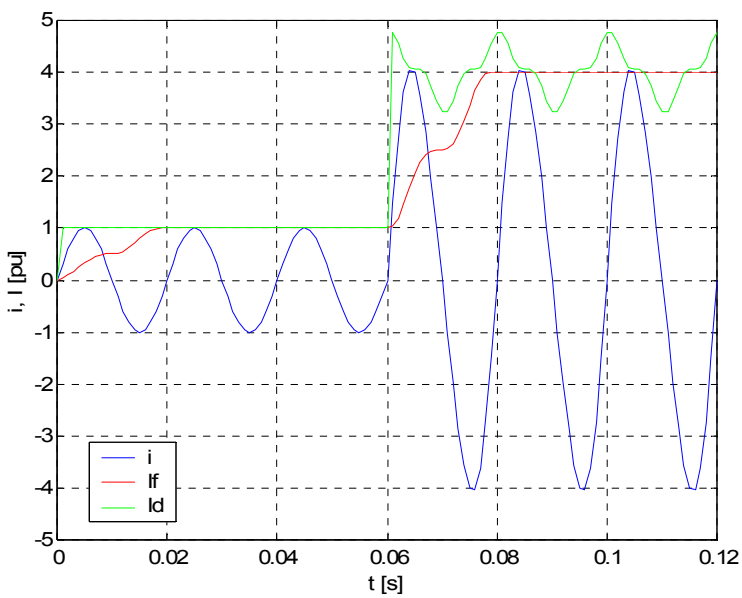

Fig. 6.2. Signal amplitude measurement with two orthogonalization methods for the signal with 2nd harmonic (after t=0.06s)

The algorithm with time delay is very fast, yet its behavior is poor when the input signal contains some noise. This is illustrated in Fig. 6.2 for the input signal being fundamental component contaminated with the second harmonic (10%). Application of Fourier filters helps to get rid of the 2nd harmonic what gives perfect measurement result, contrary to the delay method, which delivers results with significant oscillations.

6.1.2. CALCULATION BY MEANS OF MAXIMIZATION

If the signal is sinusoidal, but the orthogonal components are not available, one may calculate the amplitude by means of finding maximum of the absolute value of the signal during half a period. Therefore:

$$F_1(n) = \max\left(\left|f(n-k)\right|\right)\overset{0.5(p+1)}{\underset{k=0}{\uparrow}}. \tag{6.4}$$

This process may be accelerated, if one uses the signal and the signal delayed by a quarter of a period (here, for p=15):

$$F_1(n) = \max\left(\left|f(n-k)\right|;\left|f\left(n-k-\frac{p-3}{4}\right)\right|\right)\overset{0.25(p-3)}{\underset{k=0}{\uparrow}}, \tag{6.5}$$

where: $T_1 = (p+1)T_S$.

The same may be done if one employs the first derivative of the signal:

$$F_1(n) = \max\frac{1}{\omega_1}\left(\left|f'(n-k-0.5)\right|\right)\overset{0.5(p+1)}{\underset{k=0}{\uparrow}} \tag{6.6}$$

or, in the mixed form:

$$F_1(n) = \max\left(\left|f(n-k-0.5)\right|;\frac{1}{\omega_1}\left|f'(n-k-0.5)\right|\right)\overset{0.25(p-3)}{\underset{k=0}{\uparrow}}. \tag{6.7}$$

6.1.3. CALCULATION BY MEANS OF INTEGRATION

If there is a pure sinusoidal signal, calculation of its amplitude may be performed integrating the absolute value of the signal, with the data window being a half of the period:

$$f(\tau) = F\sin(\omega_1\tau - \beta),$$

$$F = \frac{\omega_1}{2} \int_{t-0.5T_1}^{t} |f(\tau)| d\tau \tag{6.8}$$

or, in the digital form:

$$F = \frac{\pi}{p+1} \sum_{k=0}^{0.5(p+1)} |f(n-k)|. \tag{6.9}$$

Again, the process may be accelerated, if one uses the value of the signal, and the same signal delayed by a quarter of the period T_1.

6.2. CALCULATION OF ACTIVE AND REACTIVE POWER

6.2.1. CALCULATION BASED ON ORTHOGONAL COMPONENTS

The orthogonal quantities of voltage and current are given by the expressions:

$$\begin{aligned} u_-(t) &= U\sin(\omega_1 t - \beta) \\ u_+(t) &= U\cos(\omega_1 t - \beta) \\ i_-(t) &= I\sin(\omega_1 t - \beta - \varphi) \\ i_+(t) &= I\cos(\omega_1 t - \beta - \varphi) \end{aligned},$$

where: φ – phase angle between voltage and current.

Then:

$$\begin{aligned} i_+(t)u_-(t) &= 0.5UI[\sin\varphi + \sin(2\omega_1 t - 2\beta - \varphi)] \\ i_-(t)u_+(t) &= 0.5UI[\sin(-\varphi) + \sin(2\omega_1 t - 2\beta - \varphi)] \\ i_+(t)u_+(t) &= 0.5UI[\cos\varphi + \cos(2\omega_1 t - 2\beta - \varphi)] \\ i_-(t)u_-(t) &= 0.5UI[\cos\varphi - \cos(2\omega_1 t - 2\beta - \varphi)] \end{aligned}. \tag{6.10}$$

Therefore, active and reactive powers in the digital form will become:

$$Q = 0.5[i_+(n)u_-(n) - i_-(n)u_+(n)], \tag{6.11}$$

$$P = 0.5[i_+(n)u_+(n) + i_-(n)u_-(n)]. \tag{6.12}$$

One should understand that the dynamics and accuracy of measurement is dependent on the algorithms that were used for calculation of orthogonal components.

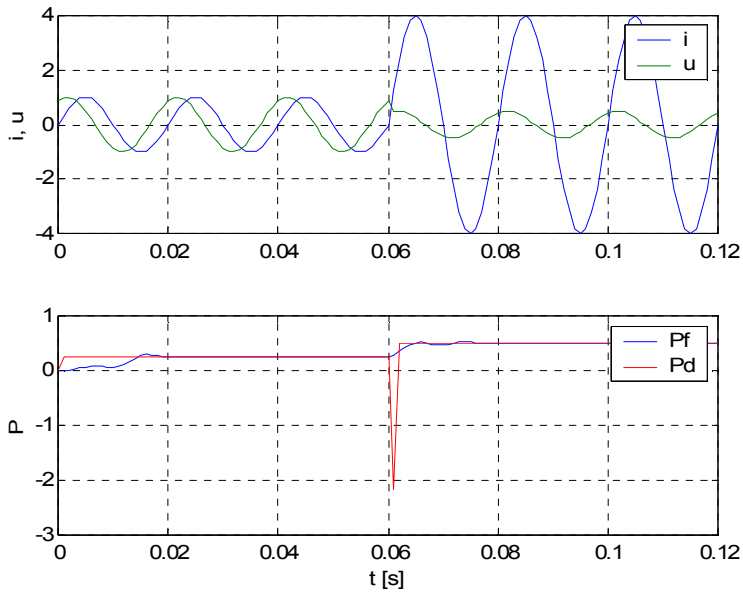

Fig. 6.3. Active and reactive power measurement with two orthogonalization methods for pure sine current and voltage input signals

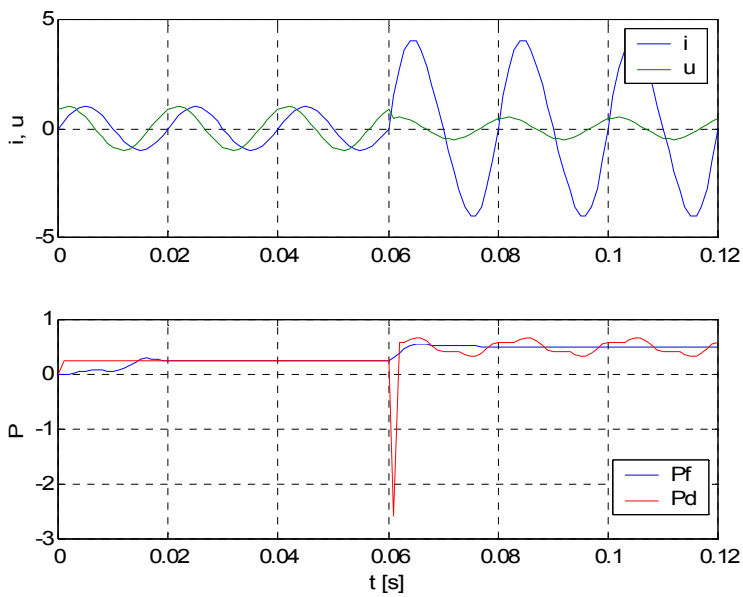

Fig. 6.4. Active and reactive power measurement with two orthogonalization methods for the current signal with 2nd harmonic (after t=0.06s)

The results of measurement of active power for the cases when both current and voltage signals are pure sine waves and when the current signal contains additional second harmonic component are shown in Figs. 6.3 and 6.4, respectively. Two methods or signals orthogonalization were applied – with full-cycle filtering (curve Pf) and with time delay (curve Pd). One can see that, similarly as for measurement of current amplitude presented in Figs. 6.1, 6.2, faster stabilization of active power is obtained for the time delay algorithm. On the other hand, when the current signal contains higher harmonics, better accuracy is assured for the measurement with use of Fourier filters.

6.2.2. CALCULATION BASED ON INTEGRATION OF THE PRODUCT OF CURRENT AND VOLTAGE

If the voltage and current are given by the following formulas:

$$u(t) = U\sin(\omega_1 t - \beta)$$
$$i(t) = I\sin(\omega_1 t - \beta - \varphi)'$$

then|:

$$\int_{t-0.5T_1}^{t} u(\tau)i(\tau)d\tau = \left(\frac{T_1}{4}\right)UI\cos\varphi = \left(\frac{T_1}{2}\right)P. \tag{6.13}$$

In the digital form it will be:

$$P = 2\left(\frac{T_S}{T_1}\right)\sum_{k=0}^{0.5(p-1)} i(n-k)u(n-k) = \left(\frac{2}{p+1}\right)\sum_{k=0}^{0.5(p-1)} i(n-k)u(n-k). \tag{6.14}$$

If the values of current and voltage amplitudes were calculated before, then:

$$S = 0.5UI = \sqrt{P^2 + Q^2}$$

and consequently:

$$Q = \sqrt{S^2 - P^2}\ , \tag{6.15}$$

where: S - apparent power.

Alternatively, the reactive power may be calculated if the current signal is delayed by $\pi/4$:

$$\int_{t-0.5T_1}^{t} u(\tau)i(\tau - 0.25T_1)d\tau = \left(\frac{T_1}{4}\right)UI\sin\varphi = \left(\frac{T_1}{2}\right)Q \tag{6.16}$$

and in the digital form (again – for p=15):

$$Q = 2\left(\frac{T_S}{T_1}\right)\sum_{k=0}^{0.5(p-1)} u(n-k)\,i(n-k-0.25(p-3)) = \left(\frac{2}{p+1}\right)\sum_{k=0}^{0.5(p-1)} u(n-k)\,i(n-k-0.25(p-3)) \tag{6.17}$$

6.3. CALCULATION OF ACTIVE AND REACTIVE COMPONENTS OF CURRENT SIGNAL

6.3.1. CALCULATION BASED ON ACTIVE AND REACTIVE POWER

Perhaps the most straightforward way to calculate the active components of current and reactive power is to derive them directly from active and reactive power formulae:

$$\begin{aligned} I\sin\varphi &= \frac{2Q}{U} \\ I\cos\varphi &= \frac{2P}{U} \end{aligned}. \tag{6.18}$$

However, it requires that the values of active and reactive powers and the amplitude of voltage have been calculated before:

$$\begin{aligned} U &= \sqrt{u_+^2(n) + u_-^2(n)} \\ Q &= 0.5\left[i_+(n)u_-(n) - i_-(n)u_+(n)\right] \\ P &= 0.5\left[i_+(n)u_+(n) + i_-(n)u_-(n)\right] \end{aligned}. \tag{6.19}$$

6.3.2. CALCULATION BASED ON WAVESHAPES RELATIONS

If current and voltage signals are sinusoidal, and the phase shift between them is positive (the voltage leads), then:

$$\begin{aligned} u(\tau) &= U\sin(\omega_1\tau - \beta) \\ i(\tau) &= I\sin(\omega_1\tau - \beta - \varphi) \end{aligned}.$$

One may observe that the value of reactive component of the current corresponds to the values of current at the instants of zero crossing of the voltage waveshape, what is illustrated in Fig. 6.5.

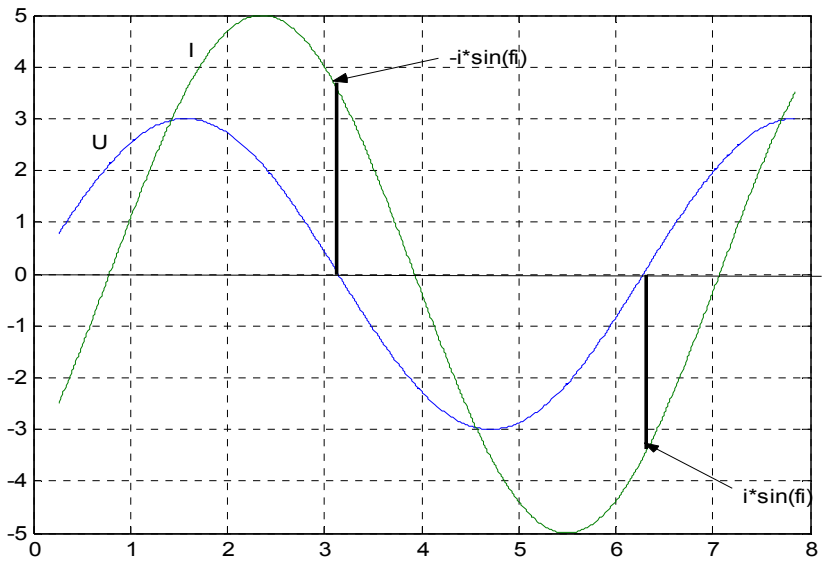

Fig. 6.5. Illustration how reactive part of the current is determined

Therefore:

$$I \sin \varphi = -i(t_1) sign\left[u'(t_1)\right] \tag{6.20}$$

where: t_1 - instant of the voltage zero crossing.

Then:

$$I \sin \varphi = i(t_1)$$
$$I \sin \varphi = -i(t_2)$$

However, the zero crossing of voltage may be located somewhere between the samples (see Fig. 6.6).

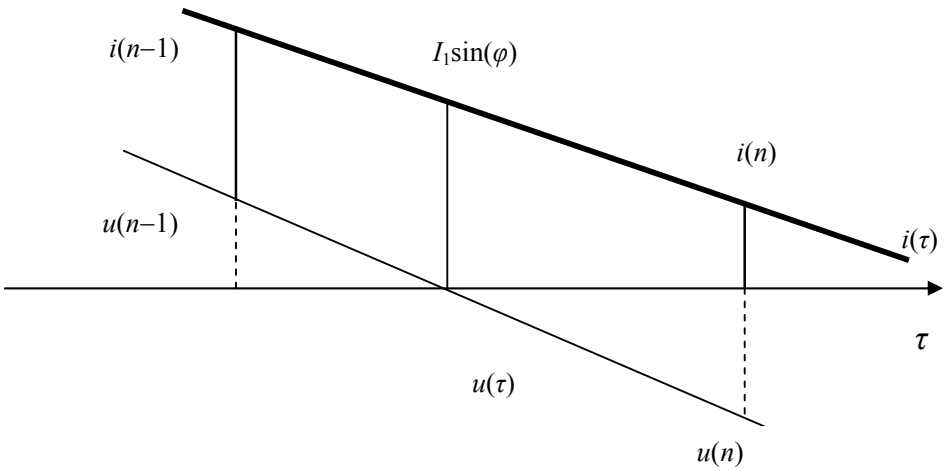

Fig. 6.6. Increased accuracy of the calculation

Therefore, to minimize the error one may assume that the zero crossing is between the samples (Fig. 6.6). Therefore in the digital form the reactive part of the current is:

$$I\sin\varphi \approx -\frac{i(n)\left|u(n-1)\right| + i(n-1)\left|u(n)\right|}{\left|u(n)\right| + \left|u(n-1)\right|} sign\left[u(n) - u(n-1)\right]. \tag{6.21}$$

The active part of the current may be calculated indirectly:

$$I\cos\varphi = \sqrt{I^2 - (I\sin\varphi)^2}\ . \tag{6.22}$$

The alternative way in calculation of the active part of the current is to determine the value of the current at the instant, when the first derivative of voltage crosses zero.

$$I\cos\varphi = -i(t_3)sign\left[u''(t_3)\right], \tag{6.23}$$

where t_3 – instant of zero crossing by the first derivative of voltage.

6.4. CALCULATION OF IMPEDANCE, REACTANCE AND RESISTANCE

The circuit for which the quantities are to be calculated is presented in Fig. 6.7.

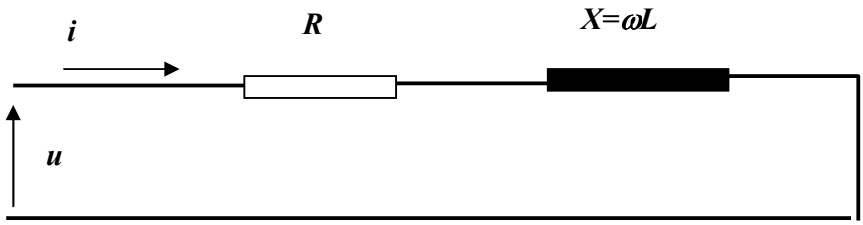

Fig. 6.7. Series R–X circuit

If the active and reactive power is known, and so are amplitudes of current and voltage, the basic formulas to calculate Z, R and X are very simple:

$$\begin{aligned} Z &= \frac{U}{I} = \sqrt{R^2 + X^2} \\ R &= \frac{2P}{I^2} \\ X &= \frac{2Q}{I^2} \end{aligned} \tag{6.24}$$

or, using the orthogonal components of current and voltage:

$$Z(n) = \sqrt{\frac{u_-^2(n) + u_+^2(n)}{i_-^2(n) + i_+^2(n)}}\,, \tag{6.25}$$

$$R(n) = \frac{i_-(n)u_-(n) + i_+(n)u_+(n)}{i_-^2(n) + i_+^2(n)}, \tag{6.26}$$

$$X(n) = \frac{i_+(n)u_-(n) - i_-(n)u_+(n)}{i_-^2(n) + i_+^2(n)}. \tag{6.27}$$

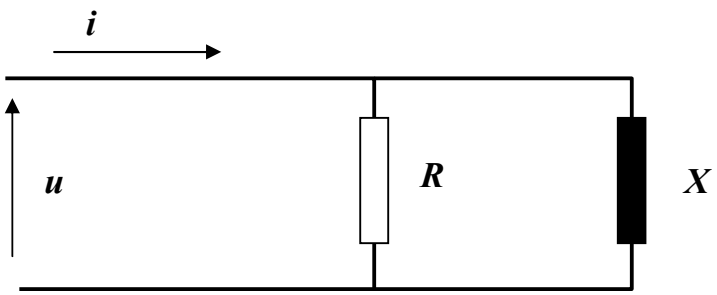

Fig. 6.8. Parallel R – X circuit

In a similar way one may calculate admittance, susceptance and conductance, for a circuit presented in Fig. 6.8.

$$G = \frac{1}{R}$$

$$B = \frac{1}{X}$$

$$Y = \sqrt{G^2 + B^2}$$

Therefore:

$$Y(n) = \frac{I(n)}{U(n)} = \sqrt{\frac{i_-^2(n) + i_+^2(n)}{u_-^2(n) + u_+^2(n)}}, \tag{6.28}$$

$$G(n) = \frac{2P(n)}{U^2(n)} = \frac{i_-(n)u_-(n) + i_+(n)u_+(n)}{u_-^2(n) + u_+^2(n)}, \tag{6.29}$$

$$B(n) = \frac{2Q}{U^2(n)} = \frac{i_+(n)u_-(n) - i_-(n)u_+(n)}{u_-^2(n) + u_+^2(n)}. \tag{6.30}$$

6.5. CALCULATION OF RESISTANCE AND INDUCTANCE

In the circuit from Fig. 6.7 one may calculate the resistance and inductance on the ground of differential equation taken at two instants t and $(t–t_0)$

$$\begin{aligned} u(t) &= Ri(t) + Li'(t) \\ u(t-t_0) &= Ri(t-t_0) + Li'(t-t_0) \end{aligned}. \tag{6.31}$$

From the two equations the unknown R and L values may be calculated by means of the final relationships:

$$R = \frac{u(t)i'(t-t_0) - u(t-t_0)i'(t)}{i(t)i'(t-t_0) - i(t-t_0)i'(t)}, \tag{6.32}$$

$$L = \frac{u(t-t_0)i(t) - u(t)i(t-t_0)}{i(t)i'(t-t_0) - i(t-t_0)i'(t)}. \tag{6.33}$$

In the digital form, if ($t_0 = kT_S$) the values of signals and their derivatives are:

$$u(n)=\frac{u(n)+u(n-1)}{2\cos\left(\frac{\omega T_S}{2}\right)} \qquad u(n-k)=\frac{u(n-k)+u(n-k-1)}{2\cos\left(\frac{\omega T_S}{2}\right)}$$

$$i(n)=\frac{i(n)+i(n-1)}{2\cos\left(\frac{\omega T_S}{2}\right)} \qquad i(n-k)=\frac{i(n-k)+i(n-k-1)}{2\cos\left(\frac{\omega T_S}{2}\right)}$$

$$i'(n)=\omega\frac{i(n)-i(n-1)}{2\sin\left(\frac{\omega T_S}{2}\right)} \qquad i'(n-k)=\omega\frac{i(n-k)-i(n-k-1)}{2\sin\left(\frac{\omega T_S}{2}\right)}$$

The shortest delay is for one sampling period, therefore in such a case $k = 1$.

Having known R and L one may easily calculate the time constant of the circuit:

$$T_a=\frac{L}{R}=\frac{u(n-k)i(n)-u(n)i(n-k)}{u(n)i'(n-k)-i(n-k)i'(n)}. \tag{6.34}$$

The method is insensitive to the decaying DC components in currents, therefore in this respect it is very accurate. However, the errors may be caused by the higher frequency components, which have not been removed by the antialiasing input filters. To minimize the errors one may modify the process of calculation, by means of applying the basic equation in which this error e exists:

$$u(t)=Ri(t)+Li'(t)+e. \tag{6.35}$$

To minimize the mean square error one may solve two equations, thus calculating R and L:

$$\frac{d}{dR}\int_{t-t_0}^{t}e^2(\tau)d\tau=R\int_{t-t_0}^{t}i^2(\tau)d\tau+L\int_{t-t_0}^{t}i(\tau)i'(\tau)d\tau-\int_{t-t_0}^{t}i(\tau)u(\tau)d\tau=0, \tag{6.36}$$

$$\frac{d}{dL}\int e^2(\tau)d\tau=R\int_{t-t_0}^{t}i(\tau)i'(\tau)d\tau+L\int_{t-t_0}^{t}i'^2(\tau)d\tau-\int_{t-t_0}^{t}i'(\tau)u(\tau)d\tau=0, \tag{6.37}$$

which leads to the following equations:

$$\begin{aligned} RA_1+LA_2&=A_4\\ RA_2+LA_3&=A_5 \end{aligned}.$$

In the digital form the integrals will be calculated by summations, and therefore the coefficients $A_1 - A_5$ become:

$$A_1 = \sum_{k=0}^{p} i^2(n-k)$$

$$A_2 = \sum_{k=0}^{p} i(n-k)i'(n-k)$$

$$A_3 = \sum_{k=0}^{p} i'^2(n-k) \quad ,$$

$$A_4 = \sum_{k=0}^{p} i(n-k)u(n-k)$$

$$A_5 = \sum_{k=0}^{p} i'(n-k)u(n-k)$$

where: $(p+1)\ T_S = t_0$.

And finally:

$$R = \frac{A_4 A_3 - A_5 A_2}{A_1 A_3 - A_2^2}$$
$$L = \frac{A_5 A_1 - A_4 A_2}{A_1 A_3 - A_2^2} \quad . \tag{6.38}$$

6.6. DETERMINATION OF FREQUENCY OF THE SINUSOIDAL SIGNAL

6.6.1. MEASUREMENT WITH IMPULSE COUNTING

The most straightforward way to determine frequency of input sinusoidal signals (in most cases voltages) is to count the number of sampling pulses for one period of the sine wave. In such cases:

$$f_x = 50\frac{m}{m_1}, \tag{6.39}$$

where:

f_x – measured frequency of the signal,

m – number of pulses in one period of the input signal. If the period is equal to T_1 the value of m becomes: $m=T_1/T_S$,

m_1 – number of sampling pulses counted between the instants of zero crossing of the signal, when it increases.

However, this method shows the error, which may reach the value:

$$e = \pm 100 \frac{T_S}{T_1} = \pm 100 \frac{1}{m} [\%].$$

To make the error as low as possible one must use very short sampling periods, or in the other words, very high sampling frequency. In most of the relays the sampling period is not very high. For example, if the sampling frequency is 1000 Hz (20 samples in the period T_1, m=20), the error may be as high, as 5%, what is unacceptable.

The accuracy may be drastically improved, if the moment of zero crossing by the signal is better estimated. It is demonstrated in Fig. 6.9.

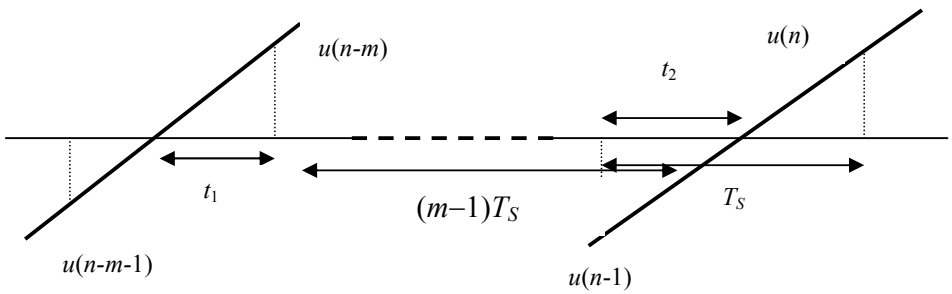

Fig. 6.9. Illustration of the frequency measurements

Therefore the measured period of the signal T_X becomes:

$$T_X = (m-1)T_S + t_1 + t_2 \tag{6.40}$$

And, if the voltage at the moment of zero crossing is approximated by the straight line:

$$t_1 \approx \frac{T_S u(n-m)}{u(n-m) - u(n-m-1)}, \tag{6.41}$$

$$t_2 \approx \frac{-T_S u(n-1)}{u(n) - u(n-1)}. \tag{6.42}$$

Therefore, the existing frequency of the signal f_X is:

$$f_X = \frac{1}{T_X} \approx \frac{1}{(m-1)T_S + t_1 + t_2}. \tag{6.43}$$

One must remember that:

n – first sample after the voltage crossed zero while increasing,

n-m – first sample after the previous voltage zero crossing while increasing,

m – number of samples between two consecutive zero crossings when the voltage waveshape increases.

The accuracy of the method is much improved. If for example the sampling frequency is 1000 Hz, and the signal frequency is close to 50 Hz, the accuracy of frequency measurement is in order of 0.1%, what is sufficient for protective algorithms.

6.6.2. UTILISATION OF SIGNAL ORTHOGONAL COMPONENTS

If the orthogonal components of input signal are known (have been calculated), the frequency of the signal can be obtained using the following formula:

$$f(n) = \frac{f_S}{2\pi k} \cos^{-1}\left\{0.5 \frac{u_+(n)u_-(n-2k) - u_-(n)u_+(n-2k)}{u_+(n)u_-(n-k) - u_-(n)u_+(n-k)}\right\} \tag{6.44}$$

where: k – any delay value (in samples)

The accuracy of (6.44) is very good. In the range of frequencies from 48 to 52Hz the measurement error does not exceed the level of 2.5mHz.

7. CORRECTION OF ERRORS INTRODUCED BY MEASURING TRANSFORMERS

7.1. CORRECTION OF VOLTAGE TRANSFORMER PERFORMANCE

Inductive voltage transformers selected in the proper way do not introduce errors, which could affect operation of protective devices. It is so in both steady states and transients. Therefore, there is no need to make special arrangements which would correct the errors.

However, in cases of capacitive voltage transformers (CVTs) it is otherwise. Because they are equipped with the compensating inductance and the ferroresonance suppressing circuits they may introduce substantial errors if there is a sudden change of the primary voltage. The errors may cause maloperation of protective devices, particularly if there is a sudden drop of primary voltages. Therefore correction of the expected errors may be advantageous.

The circuit of a capacitive voltage transformer is presented in the Fig. 7.1. The ferroresonance suppressing circuits are represented by FSC (parallel circuit).

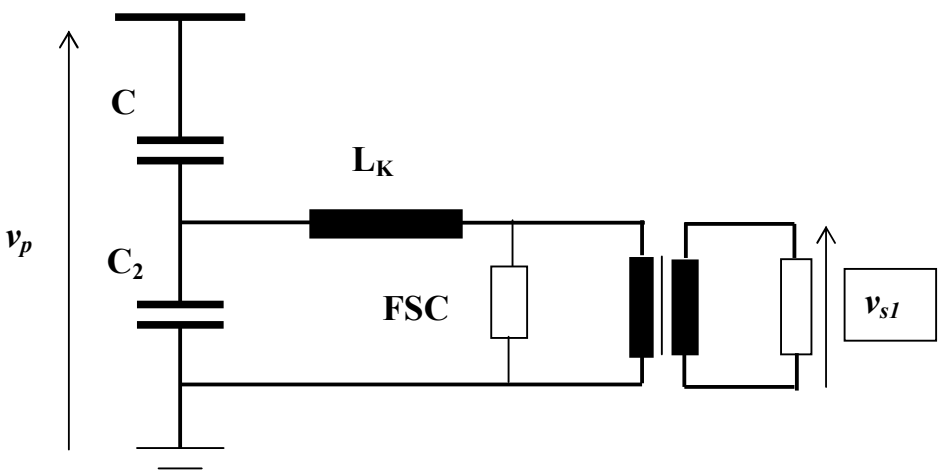

Fig. 7.1. Equivalent circuit of a capacitive voltage transformer

The whole circuit may be considered as linear, therefore one may write the Laplace transform relation:

$$\frac{v_{S1}}{v_P} = N_V F(s), \tag{7.1}$$

where: N_V – transformation ratio of the voltage transformer,
$F(s)$ – Laplace transfer function of the circuit.
v_{S1} – secondary voltage at the terminals of the transformer.

The correction algorithm ought to process the secondary voltage by a transfer function which is equal to inverse of the CVT transfer function. Therefore the corrected secondary voltage v_S becomes:

$$v_S = v_{S1} F_1(s) \approx v_P N , \tag{7.2}$$

where: $F_1(s) = \dfrac{1}{F(s)}$.

Digital representation of the transfer function $F_1(s)$ may be obtained by the discrete operators of integration, for example the Euler's operator (5.59):

$$s^{-1} \Rightarrow \left(\frac{T_S z^{-1}}{1 - z^{-1}} \right), \tag{7.3}$$

remembering, that multiplication by z^{-1} in the z-transform domain represents delay by one period of sampling T_S in the time domain.

7.2. CORRECTION OF CURRENT TRANSFORMER ERRORS

7.2.1. FORMULATION OF THE PROBLEM

The problems due to errors of current transformers are much more significant than the ones of in case voltage transformers. It is so because:

- errors of the CTs are much more harmful for proper operation of digital devices,
- current transformers are strongly nonlinear, because of the nonlinear magnetizing characteristic of the cores, therefore their errors are much more difficult to calculate and correct,
- due to the hysteresis loop of the magnetization characteristic of the core it is hardly possible to establish the initial value of the core flux,
- range of primary currents levels and the time constants of their DC components are relatively high.

If during the steady state operation the primary currents of the transformer are within the accuracy range (if they are below the rated level multiplied by the accuracy limit factor) the errors of transformation do not affect operation of protective relays. However, if they are larger, it is otherwise.

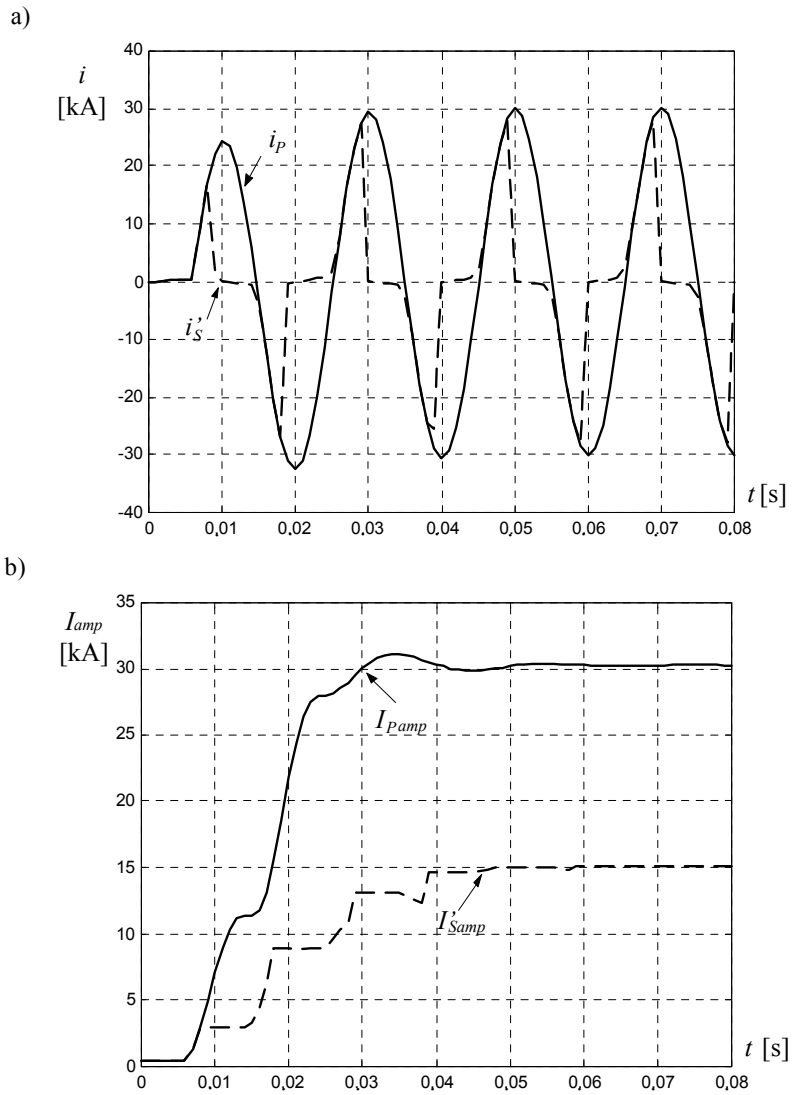

Fig. 7.2. Primary and secondary CT currents: a) instantaneous signals, b) measured amplitudes (algorithm with full-cycle Fourier filters used).

In Fig. 7.2 as an example the CT primary and secondary currents as a function of time are shown. It is obvious that protection criterion values calculated on the basis of saturated CT secondary signal may fall quite distantly from their correct values, which might have been determined if the CT primary unsaturated signal was available. Erroneous measurement may, in consequence, lead to wrong decisions (e.g. underreaching of overcurrent relays, overestimation of fault loop impedance in distance relays) and protection maloperation. Thus it can be stated that CT saturation phenomenon may impair protection system reliability if appropriate algorithms for saturation detection and/or correction are not applied to minimize the problem.

There are three basic ways of overcoming the problem which make correct operation of the protective devices possible. They are:

- application of the CTs with larger accuracy limit factor, CTs which do not saturate during steady state operation,
- application the relay algorithms which are insensitive to the errors (for example they make measurements only within the fraction of periods, when the transformation is correct).
- calculation of the primary current on the ground of the secondary, corrupted waveshape.

The first way is obvious, but in some cases it requires the CTs with the cores of very large cross sections. The second and third ways do not require very large cross sections, but they demand correction of the secondary currents.

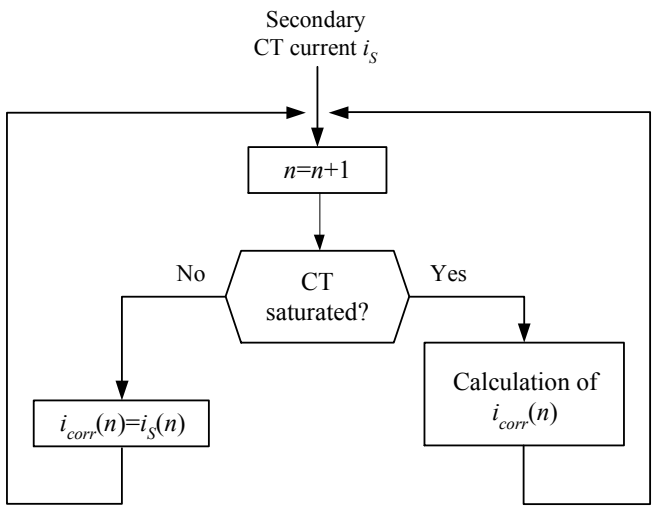

Fig. 7.3. Block scheme of CT saturation compensation.

The basic idea of handling the CT saturation problem may be based on splitting the task into two subtasks, namely saturation detection and correction of the distorted

secondary current (Fig. 7.3). When the CT is not saturated (i.e. the detection block has not detected it) the correction block is not activated. Starting from the point of saturation beginning the procedure of secondary current correction is activated. The procedure is operative until the CT goes out of saturation. The process is repeated when the detection block affirms saturation beginning again.

7.2.2. DETECTION OF THE UNSATURATED FRAGMENT OF THE WAVESHAPE

Saturation of the CT core is particularly likely during transient states, when the primary currents contain large DC components, and the residual flux in the transformer core is high. In such cases the secondary current waveshape in each cycle may be divided into two time spans. The first covers the time, when the CT is not saturated and the transformation is correct. The second corresponds to the saturation of the transformer magnetic core, what results in very large errors of transformation. Correction of the transformation requires identification of the moment of saturation, which in Fig. 7.4 is between the samples n and $n-1$. The saturation ends between the samples $m-1$ and m. Therefore, the transformation is correct, what means that the secondary current is proportional to the primary current ($i_2 = N_i i_1 = i_p$), until the sample n, and after the sample m.

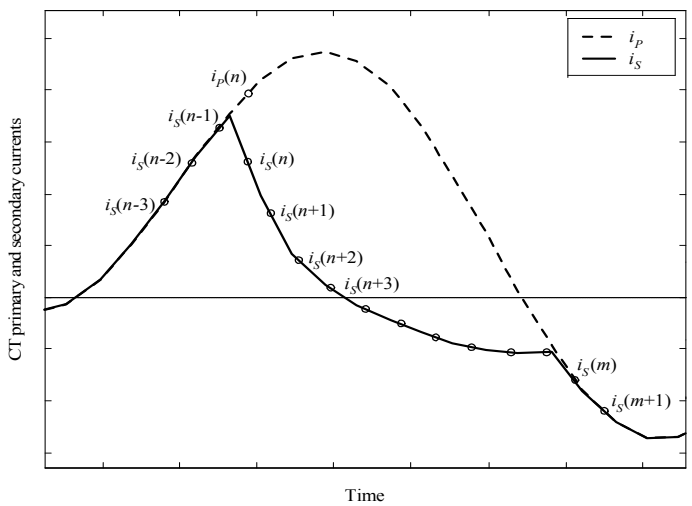

Fig. 7.4. Primary and secondary current waveshape of the saturated CT

Determination of the sample n can be based on the comparison of the measured secondary current $i_s(n)$ and the estimated secondary current $i_{se}(n)$. If the difference between the two exceeds a part Δ of the estimated level it means that there was a

change of the waveshape and that the saturation happened between the samples. It is so if:

$$\left|i_{se}(n)-i_s(n)\right| \geq \Delta\left|i_{se}(n)\right| \tag{7.4}$$

and:

$$\left|i_{se}(n)\right|-\left|i_s(n)\right| \geq 0\,. \tag{7.5}$$

If the condition (7.4) is satisfied, but :

$$\left|i_{se}(n)\right|-\left|i_s(n)\right| \leq 0\,, \tag{7.6}$$

like between the samples m and $m-1$ in Fig. 7.2, it marks the end of saturation. Estimation may be done through the assumption, that the derivatives of the secondary current between the samples $n-1$and $n-2$ are the same, as between the samples n and $n-1$. The simplest way is to assume, that the first order derivatives are equal:

$$\frac{i_{se}(n)-i_s(n-1)}{T_S} \approx \frac{i_s(n-1)-i_s(n-2)}{T_S}\,. \tag{7.7}$$

This leads to the formula:

$$i_{se}(n) \approx 2i_s(n-1)-i_s(n-2)\,. \tag{7.8}$$

And now one may apply the condition (7.4) to find out, if there was a rapid change in the waveshape.

The second and third order derivatives may be calculated by the well known formulae:

$$i''(n) \approx \frac{i'(n)-i'(n-1)}{T_S} \tag{7.9}$$

$$i'''(n) \approx \frac{i''(n)-i''(n-1)}{T_S} \tag{7.10}$$

If one assumes that the second order derivative is to be the same in n-th sampling period then, in the $n-1$-th sampling period, the value of $i_{se}(n)$ may be estimated from the formula:

$$i_{se}(n) \approx 3i_s(n-1)-3i_s(n-2)+i_s(n-3) \tag{7.11}$$

The formula (7.11) is more accurate than (7.8). However, if one wants to increase accuracy even more, one may assume, that the third derivative is to be the same between the samples n - $n-1$, and $n-1$ - $n-2$, what gives the condition:

$$i_{se}(n) \approx 4i_s(n-1)-6i_s(n-2)+4i_s(n-3)-i_s(n-4)\,. \tag{7.12}$$

The detection of the end of saturation is not that important as detection of saturation beginning, since some of the correction methods may perform quite well (properly estimate the signal) even during unsaturated periods of CT operation. It is however advantageous to know the end-of-saturation time instant for at least two good reasons:

a) the estimate of the corrected CT current is always somewhat worse than the original CT signal (the primary current is known when CT is not saturated), therefore it is better to stop the procedure of secondary current correction at that point,
b) some correction methods may require the information on the end-of-saturation time instant simply to calculate the interval of unsaturated period before they start their operation for the next saturation period.

The end-of-saturation determination can be based on calculation of the integral of the secondary current, starting from the saturation beginning instant. If the secondary impedance of the current transformer is purely resistive, then during the saturation period the magnetic induction in the core rises at the beginning, reaches maximum when the secondary current is zero, and after that decreases to the saturation level. Therefore the integral of the secondary current in the time span of saturation must be:

$$\int_{t_{SB}}^{t_{SE}} i_s(t)\,dt = 0 \tag{7.13}$$

where: t_{SB} – beginning of saturation, t_{SE} – end of saturation.

Tracking the value of integral (7.13) enables determination of the end of saturation.

7.2.3. CORRECTION OF THE SECONDARY CURRENT

During transient state the primary current may be presented in the following form:

$$i_p = \left(\frac{1}{N_i}\right) i_1 \cong I_0 \exp\left(-\frac{t}{T_a}\right) - I_1 \cos\left(\omega t - \alpha\right), \tag{7.14}$$

where: N_i – current transformer ratio,
i_1 – primary current,
I_0 – DC decaying component,
T_a – time constant of the decay,
I_1 – amplitude of the AC component,
α - phase angle of the AC component.

In spite of the transient errors caused by the CT core saturation, operation of the protective devices may be correct. However, it demands careful processing of the signal, what may be done in a number of ways.

If the aim of processing is to make proper operation of differential relays, the best way is to use current signals only in the fraction of periods, when the CTs at both sides are not saturated. Therefore, the differential current is detected taking into considera-

tion non corrupted current samples of the input currents: $i_s n-1$; $i_s(n-2)$; $i_s(n-3)$… etc., and $i_s(m)$; $i_s(m+1)$; $i_s(m+2)$, etc. until the beginning of saturation in the next period. In fact, this unsaturated fragment may be artificially expanded particularly in the cases, when the secondary current samples $i_{se}(n)$ and $i_{se}(n+1)$ are estimated by the formula (7.12), which returns sufficiently accurate results.

If the aim of the processing is the proper operation of protective devices, which are based on the calculation of the fundamental frequency components (overcurrent, distance etc…), the amplitude I_1 of the current ought to be determined, on the ground of the distorted current signals.

A. Calculation of the amplitude I_1 based on the unsaturated fractions of the waveshape

There are several methods of determination of the amplitude, considering only the samples of the secondary current taken in the fraction of each period during which the CT core is not saturated. Perhaps the easiest one is to consider the value of the secondary current i_s, and the first derivative of it i'_s, correlating both of them with the sinusoidal function:

$$b_1(n)=\left(\frac{2T_S}{(T_w-T_1\sin(\omega T_w)/2\pi)}\right)\sum_{r=n-p}^{n} f_c(r)\sin\left[\omega_1(r-n)T_S+\frac{T_w}{2}\right]=f_-, \qquad (7.15)$$

$$a_1(n)=\left(\frac{T_1}{2\pi}\right)\left(\frac{2T_S}{(T_w-T_1\sin(\omega T_w)/2\pi)}\right)\sum_{r=n-p}^{n} f_c'(r)\sin\left[\omega_1(r-n)T_S+\frac{T_w}{2}\right]=f_+ \qquad (7.16)$$

where:

$$f_c(r)\approx\frac{i(r)+i(r-1)}{2},$$

$$f_c'(r)\approx\frac{i(r)-i(r-1)}{T_S}$$

and:

$$I_1=\sqrt{f_-^2+f_+^2}\,. \qquad (7.17)$$

One must bear in mind that this method does not reproduce the waveshape of the primary current. It only estimates the fundamental and DC components in each period. The accuracy of calculation is good even if the primary current contains a substantial level of the higher harmonics, providing the unsaturated time span is longer than 6-7 ms. The method is not very sensitive to the small errors in determining the beginning of the unsaturated time span.

Besides, it ought to be remembered that the method is not suitable in cases when extraction of the higher harmonics in the current is required (e.g. when protecting a power transformer).

B. Reproduction of the distorted waveshape

Equivalent circuit of the CT reduced to the secondary side is presented in Fig. 7.5 and the magnetizing characteristic of the core in Fig. 7.6.

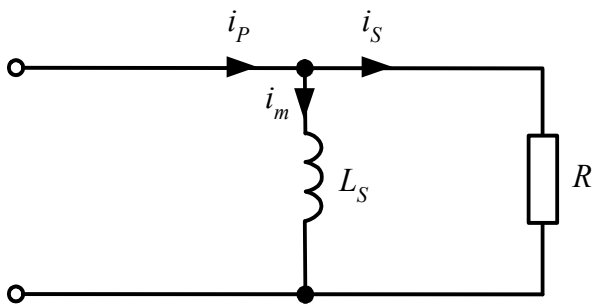

Fig. 7.5. Equivalent circuit of the CT

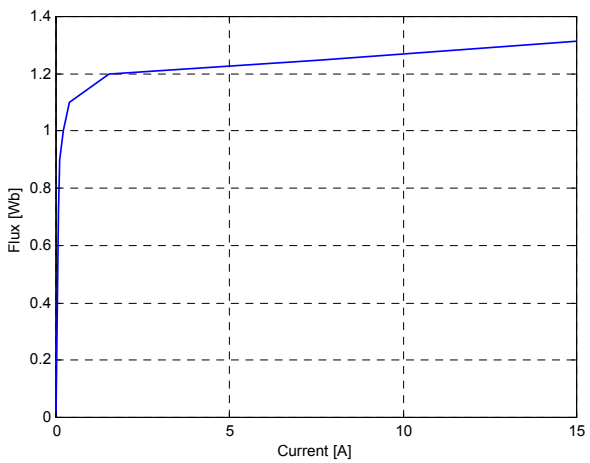

Fig. 7.6. Simplified magnetizing characteristic of the transformer core

Estimation of the true values of the secondary current by means of the formula (7.12) is sufficiently accurate while calculating two samples of the current after saturation. Therefore one may assume that:

$$i_{se}(n) \approx i_p(n),$$

$$i_{se}(n+1) \approx i_p(n+1).$$

Therefore, the samples of the magnetizing current become:

$$i_m(n) \approx i_{se}(n) - i_s(n), \tag{7.18}$$

$$i_m(n+1) \approx i_{se}(n+1) - i_s(n+1). \tag{7.19}$$

Thus, the change of the magnetizing current between the samples n and n+1 becomes:

$$\Delta i_m(n+1) \approx i_m(n+1) - i_m(n). \tag{7.20}$$

If the secondary inductance is negligible then the mean value of voltage between the samples n+1 and n+2 becomes:

$$u(n+1) \approx \frac{i_s(n+1) + i_s(n)}{2} R. \tag{7.21}$$

Therefore, the increase of the flux linkage ψ in one sampling period becomes:

$$\Delta\psi(n+1) \approx T_S u(n+1). \tag{7.22}$$

The value of the magnetizing inductance between the samples is given by the formula:

$$L_m(n+1) \approx \frac{\Delta\psi(n+1)}{\Delta i_m(n+1)}. \tag{7.23}$$

Now, assuming that the magnetizing inductance L_m between the samples n+2 and n+3 has the same value, as during the previous sample, one may write:

$$\Delta i_m(n+2) \approx \frac{\Delta\psi(n+2)}{L_m(n+1)} \approx \Delta i_m(n+1) \frac{\Delta\psi(n+2)}{\Delta\psi(n+1)}, \tag{7.24}$$

where:

$$\Delta\psi(n+2) \approx T_S u(n+2), \tag{7.25}$$

$$u(n+2) \approx \frac{i_{se}(n+2) + i_{se}(n+1)}{2} R. \tag{7.26}$$

Therefore:

$$i_m(n+2) \approx i_m(n+1) + \Delta i_m(n+2). \tag{7.27}$$

In consequence:

$$i_{se}(n+2) \approx i_s(n+2) + i_m(n+2). \tag{7.28}$$

This algorithm may be repeated, bearing in mind that:

$$L_m(n+2) \approx \frac{\Delta\psi(n+2)}{\Delta i_m(n+2)}, \tag{7.29}$$

$$\Delta i_m(n+3) \approx \Delta i_m(n+2)\frac{\Delta\psi(n+3)}{\Delta\psi(n+2)} \tag{7.30}$$

and consequently:

$$i_{se}(n+3) \approx i_s(n+3) + i_m(n+3). \tag{7.31}$$

The calculation of the estimated values of the secondary current samples continues until the end of the saturated fraction of the period.

If the waveshape of the secondary current is reproduced, the phasor may be calculated using the data window duration T_w equal to the period of the fundamental frequency component T_1, either calculating the non-rotating phasor components (3.22), (3.23), (3.24), (3.25), (3.19) or calculating rotating phasor components (3.26), (3.27), (3.19).

The above considerations show, how digital representation of the secondary current may be efficiently used for determination of time intervals in which the CT magnetic core is not saturated and transformation is correct, and how distorted waveshape may be processed to determine phasors. The presented methods are not unique, but perhaps represent the best compromise between the accuracy and efficiency.

An example of application of the above described methods for CT saturation detection and correction is shown in Fig. 7.7 for the case of a fault on transmission line simulated with use of EMTP-ATP program. In this case the CT saturation time constant was equal to 3ms while the input signal was sampled at 1kHz. One can see that in each period the CT is saturated transiently, mainly due to the presence of decaying DC component. When this component decreases, the CT saturation becomes shorter. It can be observed that the saturation detection, marked with red line in Fig. 7.7a, is correct both for positive as well as negative halves of the current waveshape. It is also seen that the primary current is reconstructed with quite a good accuracy (red curve in Fig. 7.7b).

a)

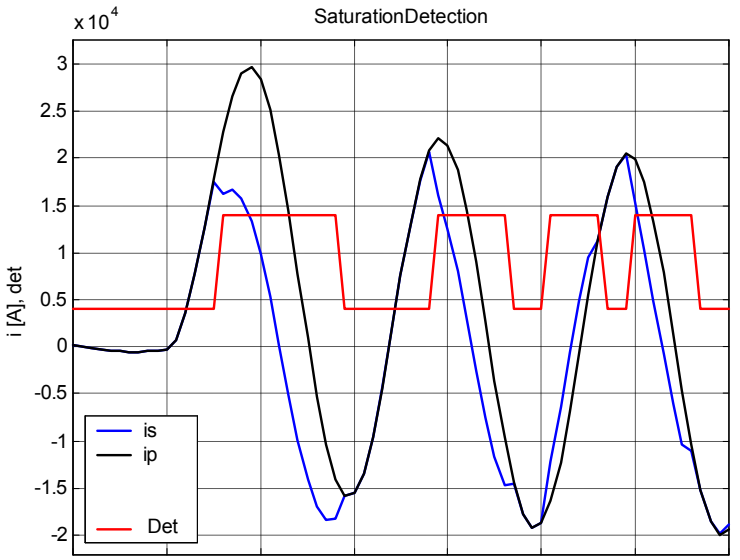

b)

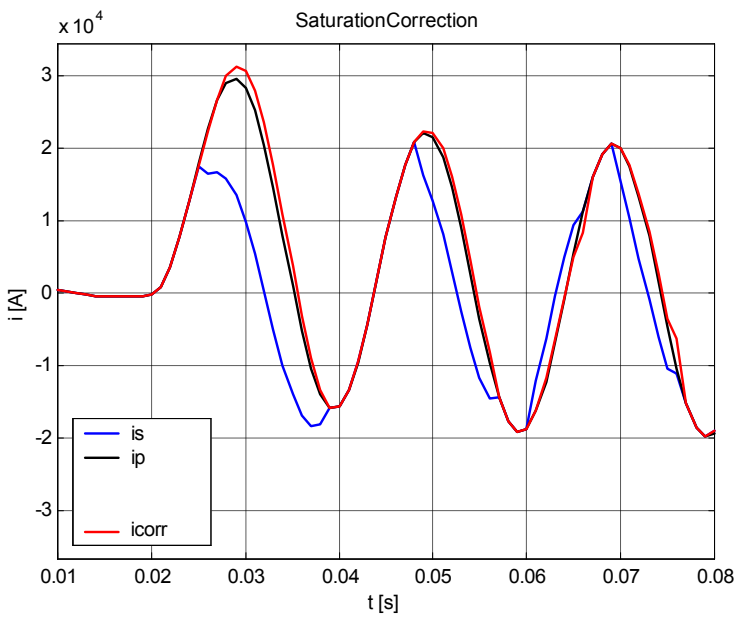

Fig. 7.7. Performance of the algorithms for: a) CT saturation detection, b) correction of the secondary current

8. DECISION MAKING

8.1. GENERAL CONSIDERATIONS

The protective relays are devices that are supposed to evaluate the state of the protected plant and to react properly in case of abnormal operating conditions. The relay final output is usually the command to trip the protected element or to raise an alarm, whenever it is necessary. The protection decision is mostly based on the locally measured criteria values and additional information from other protective relays and/or control centers. In this paragraph the possible approaches to the decision making are briefly outlined.

The protective devices of previous generations (electromechanical, also static) were frequently designed to generate its final output (trip signal) basing on comparison of selected signals and/or their combinations, often without direct measurement of the protection criteria. Numerical relays, on the contrary, first digitally measure the criteria values that are further compared with appropriate threshold values or characteristics.

The final decision-making is only one of the numerous logic operations performed by the protection relays. The logic structure of the protection embraces the following functional areas:

- detection of the abnormal or emergency condition (e.g. a short circuit),
- checking if the fault is within the protected zone,
- determination of the phases involved,
- exchange of information with other protection units, e.g. those from the opposite line ends,
- choice of the way of reaction (alarm, tripping, …),
- communication with personnel,
- automatic self-testing,
- auxiliary functions.

8.2. CLASSICAL APPROACH

Depending on the plant to be protected the protection relays generate their final decision basing on a single or multiple criteria signals. The number of criteria used in given case is a function of the plant complexity, size, rated power and its importance in power system.

8.2.1. DECISION MAKING WITH A SINGLE CRITERION

The simplest approach, adopted e.g. in overcurrent or over/undervoltage relays, consists in tracking the values of a single criterion signal. After the value has been measured, it is further compared with a pre-set threshold or located with respect to an appropriately shaped protection characteristic.

For the single dimension decision problem (single criterion taken into account) the discrimination is made when the criterion signal crosses or exceeds the pre-defined border value (threshold) separating two classes of events to be distinguished, e.g. normal operation vs. fault conditions. Depending on the problem the discrimination may be of one of the two types:

- overreaching, when the criterion value is higher than a threshold, e.g. for overcurrent protection, see illustration in Fig. 8.1, or
- underreaching, when the criterion value is lower than a threshold, e.g. for undervoltage protection.

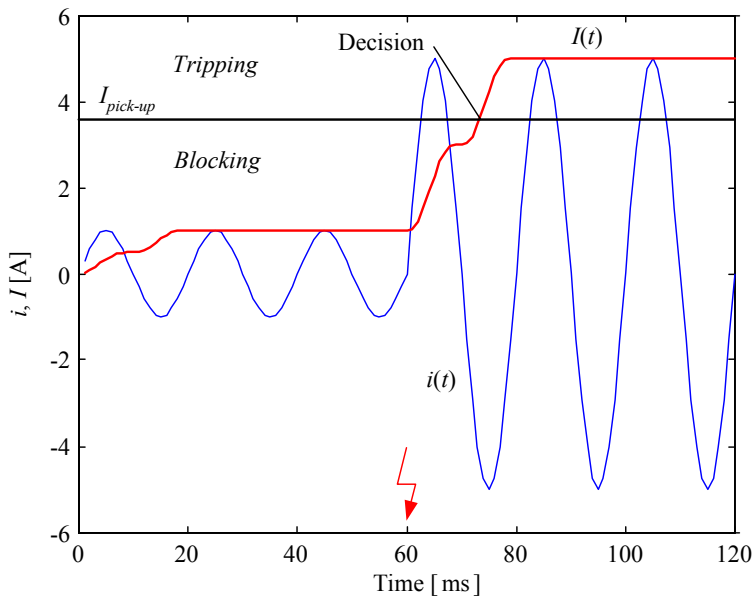

Fig. 8.1. Comparison of measured current amplitude with a threshold

With reference to Fig. 8.1, the decision to trip the protected element is taken when the measured current (instantaneous value or signal magnitude) exceeds the pick up value:

$$I(n) > I_{pick-up} \tag{8.1}$$

The decision threshold is to be set with care, i.e. taking into account the maximum expected load current and minimum fault current in the protected element. One should also note that the speed of decision-making may depend on the type of the measurement algorithm. The shorter data window is adopted, the faster reaching of the measurement steady-state and exceeding of the pick-up value.

Another situation exists when the applied criterion is a multi-dimension variable, as in case of impedance measures in distance relays. In such a case the decision is not taken by simple checking of (8.1) but by comparing mutual location of the measured complex variable with appropriately set characteristic. With reference to Fig. 8.2, the protection decision is made when the measured impedance vector is seen within the prescribed protection decision curve (here – Mho type). The protection characteristic should embrace the region of fault loop impedance for all in-zone fault cases, separating it from the region of normal operating conditions, as shown in Fig. 8.2b.

Distance protection relays of different manufacturers offer decision characteristics of various types, including Mho and polygon ones, with possibility of their quite easy shaping by setting a number of parameters.

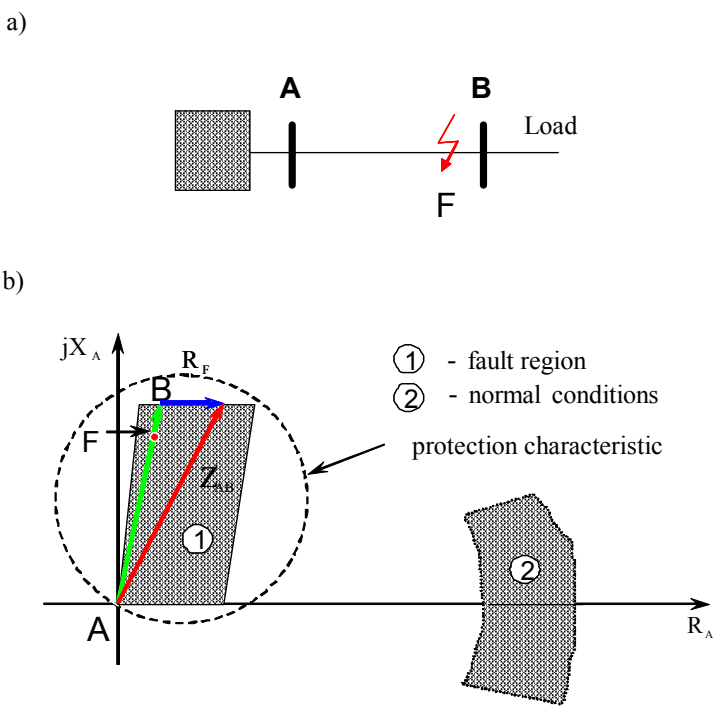

Fig. 8.2. Decision making in a distance relay:
a) simple power system with faults, b) impedance plane and zone concept

In the above-presented cases it was assumed that the protection decisions were taken without any intentional time delay. Usually one allows for some delay, waiting until the decision signal exceeds the threshold/characteristic for a number of consecutive time instants. Such a measure makes the relay less dependent on signal noise and sudden signal jumps or peaks, which results in more reliable final decisions.

Intentional delays are introduced, when the time dependency is needed, mainly for time grading, which should assure protection coordination, e.g. in:

- overcurrent protection of distribution networks,
- distance protection, with appropriate tripping time set for particular protection zones.

8.2.2. MULTICRITERIA AND ADAPTIVE PROTECTION

For the plants of complex structure or installed at a point where the operating conditions might be difficult to analyze, the single criterion decision making may be not secure enough, like it is e.g. in case of protecting of big power transformers or generators. For such objects, another option with multiple criteria is usually applied. In such a case some additional signals are delivered and processed by the relay. Thus the multi-criteria decision making brings improvement of protection reliability in terms of increased decision confidence, elimination of wrong decisions and higher speed of decision making.

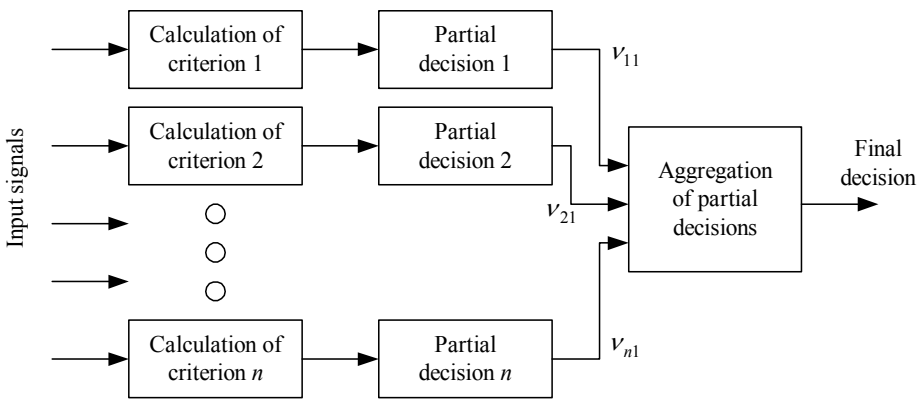

Fig. 8.3. Decision making with multiple criteria

A very basic scheme of multi-criteria decision making is shown in Fig. 8.3. The final decision is worked out in several steps including:

- calculation of particular criteria values,
- generation of partial decisions for all criteria (e.g. by comparing their values with some thresholds or characteristics, as described above),

– aggregation of partial decisions.
  Aggregation of partial decisions can be done with use of:
– simple Boolean logic operators (AND, OR),
– the strategy 'some-out-of-all' (the decision is taken when not less then the minimum number of partial decisions support one of the possible protection options),
– weighting factor method (confidence coefficients for particular criteria are used to express their relative strength or quality and to calculate the weighted support for final decision),
– decision rules of the IF … THEN form (certain knowledge is required to set up the rules),
– decision trees (equivalent to logic structure with combination of AND/OR operands),
– other techniques.
  Deterministic aggregation with weighting factors can be expressed as follows:

$$\delta_1 = w_1 v_{11} + w_2 v_{21} + ... + w_n v_{n1} \tag{8.2}$$

$$\delta_2 = 1 - \delta_1 \tag{8.3}$$

$$\delta_1 - \delta_2 > \Delta \rightarrow Dec_1 \text{ confirmed} \tag{8.4}$$

where:

v_{i1} - partial support values for the decision Dec_1 from the i-th criterion,

w_i - weighting factors for particular criteria,

δ_1 - total support for the decision Dec_1,

δ_2 - support for the opposite decision Dec_2,

Δ - discrimination threshold.

The partial decision support values v_{i1} may be crisp (taking values 0 or 1, where 0 stands for no support and 1 – for full support) or fuzzy (here any value between 0 and 1 is permissible, the larger the value, the higher the support).

The multi-criteria decision-making in a relay may sometimes be supported by the signals transmitted from other protection units or from the higher level control. Exchange of information between relays is often a source of information for protection blocking or stabilization.

External signals may also be a source of data for realization of adaptive or wide-area protection schemes. As an example of adaptive schemes application one could mention:
– adjustment of the power transformer differential relay sensitivity to the tap changer position,
– adjustment of the distance protection settings to the operating conditions of the parallel line (in operation / switched off),

– adaptation of the under-frequency load shedding strategy to the current loading of particular feeders,
– adaptive distance overreaching/underreaching schemes (first zone extended or shortened according to the information gained from the opposite line terminal/-s),
– a proposal of wide-area adaptive on-line coordination of the relay settings based on the so called multi-agent approach, etc.

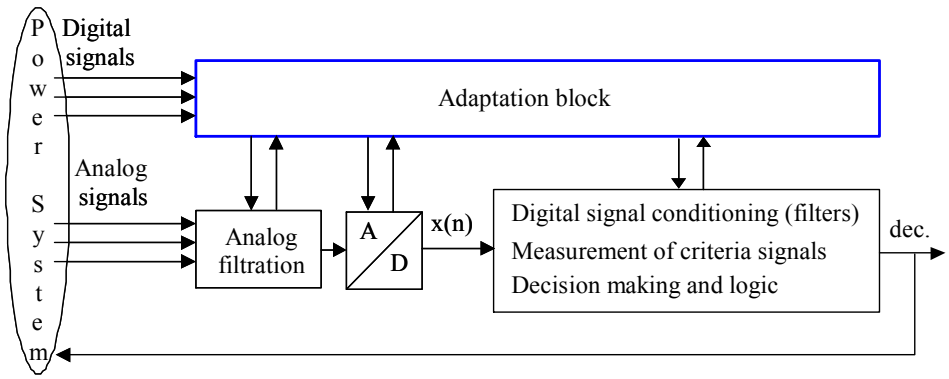

Fig. 8.4. Block scheme of an adaptive protection

Internally, from the functional point of view, the adaptation may be related to some changes in one or more of the following protection units (Fig. 8.4):
– analog filtration (switching to another set of filters),
– analog-to-digital conversion (change of sampling frequency),
– digital signal processing (selection of the processing algorithm, modification of the filters' frequency characteristics),
– measurement of protection criteria (change of the algorithm parameters and/or type),
– decision making (change of thresholds and decision characteristics, selection of new or additional criteria and logic signals).

Changes initiated by the adaptation block may include not only certain modification of selected algorithms but also their exchange for the ones better suited for given power system operating conditions.

8.3. NOVEL TECHNIQUES FOR DECISION MAKING

In the field of decision making several new techniques and tools have recently been developed and proposed in the literature to be applied for complex technical problems, also in power systems. Among the others the following are worth mentioning:

– statistic decision making (that mostly reduces to testing of statistical hypotheses related to the state of protected plant),
– application of fuzzy logic (instead of crisp signals and thresholds fuzzy signals and fuzzy settings are introduced),
– decision making by pattern recognition (application of neural networks),
– analysis of multiple alternatives (application of expert systems).

The latter three belong to the family of Artificial Intelligence and are described in more detail in Section 9. Here the technique based on statistical reasoning is presented only.

Unlike to deterministic approach, where the decision algorithm is precisely defined by decision thresholds either fixed or being changed according to a prescribed scenario, the statistic approach assumes that the decision signals may have probabilistic nature, thus calling for an appropriate procedure of reasoning. One may say that many parameters which affect phenomena in power systems are not known and may only be described by probability distributions. Similarly, in many cases the decision areas (representing classes of events to be distinguished) which often overlap in statistic terms can be viewed as overlapping of the probability density functions - see illustration in Fig. 8.5.

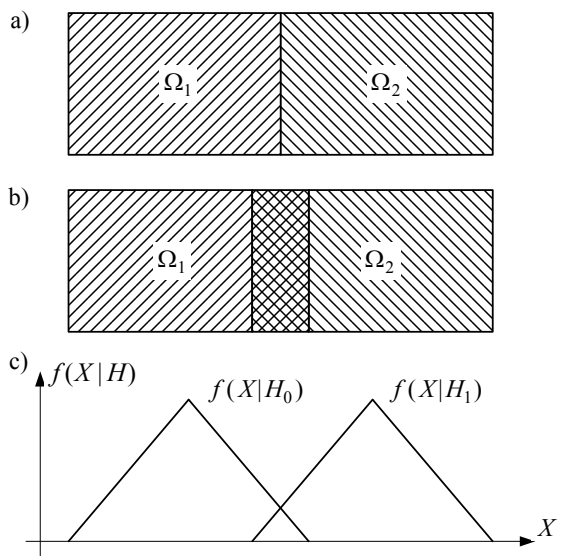

Fig. 8.5. Decision space and decision areas: a) ideal situation, b) real case, c) statistic interpretation

Statistical approach to the decision-making problem in digital protection assumes that criterion values can be considered as random variables and that required conditional statistics are known. Probabilistic nature of the decision vector is a result of

random localization of fault or such other conditions as fault resistance, fault angle, pre-fault load etc.

With statistical approach to the decision making problem various algorithms of hypothesis testing can be applied. The fundamental decision theory with probabilistic roots is the Bayesian approach. For practical technical problems the application of methods based on statistical hypothesis testing is recommended, where the hypotheses advanced could represent normal and faulty/abnormal operating conditions. When distinguishing between two hypotheses is required, one can use the Sequential Probability Ratio Test (SPRT). The approach can also be adapted for multiple hypotheses testing and in such a case so called Multi-hypotheses Sequential Probability Ratio Test (MSPRT) can be used. The SPRT methods use conditional probability density functions (PDFs) of the decision vector (for given classes of events) to generate the decision.

The Sequential Probability Ratio Test belongs to decision methods in which number of samples of the decision vector necessary to issue the decision is not pre-defined. The algorithm of the SPRT can be written in the form:

$$\Theta_k = \prod_{l=1}^{k} \frac{f_l(\boldsymbol{X}_l \mid H_1)}{f_l(\boldsymbol{X}_l \mid H_0)}, \tag{8.5}$$

$$If\left\{\begin{array}{c}\Theta_k \geq A\\ A > \Theta_k > B\\ \Theta_k \leq A\end{array}\right\} then\left\{\begin{array}{c}stop\ \&\ accept\ H_1\\ continue\ test\\ stop\ \&\ accept\ H_0\end{array}\right\}, \tag{8.6}$$

$$A = \frac{1-\varepsilon_1}{\varepsilon_0}, \quad B = \frac{\varepsilon_1}{1-\varepsilon_0}, \tag{8.7}$$

where:

$f_l(\boldsymbol{X}_l \mid H_i)$ - probability density functions (PDFs) of the decision vector $\boldsymbol{X}$ at the instant l after test starting for hypothesis H_i,

Θ_k - test index at the instant k,

A, B - probabilistic thresholds,

$\varepsilon_0, \varepsilon_1$ - assumed values of the first and second order error probabilities.

The above procedure minimizes values of the first and the second type error probabilities $\varepsilon_0, \varepsilon_1$. The first type error concerns situations in which hypothesis H_1 is recognized instead of H_0 (underfunction), while the second type error corresponds to the decision H_0 instead of H_1 (overfunction).

Application of the SPRT method is possible when the following conditions are satisfied:

- random decision quantities are at two different time steps stochastically independent,
- conditional probability density functions of the decision vector are known.

The required distributions $f_l(\boldsymbol{X}_l \mid H_i)$ may be calculated on basis of simulation cases or estimated taking into account distributions of all factors possibly affecting system behavior for given hypothesis (with the latter method sought functions can be assessed rather roughly, especially when dynamic distributions are to be found). One should understand that proper operation of the SPRT test depends heavily on the choice of an appropriate decision variable. Such a variable has to carry a lot of information on the phenomena being analyzed and its conditional PDFs for hypotheses H_0 and H_1 should be separated from each other to the highest possible degree.

The application of the SPRT algorithm for fault detection and fault type identification may serve as an example how the probabilistic technique can be used for decision making [B]. The conditional probability density functions of the decision variable $X=I_0$ (zero sequence current amplitude) for successive samples k after fault inception are shown in Fig. 8.6. It is seen that the PDFs change with time and their divergence for both hypotheses (ground vs. isolated fault) increases sample by sample, which also means that more and more information is delivered to the decision algorithm. For time instant k=6 first signs of CT's saturation can be seen (due to inaccuracy of current transformation some zero-sequence current is measured, distribution for hypothesis H_1 is no longer zero).

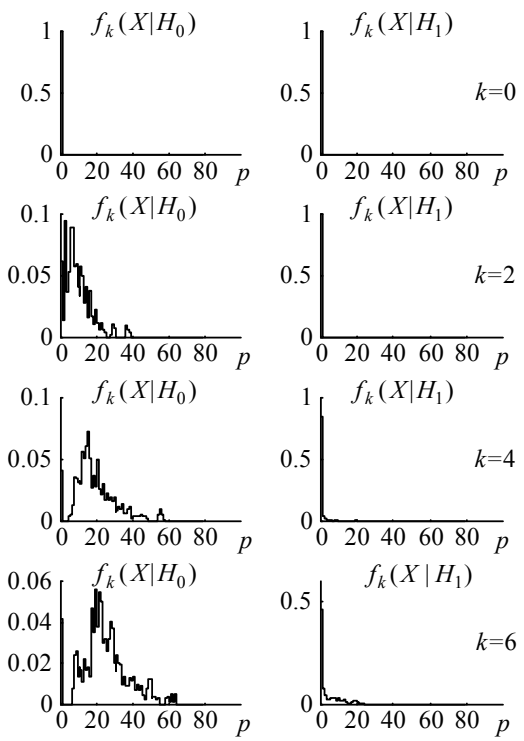

Fig. 8.6. Conditional PDFs for hypothesis H_0 - „ground fault“,H_1 - „isolated fault“

The simulative tests confirmed that the SPRT algorithm demonstrated excellent ability of fault detection. All cases were detected properly, mostly in the first or second sample after fault inception (in rare cases only more time was needed). Fault classification was made with exactitude of 97.2% and average time of 3 ms, which should be considered as a good result.

One has to admit that the application of SPRT based decision methods requires of course intensive simulative investigations and calculations to be done (conditional PDFs for the considered hypotheses must be known). Similar introductory work (off-line) is also necessary if other novel approaches (with use of Kalman filtering or neural networks) are to be applied. Contrary, on-line computational complexity of SPRT algorithm is relatively small; therefore it may be easily implemented in real time protection systems.

9. ARTIFICIAL INTELLIGENCE TECHNIQUES

9.1. GENERAL CONSIDERATIONS

Even though the digital protection devices become better and better, offering fast and accurate signal processing algorithms, possibilities of almost free shaping and setting of decision characteristics, as well as number of additional auxiliary functions, there are some situations and plants where classical approach and methods may not guarantee proper relay operation. It is so e.g. for:

- overcurrent protection of highly loaded transmission/distribution lines,
- differential protection of contemporary power transformers (low value of second harmonic signal used for stabilization),
- protection on distribution network with high penetration of distributed generation,
- protection of networks with FACTS devices, etc.

In all abovementioned cases the normal operation and overload/fault regions may overlap and thus it is difficult or even impossible to set a threshold that would separate the operation and blocking areas completely. Besides, even if the steady-state loci of measured criteria values are situated within proper decision areas, they may be seen in wrong part of the decision space during measurement transients. Therefore, new intelligence is needed to improve operation of protection devices for such situations.

Artificial Intelligence (AI) is a sub-field of computer science that investigates how the thought and action of human beings can be mimicked by a machine. The intelligence can be understood as the ability of a living being or a machine to organize external information, observations and experiences and to discover relationships that can be used to evaluate the information. The mimicking of human intelligence should include the following aspects:

- making rational decisions,
- dealing with missing or corrupted data,
- adapting to existing situations,
- improving the scheme in the long time horizon basing on the accumulated experience.

Considering the digital protection (Fig. 9.1) as a device processing the input signals (analog and digital signals from power system) with the aim of generating the final decision (alarm or trip command), one can say that the protection realizes in fact one of the two functions. If the relaying task is treated as a decision-making problem, then by using its algorithm (knowledge) the relay should decide whether to trip or restrain itself from tripping. Here the fuzzy reasoning or expert systems are well suited and

find their application for many protection problems. On the other hand, if the protection task is considered as a kind of pattern recognition problem (monitoring chosen input signals, called patterns, should lead to the protected plant state classification), then the artificial neural networks may seem a proper tool for realizing given protection function.

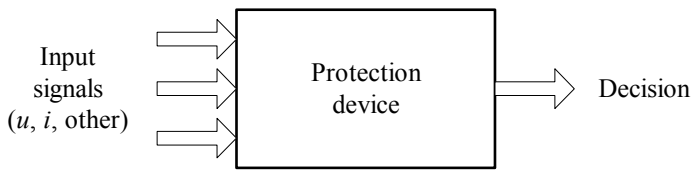

Fig. 9.1. Protection relay seen from outside

The literature survey shows that in most cases the neural networks and expert systems are applied for power system protection tasks. A number of proposals of AI techniques applications have been issued, mainly for protection of transmission and distribution lines, power transformers, as well as for diagnostics and analysis of disturbances.

In the following sections the key features, advantages and disadvantages, as well as fields of applications of particular techniques of Artificial Intelligence are described.

9.2. ARTIFICIAL NEURAL NETWORKS

9.2.1. BASIC INFORMATION

Artificial Neural Networks (ANN) represent a modern approach to decision making that is nowadays quite frequently proposed also for power system protection and control applications. The ANNs perform actions similar to human reasoning which rely on experience gathered during so called training. Advantages of neural computing methodologies over conventional approaches include faster computation, learning ability, robustness and noise rejection. Once trained the ANN should possess the feature of knowledge generalization, which means that they should reasonably respond to the situations that had not been presented during training. The ANNs are mainly used for classification and decision-making in case of problems that are not fully described in the deterministic way or when their description (model) is non-linear or heavy complicated.

The ANNs are artificial units resembling the structure, internal connections and the way of functioning of the human brain. Application of ANNs results from the possibility of their training for particular task, so that the neural network becomes a mathe-

matical model of the system or process being analyzed. Independently of the ANN structure, the neural networks consist of small computational units called neurons. Single neuron performs computation of the weighted sum of its input signals:

$$a = \boldsymbol{X} * \boldsymbol{W} + b, \tag{9.1}$$

where: $\boldsymbol{X}$ – vector of input signals [N×1],
$\boldsymbol{W}$ – vector of synaptic weights [1×N],
b – bias coefficients.
on which then a usually non-linear activation function is imposed.

The design of a neural pattern recognition unit (both single-neuron and more complex structures) is based on the ANN training, which is realized with use of a set of prepared learning patterns and appropriate training algorithm.

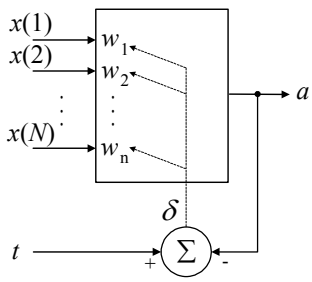

Fig. 9.2. Single neuron training scheme

In the process of neuron training the values of synaptic weights are automatically adjusted in such a way that at the output of the neuron (generally – an ANN) a signal of desired level (value) is generated. With the so called *supervised training* methodology (illustration in Fig. 9.2) the synaptic weights are corrected after successive presentations of the input-output pairs ($\boldsymbol{X} - t$), with minimization of an appropriate goal function. The goal function can be e.g. the mean-square error, defined as:

$$mse = \sum_{k=1}^{Q} \delta(k)^2 = \sum_{k=1}^{Q} (t(k) - a(k))^2 , \tag{9.2}$$

where: Q – number of signal patterns.

The neuron weights are modified according to:

$$w(j+1) = w(j) + \eta(j)\delta(j)x(j) , \tag{9.3}$$

where $\eta(j)$ – time-dependent learning rate.

Understanding that the efficiency of single neuron in solving of more complex problems is quite low, various type neuron connections, called neural networks, have found practical applications. An example of such a network (multilayer perceptron) is

shown in Fig. 9.3. The multilayer perceptron consists of several layers of neurons, being interconnected, that process input signals with unidirectional flow of information (feed forward).

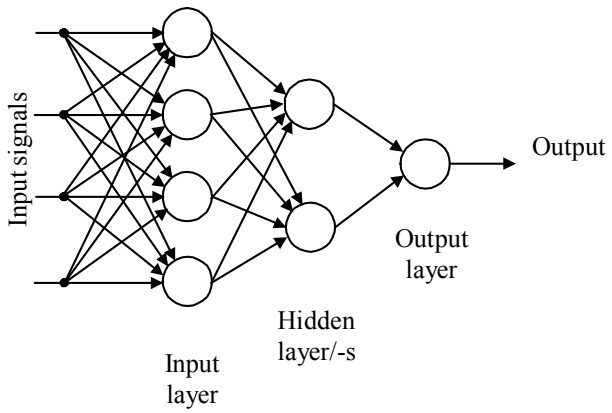

Fig. 9.3. Multilayer perceptron architecture

There exist a number of neural network types. The most frequently applied are (in brackets the frequency of application for power system protection and control tasks are given):

- multilayer perceptron networks (81%) – three- or four-layer feed-forward networks, networks with radial basis function,
- Hoppfield networks (6%) – Bolzmann machines, Gauss networks, chaotic networks,
- Kohonen networks (8%) – two- or three-dimensional grid nets,
- others – less frequently used.

In case of multilayer networks more complex training algorithms are utilized, like the method of error backpropagation. The *backpropagation* (BP) is a recursive algorithm based on a gradient-search optimization method applied to an error function. The neurons' weights are iteratively adjusted until the desired accuracy level is achieved. The net errors are propagated back from output layer to hidden layers. Variable „learning rate" and „momentum" techniques are often utilized with the aim of reaching faster convergence and more accurate results.

The other mode of training, called *unsupervised training* (data self-organization concept), is based on comparison of the inputs with previously encountered patterns. If coming input is similar to any of the patterns, it will be placed in the same category, otherwise a new category (cluster) will be assigned, whereas category proliferation is controlled by a threshold. After the learning (cognition phase) the user defines or labels the clusters according to some criterion.

9.2.2. ANN APPLICATION TO PROTECTION PROBLEMS

The neural networks are believed to possess a generalization feature, which similarly to human reasoning makes them good tools for identification of patterns, even if not all representative features of the patterns are well defined or when some data is missing. Due to built-in neuron activation functions the ANNs are well suited to represent non-linear problems and bring answers to difficult protection and control questions, some of them being outlined in this section.

The neural networks for pattern classification are usually single-output structures. They may, however, also have multiple outputs, each of them assigned to specific purpose. Such networks can be used e.g. in fault classification or in multidimensional control schemes, where the outputs of particular neurons of the output layer are sent to appropriate points of the control structure.

The following (selected) examples of the ANN applications for power system protection and control tasks are quite representative:

- protection of transmission and distribution lines (fault detection and classification, fault direction discrimination, adaptive distance protection, distance relay for series compensated lines, autoreclosing and fault location functions, high impedance faults detection, high frequency based relaying),
- power transformer monitoring, protection functions (e.g. stabilization against inrush conditions), diagnostics,
- generator protection (e.g. out-of-step – described in more detail below),
- fault location and analysis in substations,
- other non-protection tasks (on-line security assessment, load forecasting, optimisation tasks in power plants, signal analysis, process control and automation).

It is good to know what are the problems and issues that should be addressed when an ANN-based solution is to be developed for an application at hand. Generally, one should take into consideration the following points:

- ANN structure type,
- ANN size (number of layers and neurons in particular layers),
- neuron activation function (may be different in given layers),
- number and type of input signals,
- representative set of patterns,
- initial values of synapse weights and biases (usually random values),
- the training algorithm itself (depends on the ANN type),
- generalisation vs. memorisation dilemma.

Having the ANN type chosen for given task (e.g. multilayer perceptron) one should decide on the size of the neural network. It has been proven that infinitely large neural network with just a single hidden layer is capable of approximating any continuous function. In practice ANNs with one or two hidden layers are in use, with the number of neurons dependent on the number of ANN input signals and the size of training set.

The neural network size is sometimes chosen arbitrarily, but it can also be optimized, e.g. with use of a genetic procedure.

The last of the above-mentioned problems (generalization vs. memorization) results from the very fact that the well trained ANN is expected to operate correctly not only for all the patterns from the training data set, but also for all other possibly appearing data that were not presented to the ANN during training. Such a feature means generalization of the acquired knowledge, which is different from focusing on the training cases only (memorization). The knowledge generalization feature can be assured when appropriate techniques, like randomization of training set elements, are applied.

Out-of-step (OS) protection with application of ANN

The out-of-step conditions (loss of synchronism) of a synchronous machine may occur as a result of loss of excitation or during pole slipping. The pole slipping condition can arise after a long power system fault or when a tie line between two systems is opened. The parameter that supervises the detection of pole slipping is the impedance vector measured at the machine terminals. Crossing of the impedance vector trajectory with properly set characteristic on the impedance plane is checked to detect the pole slipping. The other methods used for OS protection are based on the equal area criterion, direct method of Liapunov or rate of change of apparent resistance augmentation. With a communication channel available, an OS protection system may use observations of phase difference between substations. It must be said that all the above methods allow detecting the OS conditions not before the first slip actually occurred.

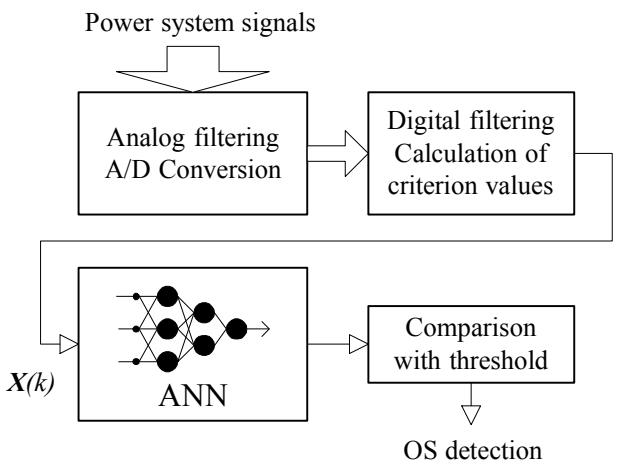

Fig. 9.4. Neural OS protection arrangement

Since the commonly used methods of loss of excitation and pole slipping protection are not always fast and secure enough, it is justified to search for new solutions applying AI approach. Hence, appropriate relaying procedures have been considered and adequate ANN solutions have been developed and tested [C]. The general scheme of the neural OS protection scheme developed is shown in Fig. 9.4. The decision part of the protection is realized with help of an ANN performing typical pattern recognition with appropriately chosen vector of criterion signal samples ***X(k)***. The decision (criterion) values have to be previously calculated from available power system signals with use of dedicated digital processing algorithms. The ANN was assumed to produce output equal to 0 for stable patterns and 1 for OS conditions. For the classification purpose a threshold value set to 0.5 was introduced. All the cases for which the ANN output is lower than 0.5 were classified as stable and those for which the threshold was exceeded were recognized as OS cases.

To obtain data for training of ANNs and further testing of the OS protection, the following simple single machine – infinite bus system has been modeled (Fig. 9.5) with use of the ATP software package. The synchronous machine G1 is connected to the infinite bus system S1 (220 kV) via the block transformer T1 and a 200-km long double-circuit line L1. Within the transmission line L1 a number of symmetrical faults on one of the line circuits were applied, some of them responsible for further developing OS conditions.

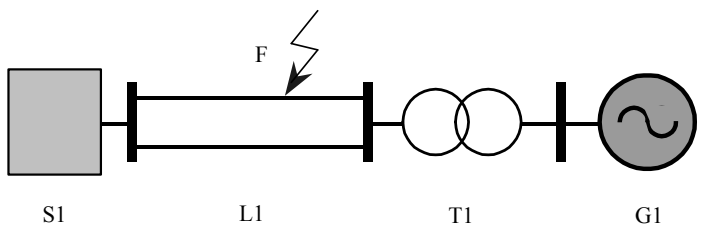

Fig. 9.5. Test power system modelled

Generator output voltages and currents as well as its angular speed were registered in ATP output files. Additional features like voltage/current amplitudes, components of generator power etc. were obtained after digital processing of voltage and current signals. In order to choose the best signals for application as ANN input features, the statistical properties of available signals were determined. The analysis of calculated conditional PDFs allowed sorting the decision signals according to their relative recognition strength. Ultimately, the machine angular frequency deviation $\Delta\omega$ was taken as the most valuable recognition feature in the investigated case.

The ANN input vector ***X(k)*** was being created on-line from a number of signal samples captured with use of a sliding data window (DW). The criterion signal $\Delta\omega$ is observed with the measurement rate MR (time distance between two successive sam-

ples, not necessarily equal to the sampling period) within the DW having the length being a whole multiple of MR and number of samples *m* (DWL=MR*m). The data window beginning (DWB, measured from the fault inception time) is moving and thus consecutive sets of signal samples (input vectors) are delivered to the ANN-based reasoning unit. The case studies have been done for ANNs fed with input vector *X(k)* consisting of $\Delta\omega$ samples captured with MR=120 ms within the data window having DWL=360 ms (m=3).

The choice of the ANN structure and size for the neural OS protection scheme developed has been done with use of the genetic optimisation procedure (see section 9.4 for more details). The nets constituting the population of individuals were graded according to two different quality indices, i.e. mean square error of the net output Q_{ms} (squared difference between desired and actual output values) and testing efficiency Q_{eff} (percentage of properly recognized OS cases). Consequently, different results of the genetic process have been reached. After performing the training the "best" nets obtained after 50 generations had 6-1 and 3-1 neurons for the Q_{mse} and Q_{eff} grading indices, respectively.

The ANN-based OS protection scheme developed has been thoroughly tested with ATP-generated power system signals. The scheme displayed high efficiency and very short time of OS detection. The OS protection equipped with the "best" ANNs (graded with quality indices equal to 1.0) displayed 100% selectivity which means that all considered ATP testing cases were correctly classified.

Comparing to other existing impedance-based OS protection devices, a kind of prediction of approaching machine instability is performed instead of traditional detection of actually occurring phenomena. The decision is taken within approx. 500ms after fault inception (some 300-900 ms before actual OS appeared), thus leaving enough time for an appropriate action (machine tripping, fast valving) to protect the generator from stresses and preserve the stability of power system. Wide robustness features of the scheme with respect to both various fault types and other synchronous machine ratings have also been confirmed.

9.3. FUZZY LOGIC SYSTEMS

9.3.1. THEORETICAL BACKGROUND

The other group of methods that have found application in power system protection and control is based on so called fuzzy sets theory or fuzzy logic. Fast development of fuzzy techniques has been connected with the need of finding an adequate way of description of problems and phenomena being ambiguous and/or imprecise in nature. Since utilization of classical theories with two-valued logic was inefficient for such issues, one has developed theoretical foundations for unsharp/fuzzy sets along with

respective tools and algorithms for operations on such sets. The multi-valued logic has become an extension of Boolean logic for the cases of imprecise rules and values.

The very basic definition of a fuzzy set can be expressed in the form:

$$A=\{(x,\mu_A(x)); x\in \boldsymbol{X}\}, \qquad \mu_A:\boldsymbol{X}\rightarrow[0,1]. \tag{9.4}$$

Each element of the crisp set $\boldsymbol{X}$ has been assigned a membership function μ_A describing the degree of membership of given element to the fuzzy set $\boldsymbol{A}$. Full membership corresponds with the value 1, whereas lack of membership – value 0. Values of μ_A from the range (0, 1) denote partial membership to the fuzzy set $\boldsymbol{A}$. The definition (9.4) is well suited for sets of elements of any kind, including also imprecise "linguistic" statements determining e.g. "high temperature" or "low angular velocity". Such statements, being close to intuitive and natural description of the process, can be then used to design of a fuzzy controller or regulator, provided appropriate rules of operation in the form "IF … THEN …" have been developed.

In power system protection and control issues the fuzzy sets specified on the objects being real numbers are of special importance, since the decision or control signal is usually worked out with relation to the input signals being real numbers. The fuzzy set $\boldsymbol{A}$ determined on the set of all real numbers $\boldsymbol{R}$ is called a fuzzy number, if there is defined a membership function $\mu_A:\boldsymbol{R}\rightarrow[0,1]$, being normal, convex and at least fragmentary continuous.

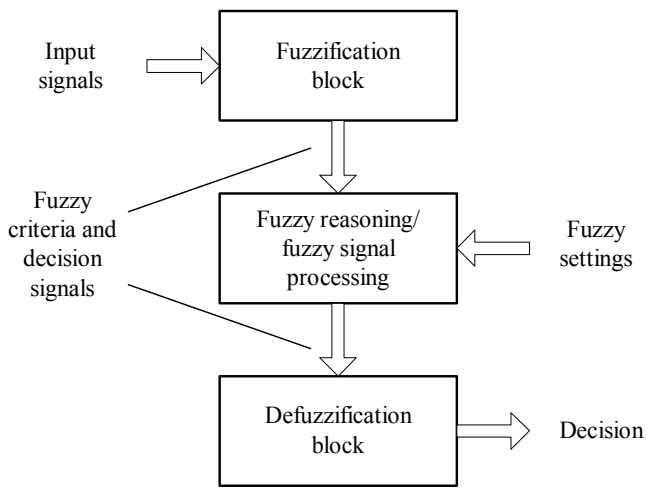

Fig. 9.6. Architecture of a fuzzy protection relay or control unit

Practical utilisation of the fuzzy set theory as well as the rules of operations on fuzzy numbers leads to the general scheme of the fuzzy protection/control device presented in Fig. 9.6. The following main blocks can be distinguished here:

- *fuzzification*, where the real input signals are converted into their fuzzy counterparts (fuzzy numbers),
- *fuzzy reasoning*, where the fuzzy criteria signals are processed and – after comparison with fuzzy settings – some fuzzy decision/output signals are generated,
- *defuzzification*, which is understood as conversion of the fuzzy outputs into crisp numbers (real output signal or decision).

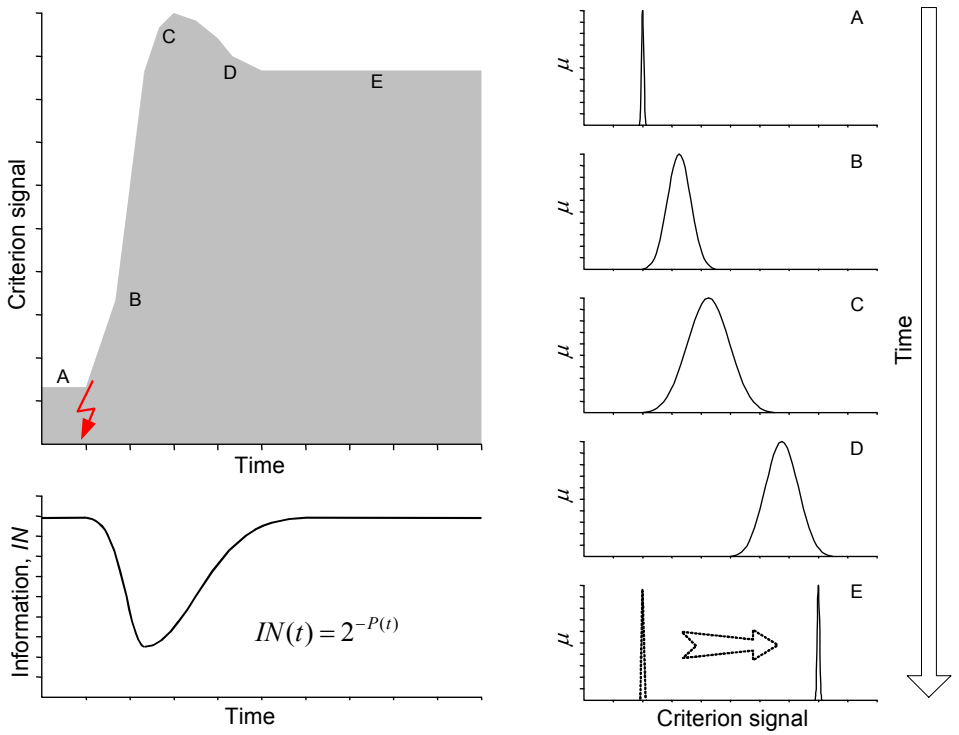

Fig. 9.7. Classical and fuzzy criteria signals

An example of the fuzzy criterion signal, defined for the measured amplitude of fault current, is shown in Fig. 9.7. Since the non-fuzzy signal is dynamic, the corresponding fuzzy signal changes with time accordingly. The location of center of the membership function μ depends on the actual current magnitude value, while the degree of fuzziness reflects the degree of confidence to the dynamic measurement results at given time instant. The width of membership function is directly related to the rate of change of the criterion signal, which is also a function of applied digital filters and specific measurement algorithms, and in a way encodes the degree of conformity between accurate (but not exactly known) and measured criterion signal values. The amount of information *IN* in the signal is inversely proportional to the degree

of fuzziness, expressed by the area P under the membership function μ, and is the highest at the steady state of measurement (points A, E), but the lowest during transient, when the signal magnitude changes dynamically (points B, C and D). Utilization of the fuzzy criteria signals instead of their real counterparts allows for mathematical depiction of the measurement uncertainty, especially during transients, that is also just after the fault/disturbance inception.

As a consequence of using fuzzy criteria signals the notion of fuzzy setting is also introduced, understood as a fuzzy number separating the two states to be distinguished. For example (see Fig. 9.8), instead of classical decision threshold I_0 of the overcurrent protection one can propose a fuzzy curve, that separates the blocking and tripping regions in a smooth way. Unambiguous decision (with the degree of confidence 1.0) can be taken for current magnitudes lower than I_1 and higher than I_2, whereas for the values within the range (I_1, I_2) appropriate value of the membership μ from the range (0, 1) is assigned, coding the grade of the signal membership to the category of fault cases. The higher the membership value μ, the more clearly (with higher certainty) the decision to trip the protected plant can be taken. One can say that application of the fuzzy settings creates a remedy for many problems with settings of classical protection relays, being often a peculiar compromise between sensitivity and selectivity.

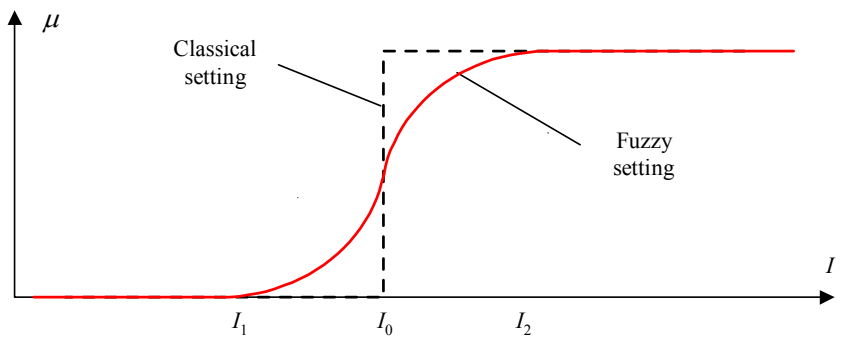

Fig. 9.8. Classical and fuzzy overcurrent decision threshold

Fig. 9.9 illustrates one of the possible ways of comparison of the fuzzy signal with fuzzy setting. The degree of the threshold exceeding (also a value within [0, 1]) is defined as a ratio of the areas P^* and P, where P* stands for this part of the area under the fuzzy signal membership function that is also situated under the fuzzy setting curve, i.e.

$$\nu = \frac{P^*}{P}. \tag{9.5}$$

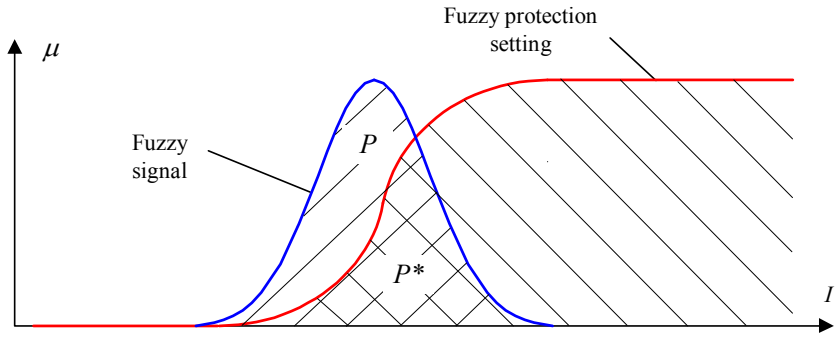

Fig. 9.9. Comparison of fuzzy decision signal with fuzzy threshold

With such a way of comparison, if the signal ν□□ (non-fuzzy number) is interpreted as the grade of meeting given criterion, it is not necessary to perform its defuzzification. It can be directly used for decision making (through comparison with simple threshold) or for working out the final decision in multi-criteria protection schemes, where a number of various criteria signals are analyzed and evaluated in parallel. Introducing the weighting factors w_i for particular criteria values, the resulting support grade for protected plant tripping can be defined as a weighted sum:

$$\delta = \sum_{i=1}^{N} w_i \nu_i \ , \tag{9.6}$$

and the final protection decision is taken after the value of δ exceeds certain non-fuzzy threshold Δ. This approach is called weighting factor aggregation method and can be treated as a simplified version of fuzzy reasoning.

Application of other comparison methods, e.g. based on product or implication of the fuzzy sets, leads to generating output signal being also a fuzzy number. Thus there is a need of its converting back to a real value (*defuzzification*). Among numerous methods of defuzzification one should mention the following three that are most frequently used: *center average defuzzification*, *center of gravity (center of area) method*, *maximum of membership function*.

9.3.2. APPLICATION EXAMPLES

Among the most important virtues of fuzzy systems that imply application of fuzzy theories in protection practice, the following should attract the reader's attention:

- ability of processing of uncertain information, inaccurate and/or corrupted data,
- possibility of expressing of non-sharp relationships and rules in a way close to natural language (linguistic variables, IF … THEN … rules),
- quite easy interpretation of the internal signals of a fuzzy system,

- improvement of efficiency and selectivity by decision-making in protective relays thanks to application of fuzzy settings and fuzzy decision characteristics,
- relatively simple, intuitive setting of the input/output membership functions (at least for the first, not-optimized scheme version),
- simple description of systems, for which a detailed mathematical model is too complex or is not known.

Among the interesting application of fuzzy logic in power systems, and especially in power system protection and control, one can enumerate the following:

- identification of fault type in transmission lines,
- fault location on a line,
- fuzzy multi-criteria protection of power transformer,

and also, being examples of non-protection applications:

- fuzzy controllers of voltage and angular speed of synchronous machines,
- diagnostics of power transformers,
- network planning and security assessment,
- reactive power control,
- load forecasting, etc.

Below an example of fuzzy scheme is described that was intended for improvement of power transformer differential protection [D]. The scheme concentrates on the aspect of protection stabilization for the situations of inrush with low level of second harmonic in the differential current.

Fuzzy Logic Based Multi-Criteria Stabilization of Transformer Differential Protection

Although differential protection has been successfully used for decades to protect power transformers against faults, its implementation (even in digital technique) is not free from errors which result in improper functioning either as undesired delay or lack of tripping for internal faults or as unwanted tripping for magnetizing inrush conditions. During normal operation of power transformers the magnetizing currents are very small, usually below 1% of the rated currents. However, due to nonlinear magnetizing characteristic an increase of the core flux amplitude by 20% causes an increase of the magnetizing current 10-20 times. In the latter case the harmonic spectrum of the current shows domination of the fundamental harmonic, however, the 2^{nd} harmonic exceeds 30-40% of the fundamental one. Magnetizing inrush currents caused by high DC components of the flux, which result from sudden increase of the terminal voltages, may also become very high. The current level depend on various factors, however the dominant ones are point on wave of the voltage signal, residual flux in the core as well as source impedances. Excessive magnetizing currents may also arise as a result of voltage recovery after clearing of a nearby fault, change of the character of a fault or out-of-phase synchronizing of a connected generator.

Numerous single or compound criteria are usually used or proposed in the literature to discriminate inrush conditions and to prevent unwanted tripping. They are based on

second harmonic restraint, current waveform analysis, model based methods, flux restraint, etc. Since all the methods mentioned display certain limitations and cannot classify all possible inrush cases correctly, a fuzzy logic based stabilization algorithm of transformer differential protection has been developed. The new fuzzy stabilization algorithm employs second harmonic content and DC ratio measured in differential signal to discriminate inrush cases. It has been noticed that when during transformer energization the second harmonic ratio drops below 10% level – at the same time DC component ratio remains at high level. Thus the performance of stabilization algorithm may be enhanced by adding DC ratio signal as an additional decision variable.

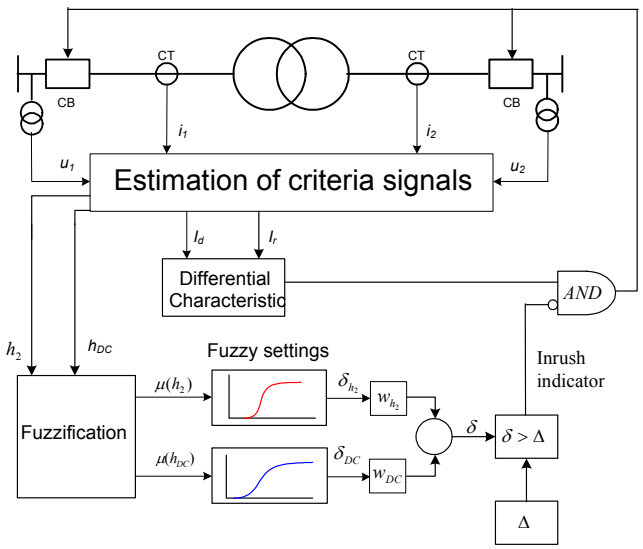

Fig. 9.10. Block scheme of the transformer differential protection with fuzzy stabilization algorithm.

In Fig. 9.10 the transformer differential protection scheme with proposed fuzzy blocking algorithm is presented. One can see that decision-making process is based on two signals. The first one comes from the standard percentage differential characteristic which is responsible for tripping signal generation. The second one is derived from fuzzy stabilization block and indicates when inrush conditions take place. All demanded criteria values are calculated in block responsible for estimation of criteria signals. The magnitudes of fundamental component I_1 and the 2nd harmonic I_2 of differential currents are extracted with use of traditional full cycle Fourier filters (a pair of sine and cosine filters), while the DC component in differential current I_{DC} is calculated using the algorithm based on full cycle averaging of the current, which corresponds to signal filtering with 0-order Walsh filter. The DC component is extracted online until potentially accurate measurement results are guaranteed, i.e. when 21 current samples (full cycle + 1 sample) after event inception are available. Then using the

determined initial value and time constant of DC component following samples of the DC signal are calculated.

Instead of crisp comparison the criteria signals are here compared with appropriate fuzzy setting. First, when 2nd harmonic ratio $h_2 = I_2/I_1$ and DC component ratio $h_{DC} = I_{DC}/I_1$ are estimated, fuzzification process takes place. In Fig. 9.11 an example of second harmonic ratio fuzzification is shown for the case of transformer energization. It is seen that during the first few ms after sudden signal increase the membership function $\mu_1(h_2)$ of the fuzzified signal obtained is quite broad, which can be understood as a very small confidence to the measurement results (not settled down yet, transient still in course). The membership function $\mu_2(h_2)$, for the period when the measurement process approaches its steady-state (e.g. at t=70ms) is much narrower (almost crisp), which allows to make protection decisions with higher confidence

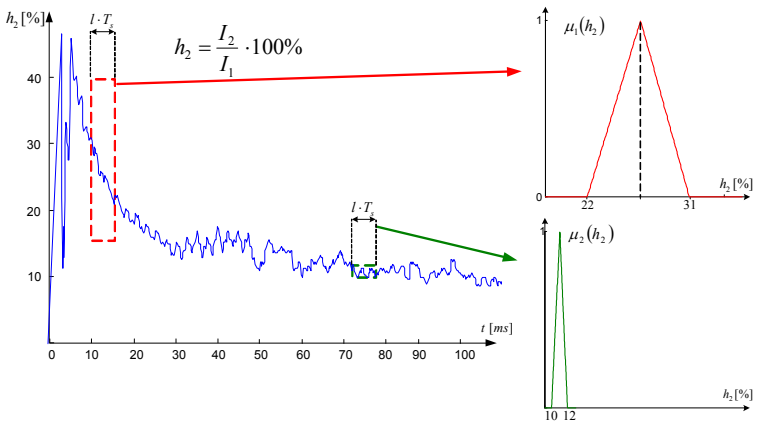

Fig. 9.11. Fuzzification and fuzzy representation of criteria signals

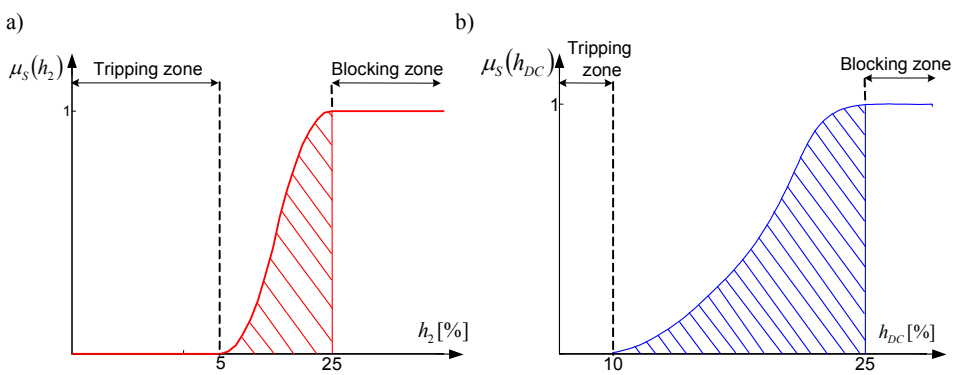

Fig. 9.12. Assumed fuzzy settings for: a) second harmonic content and b) DC component ratio

In the next step the fuzzified criteria signals are compared with appropriate fuzzy settings (see Fig. 9.12). The membership function of fuzzy setting are based on the designer's experience and results of statistical analyses of signals achieved form simulative test done in EMTP. It has been assumed that if the second harmonic content is less than 5% the inrush state is unlikely and, on the other hand, when this rate exceeds 25% transformer saturation is undeniable. As far as fuzzy setting for DC component ratio $\mu_S(h_{DC})$ is concerned the same reasoning was applied. It has been assumed that if the DC component ratio is less than 10% the inrush state is unlikely and, on the other hand, when this rate exceeds 25% transformer saturation is undeniable. According to such assumptions the fuzzy setting functions $\mu_S(h_2)$ and $\mu_S(h_{DC})$ are a kind of saturable curves changing gradually from 0 to 1 (see Fig. 9.12a,b).

The fuzzy comparison was performed according to the method illustrated in Fig. 9.9 and the formula (9.5). As a result of comparison two coefficients were achieved, namely: δ_{h2} - which specifies the degree of satisfying the 2nd harmonic restraint criterion and δ_{DC} - which defines the degree of satisfying the DC component restraint. Then both values were processed according to the multiplicative aggregation:

$$\delta = \left(w_{h_2} \cdot \delta_{h_2}\right) \cdot \left(w_{DC} \cdot \delta_{DC}\right) \tag{9.7}$$

where weighting factors w_{h2} and w_{DC} are equal to 1, but can be changed if required.

Such calculated final decision support coefficient δ was compared with additional threshold Δ equal to 0.5. If coefficient δ was greater than the threshold an indication on inrush state was issued, which should result in relay blocking.

The developed fuzzy stabilization scheme has been tested in simulative way with ATP generated signals. It has been confirmed that significant improvement of the protection stabilization function was obtained with introduction of criteria signals fuzzification. The implementation of fuzzy processing in the form proposed (triangle membership functions, filter-type calculation algorithm and simple comparison with the settings) should not pose any technical problem since the algorithm is not computationally exhaustive. Application of the proposed stabilization criteria in fuzzified form allowed for faster excluding of magnetizing inrush condition during faults, which can be also seen as a mean of relay response speed-up. The stabilization scheme with combined fuzzy second harmonic and DC restraint enabled furthermore detecting transformer internal faults that may occur during transformer energization.

9.4. EXPERT SYSTEMS

The Expert Systems (ES) can be treated as a kind of software that in certain formalized way expresses and thus simulates the way of reasoning of a human expert by solving tasks from given knowledge domain. The design and application of expert systems finds justification in situations when the traditional data processing is highly time-consuming, because of either complex computational algorithm or big amount of

data. Then (see Fig. 9.13) instead of algorithmic methods one can utilize techniques of intelligent searches, moving up to a higher generalization level, i.e. from processing of simple data and facts to the reasoning in the space of knowledge and rules.

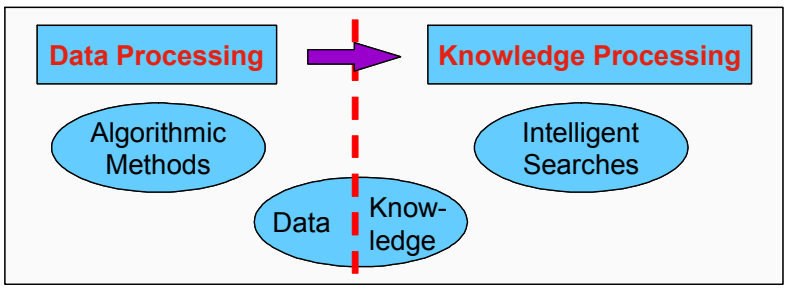

Fig. 9.13. Data processing and knowledge mining

9.4.1. EXPERT SYSTEM COMPONENTS

An expert system is usually organized as it is schematically shown in Fig. 9.14. The components of ES are:

- Knowledge Base – containing the knowledge about the system, its functioning, rules of problem solving, etc.,
- Data Base – including the facts, which generally describe the domain and the state of the problem to be solved,
- Inference Engine – with the reasoning principles and conflict resolution strategies.

The block connections in Fig. 9.14 suggest that there exist unidirectional (read-only) information flow from the KB to the Inference Engine and bidirectional exchange of data with the DB. This is because during data and knowledge processing new facts are created that should be stored in the Data Base for further usage.

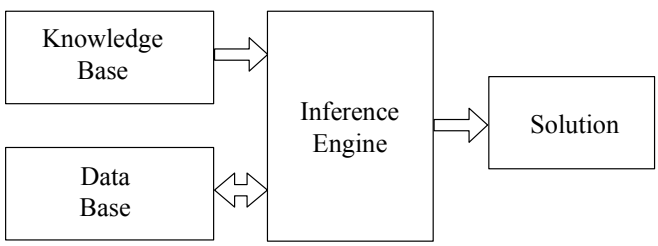

Fig. 9.14. Block scheme of an expert system

The most important blocks of the ES structure, i.e. Knowledge Base and Inference Engine contain the information provided by human experts. Potential experts are those who possess knowledge and strong practical experience in particular domain. They are often skilful persons that can do things other people cannot. The experts should, however, be capable of expressing their knowledge in the form of rules for problem solving, which is not always simple since some conclusions are sometimes drawn without deep consideration, on basis on experience and "rules of thumb" that cannot be easy explained.

Knowledge can be understood as a theoretical or practical understanding of a subject or a domain, the sum of what is currently known. For the usage in an expert system the knowledge can be represented in form of:

- mathematical logic (well suited for objects with numerical values),
- production rules (condition – action),
- meta-rules (based on meta-knowledge – knowledge about knowledge, how to use and control knowledge),
- semantic networks, consisting of nodes (concepts or meanings) and links (relations),
- frames (information is grouped in records, with multiple levels),

  or in mixed form of the above, when required.

The inference block, apart from the main task, i.e. simulation of the problem-solving strategy of an expert, fulfils also the functions of control and coordination of work of the entire expert system. It determines also, which rules or algorithms should be applied in the considered case as well as, if needed, manages the process of conflict resolution for the rules of similar strength (importance) that may lead to contradictory reasoning results.

The aim of inferencing (working out of the solution of final decision) is usually obtained as a result of checking the truth (fulfillment) of all reasonable hypotheses on the basis of available measurement data – the *forward chaining* method, or through proving of a selected hypothesis for all currently known facts – the *backward chaining* method, which is schematically illustrated in Fig. 9.15.

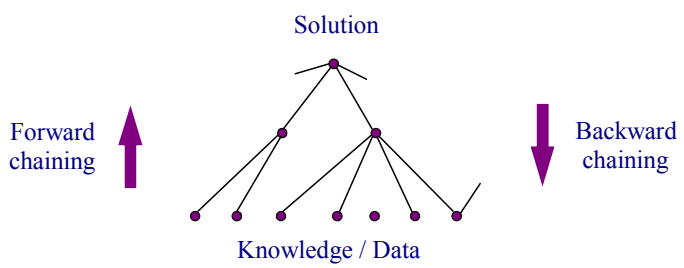

Fig. 9.15. Inference methods of an expert system

Development of an expert system for given purpose requires close cooperation of the following parties:

- Human Expert - can solve problems; one desires to implement his knowledge and solve the problems without him/her,
- Knowledge Engineer - should communicate with the HE to obtain and model the knowledge that we need in the system,
- Programmer - builds and maintains all the necessary computer programs,
- User - wants to use expertise to solve problems (better, cheaper).

9.4.2. APPLICATION OF EXPERT SYSTEMS

It should be stressed that the applications of expert systems in on-line operating protection and control devices are quite rare. The limitations arise basically from significant complexity and time-consuming execution of the expert reasoning algorithms.

As characteristic examples of expert systems for the tasks executed off-line (or possibly on-line, but with longer time horizon) one can enumerate:

- network planning,
- intelligent alarm processing in EMS and SCADA systems,
- network security analysis,
- load forecasting,
- voltage and reactive power flow control
- power quality monitoring,
- power system restoration
- post-fault diagnosis,
- coordination of protection settings (off-line, i.e. at design stage), etc.

Design of a Pilot Knowledge-based Expert System for Providing Coordinated Setting Values for Power System Protection Devices

As an example an application of expert technique for coordination of expert system is outlined. The scheme described in [E] is intended as a support for protection engineer in design and setting of protection devices, with the aim of achieving and maintaining protection selectivity, sensitivity, reliability and possibly highest speed of operation.

The problem solution strategy was based on a definition of the calculation sequence for the protection function parameters. The protection knowledge (IF… THEN… rules) was formalized in three main knowledge bases. Protected objects were grouped in the following categories:

(1) *Components*, including motor, generator, line, transformer, busbar, etc.

(2) *Group of components* that is protected together, like a generator with unit transformer, a motor with infeed cable, etc.

(3) *Subsystems*, being a set of network components and groups protected together.

The protection knowledge was formalized and documented as a decision tree for the reasoning process. Appropriate rules for protection settings coordination have been defined. Samples of solution strategy rules for overcurrent relays settings are:

- Strategy Rule 1: Find protection settings for network components and groups that always consume energy,
- Strategy Rule 2: Find protection settings of incoming feeders/bus ties/bus couplers. Consider subsystems with incoming feeders always absorb energy from upstream and deliver it to downstream feeder(s); all downstream protections are adjusted; subsystems may have local generation units,
- Strategy Rule 3: Find protection setting of Incoming Feeders/Bus ties/Bus Couplers; consider subsystems with incoming feeders having energy flow from and into the upstream substations; all downstream protections are adjusted; subsystems may have local generation units,
- Strategy Rule 4: Find protection settings for network components and groups that always generate energy.

The pilot expert system developed can be used in manual or auto mode. Auto response mode allows speeding up the protection setting process. The user's proxy runs the referenced calculation methods and calculates automatically the new value of each entity in the decision tree. It also runs database queries to retrieve required data for network components and protection devices. In manual mode the system can be used for training of new protection engineers.

More details about the system structure and utilization can be found in [E].

10. LABORATORY EXERCISES

Below an exemplary collection of laboratory exercises is provided that can be realized during labs. The students are expected to define the input signals containing the fundamental plus a set of non-fundamental components, to test the filtering/measuring algorithms in both time and frequency domains. A report from each of the exercises should be prepared.

10.1. DIGITAL RECURSIVE FILTERS (IIR)

Exercise contents:

1. Design the IIR digital filter according to the requirements defined by the teacher (analogue filter prototype, cut-off frequencies).
2. Determine/draw the frequency response of the designed IIR filter, compare with the frequency response of the analogue prototype.
3. Analyze filter response in time domain for various input signals (sinusoids of various frequencies + noise).

IIR digital filter design formulae:

$$LP: \quad G(z) = G(s)\Big|_{s \to A\frac{1-z^{-1}}{1+z^{-1}}} \quad , \quad A = \omega_{ca} ctg(\omega_{cd} T_s / 2)$$

$$HP: \quad G(z) = G(s)\Big|_{s \to B\frac{1+z^{-1}}{1-z^{-1}}} \quad , \quad B = \omega_{ca} tg(\omega_{cd} T_s / 2)$$

LP or HP – to be decided by the teacher.

Useful functions/procedures in MATLAB:

- fft, ifft
- filter
- plot, bar, stairs, hist
- bode, dbode, freqs, freqz
- hamming, hanning, blackman

10.2. ANALYSIS OF NONRECURSIVE (FIR) FILTERS

Exercise contents:

1. Define the FIR digital filters having the impulse responses as specified by the teacher
   (e.g. Walsh, triangle, sine, cosine, etc.).
2. Determine/draw the frequency responses of the FIR filters.
3. Analyze the filtering efficiency of the filters for the signals containing harmonic, inter-harmonic and decaying DC components.
4. Analyze filters' responses in time and frequency domains after their data window modification with selected smoothing filtering windows (e.g. Hamming, Blackman, …).

10.3. ALGORITHMS FOR SIGNAL AMPLITUDE MEASUREMENT

Exercise contents:

For the measurement algorithms given below make comparative analysis with regard to:

1. measurement accuracy and dynamics for the undistorted 50Hz sine signal;
2. algorithms' accuracy for the signals containing decaying DC component of various time constants (50-300ms);
3. influence of harmonic and inter-harmonic components on the measurement quality;
4. algorithms' quality for the cases of frequency change in the range 50±2Hz;
5. influence of sampling frequency on the measurement accuracy.

The algorithms to be examined are as follows (example):

A – averaging methods

$$X_m(n) = \frac{2}{m} tg\left(\frac{\pi}{2N}\right) \sum_{k=0}^{m\frac{N}{2}-1} |x(n-k)|, \qquad m=1$$

B – orthogonal components
- orthogonalisation with

$$x_c(n) = x(n), \qquad x_s(n) = \frac{x(n-k) - x(n)\cos(k\Omega_1)}{\sin(k\Omega_1)}, \qquad k=1$$

- measurement with

$$X_m(n) = \sqrt{x_c^2(n) + x_s^2(n)}$$

C – orthogonal components
- orthogonalisation with full-cycle sine/cosine filters
- measurement as above

10.4. ALGORITHMS FOR POWER AND IMPEDANCE COMPONENTS MEASUREMENT

Exercise contents:
For the measurement algorithms given below make comparative analysis with regard to:
1. measurement accuracy and dynamics for the undistorted 50Hz sine signals (current and voltage);
2. algorithms' accuracy for the signals containing decaying DC component (in current signal) of various time constants (50-300ms);
3. influence of harmonic and inter-harmonic components on the measurement quality;
4. algorithms' quality for the cases of frequency change in the range 50±2Hz;
5. influence of sampling frequency on the measurement accuracy.

The algorithms to be examined are as follows (example):

A – averaging methods

$$P_1(n) = \frac{1}{N}\sum_{k=0}^{N-1} u_1(n-k) i_1(n-k)$$

$$Q_1(n) = \frac{1}{N}\sum_{k=0}^{N-1} u_1(n-k-N_1/4) i_1(n-k) \quad \text{or} \quad Q_1(n) = \frac{1}{N}\sum_{k=0}^{N-1} u_1(n-k) i_1(n-k-N_1/4)$$

B – orthogonal components

- orthogonalisation with

$$x_c(n) = x(n), \qquad x_s(n) = x(n - N_1/4)$$

$$x_c(n) = x(n), \qquad x_s(n) = \frac{x(n-k) - x(n)\cos(k\Omega_1)}{\sin(k\Omega_1)}, \qquad k=1$$

full-cycle sine/cosine filters

- measurement with

$$P_1(n) = \frac{1}{2}\left[u_{1C}(n)i_{1C}(n) + u_{1S}(n)i_{1S}(n)\right]$$

$$Q_1(n) = \frac{1}{2}\left[u_{1S}(n)i_{1C}(n) - u_{1C}(n)i_{1S}(n)\right]$$

10.5. MEASUREMENT OF SIGNAL FREQUENCY

Exercise contents:

For the measurement algorithms given below make comparative analysis with regard to:

1. measurement accuracy and dynamics for the undistorted 50Hz sine signal;
2. algorithms' accuracy for the signals containing decaying DC component of various time constants (50-300ms);
3. influence of harmonic and inter-harmonic components on the measurement quality.

The algorithms to be examined are as follows (example):

A – algorithm with counting of impulses with zero-crossing correction

$$T_m = 2T_s\left[M_{0.5} + \left(\frac{u_{k+1}}{u_{k+1} - u_k}\right)_{|p} + \left(\frac{u_{m+1}}{u_{m+1} - u_m}\right)_{|p+1}\right], \quad f = 1/T_m$$

B – algorithm with use of orthogonal components
- orthogonalisation with full-cycle sine/cosine filters
- measurement

$$f(n) = \frac{f_s}{2\pi}\arccos\left\{0.5\frac{x_s(n)x_c(n-2) - x_c(n)x_s(n-2)}{x_s(n)x_c(n-1) - x_c(n)x_s(n-1)}\right\}$$

10.6. MEASUREMENT OF SYMMETRICAL COMPONENTS

Exercise contents:

For the measurement algorithms specified as below make comparative analysis with regard to:

1. measurement accuracy and dynamics for the undistorted 50Hz sine signals;

2. algorithms' accuracy for the signals containing decaying DC component of various time constants (50-300ms);
3. influence of harmonic and inter-harmonic components on the measurement quality;
4. algorithms' quality for the cases of frequency change in the range 50±2Hz.

The algorithms to be examined are as follows (example):

A. Algorithm in complex matrix form

$$\begin{bmatrix} \underline{x}_0(n) \\ \underline{x}_1(n) \\ \underline{x}_2(n) \end{bmatrix} = \frac{1}{3}\begin{bmatrix} 1 & 1 & 1 \\ 1 & a & a^2 \\ 1 & a^2 & a \end{bmatrix}\begin{bmatrix} \underline{x}_{L1}(n) \\ \underline{x}_{L2}(n) \\ \underline{x}_{L3}(n) \end{bmatrix}$$

Orthogonalisation
- with double delay, $k=N_1/4$

$$x_c(n) = x(n-k)$$

$$x_s(n) = \frac{x(n-2k) - x(n)}{2\sin(k\Omega_1)}$$

- with full-cycle sine/cosine filters

B. Algorithm with time delay

10.7. DESIGN AND ANALYSIS OF ANN-BASED PROTECTION UNIT

Exercise contents:

Problem: ANN-based overcurrent protection (example)

For the decision/classification task as defined above do the following particular tasks:
1. prepare the input and output matrices for training of ANN;
2. execute ANN training;
3. examine the ANN operation for training and new testing patterns;
4. check the ANN operation for distorted input signals;
5. perform comparative analysis with chosen non-AI measurement/decision procedure.

Useful Matlab functions (Matlab 5.3): newff, train, sim

```
%initialization
net = newff([min max],[n1 n2],{'tansig' 'purelin'});
%trainig
net.trainParam.epochs = 50;
net = train(net,P,T);
%simulation and comparison
Y = sim(net,P);
plot(P,T,P,Y,'o')
```

where:

P, T – input and output vector matrices, net – ANN structure
min, max – expected range od change of input signal(-s)
n1, n2 – number of neurons in particular layers

REFERENCES

[A] A. Wiszniewski, W. Rebizant, L. Schiel. ***Correction of Current Transformer Transient Performance.*** IEEE Trans. on Power Delivery, Vol. 23, April 2008, No. 2, pp. 624 – 632

[B] W. Rebizant, J. Szafran. ***Power system fault detection and classification using probabilistic approach.*** European Transactions on Electrical Power, Vol. 9, No. 3, May/June 1999, pp. 183-191.

[C] W. Rebizant, K. Feser. ***Out-of-step protection with AI methods***, Proc. of the 7th Int. IEE Conference Developments in Power System Protection DPSP 2001, 9-12 April 2001, pp. 295-298.

[D] D. Bejmert, W. Rebizant, A. Wiszniewski, L Schiel. ***Fuzzy Logic Based Multi-Criteria Stabilization of Transformer Differential Protection***. Proceedings of the 3rd International Conference on Advanced Power System Automation and Protection, APAP2009, Jeju, Korea, 19-22 October 2009, CD-ROM, paper 147.

[E] M.R. Ganjavi, R. Krebs, Z. Styczyński, ***Design of a Pilot Knowledge-based Expert System for Providing Coordinated Setting Values for Power System Protection Devices***. Proceedings of the MEPS06 Conference, Wroclaw, Poland, pp. 354-360.

FURTHER READING

[1] Leland B. Jackson. ***Digital Filters and Signal Processing*** . Kluwer Academic Publishers, 1986.

[2] Helmut Ungrad, Wilibald Winkler, Andrzej Wiszniewski . ***Protection Techniques in Electrical Energy Systems.*** Marcel Dekker Inc., 1995.

[3] Arun G. Phadke, James S. Thorp. ***Computer Relaying for Power Systems.*** John Wiley and Sons, 1988.